

***BIOLOGICAL INTERACTIONS DURING ION EXCHANGE
REMOVAL OF AMMONIA FROM TERRESTRIAL AND
MARINE WASTE WATER***

by

NATALIJA D. MILADINOVIC

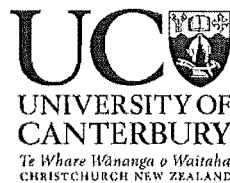
Thesis Submitted for
the Degree of Doctor of Philosophy

Chemical and Process Engineering

University of Canterbury

Christchurch, New Zealand

April 2005



)
57.5
637
1005

*This thesis is dedicated to my mother Mileva-Luisa Miladinovic
(1940-1992)*

Acknowledgements

The work carried out in this research project would not have been successful without the contributions of a number of people to whom I would like to express my appreciation. I thank my supervisor Professor Laurence Weatherley for his guidance and advice over the past four years. His comments and ideas helped me a lot through the experimental part of the work as well as through the period of analysis of the results obtained. My sincere thanks are extended to Dr Ken Morison who supported me throughout the last half year of my project and contributed a lot to the thesis writing.

Additionally, I would like to thank the technical staff at Department of Chemical and Process Engineering. Bob Gordon, Frank Weerts, Paul Tolson and Ron Boyce helped me with design and construction of the ion exchange columns and lab scale plant; Glenn Wilson was always helpful in providing consumables for my experiment; Trevor Berry was always ready to solve any problem which might occur and Tony Allen fixed any computer problems.

Thanks are also extended to Mike Flaws from Mechanical Engineering, for helping me in obtaining scanning electron microscopy pictures of materials used and to Dr Gavin Walker from Queen's University of Belfast for surface area and pore size measurements. I also wish to thank Zolve Limited from Auckland and Mr Graeme Stretch for providing us with the New Zealand zeolites as well as Professor Hose Lopez Ruiz from University of Cadiz, Spain, for providing us with modified zeolites used in this research.

I express gratitude to the New Zealand Foundation for Research, Science and Technology who provided the Bright Future Scholarship for this research.

Finally I would like to thank my family, Darko, Vukasin and Anka-Lula, who have encouraged and distracted me, but always were there to remind me what life really is about. Last but by no means least I would like to thank my parents who have provided constant guidance and support throughout my entire education.

Summary

Wastewater containing ammonia is a product of oil refineries, coal gasification plants, slaughterhouses, dairy plants, distilleries, fertilizer plants and pharmaceutical operations; ammonia is also found in municipal wastewater. The ammonia is toxic to living organisms and it is desirable that it be removed. The foremost aim of this research was to use biologically activated ion exchange materials for ammonia removal from wastewater.

In the past sand, plastic media and activated carbon as well as some ion exchange materials, e.g., clinoptilolite, have been used like a solid surface for bacteria growth. In this work some other materials were used for a combined biological and ion exchange process. The materials used were mordenite and Macronet MN 500 for terrestrial water, and modified zeolites for selective uptake of ammonia from marine waters. Clinoptilolite was used for comparison, as an ion exchanger which previously has been biologically activated.

The ammonia adsorption characteristics of the materials in saline and non-saline synthetic wastewater were determined and compared with literature data. The data was fitted using Langmuir and Freundlich isotherms. The effect of the individual presence of potassium, calcium and magnesium ion upon ammonium ion uptake onto each material was also investigated.

Bench scale ion-exchange stirred cell experiments were conducted to assess the uptake kinetics of ammonium ion. Process parameters include: initial ammonia concentration, the agitation rate, material particle size and mass of the material. The suitability of the ion exchange materials as a support for the growth of nitrifying bacteria was determined by observing the nitrification process in the flasks containing different materials, for the fresh and saline media. The ion exchangers were tested in continuous columns initially without bacterial growth and later with. To overcome the problem of low oxygen levels in the column and to avoid over aeration of the system, a novel design of columns was introduced,

where aeration through the column was achieved by the air permeable silicon tubing.

The synthetic material MN 500 exhibited the highest uptake capacity but the natural zeolites had the highest preference for ammonium ions in the presence of interfering cations. The ion exchange materials removed ammonia from saline water. A product of zeolitic nature, ZZ, exhibited the highest uptake capacity for ammonia removal from saline water. Natural zeolites were shown to be better media for bacterial growth in non-saline water. MN 500 exhibited better ammonia removal performance for the combined process in sea water compared to modified zeolite, ZZ. Both the clinoptilolite and mordenite used in non-saline medium, exhibited higher uptake capacity during the column experiments than for batch experiments.

By introducing bacteria into the column, the uptake capacity was increased from the value of 0.15 to the value of 0.22meq/g for clinoptilolite. The improvement for the biologically active mordenite was from the value of 0.30meq/g without bacteria to the value of 0.41meq/g with bacteria. The aeration of 2.88dm³/h, achieved by the tubing, provided better condition for the nitrification within the column, compared to the commonly used tank pre-aeration at the rate of 180dm³/h.

The biologically active ion exchange column was not efficient in removing ammonia from saline water. High salt concentrations and slower nitrification in saline medium interfered the process significantly.

It could be concluded that biologically active ion exchange is acceptable method for ammonia removal from non-saline wastewater. The possible way to improve the efficiency of the process in saline water would be to apply it in wastewaters in which nitrifying bacteria are already established. Mordenite proved to be more adequate for biological activation compared to commonly used clinoptilolite, which indicates that more ion exchange materials should be tested for combined process. The new aeration system within the columns proved to be more efficient compared to the commonly used tank pre-aeration.

Table of contents

Acknowledgements.....	iii
Summary.....	iv
Table of contents.....	vi
1 Introduction	1
1.1 Wastewater treatment	1
1.1.1 Pre-treatment	4
1.1.2 Primary treatment	4
1.1.3 Secondary treatment	4
1.1.4 Tertiary treatment	5
1.2 Nitrogen cycle.....	6
1.2.1 Nitrogen fixation	7
1.2.2 Decay	7
1.2.3 Nitrification	7
1.2.4 Denitrification.....	11
1.3 Ammonia	11
1.3.1 Ammonia in the environment	14
1.3.2 Ammonia toxicity	15
1.3.3 Removal of ammonia	16
1.4 Ion-exchange	19
1.4.1 Ion exchange equilibrium	21
1.4.2 Ion exchange capacity.....	22
1.4.3 Ion exchange selectivity	23
1.4.4 Ion exchange regeneration	25
1.4.5 Kinetics of the ion exchange	26
1.4.6 Natural zeolites	29
1.4.7 Products of zeolitic nature	35
1.4.8 Synthetic ion exchanger, Purolite MN 500	36
1.5 Bacteria adhesion	37
1.6 Saline water	37

2	Literature review	39
2.1	Nitrification	39
2.1.1	Substrate ammonia concentration	40
2.1.2	pH role in nitrification process	41
2.1.3	Temperature effect on nitrification	42
2.1.4	Oxygen concentration	43
2.1.5	Role of the surface in the nitrification process	44
2.1.6	Other influencing factors on nitrification	45
2.1.7	Nitrification in saline water	47
2.2	Ion Exchange	49
2.2.1	Removal of ammonia by ion exchange	49
2.2.2	Ion exchange capacity	50
2.2.3	Ion exchange selectivity	52
2.2.4	Ion exchange kinetics	53
2.2.5	Ion exchange regeneration	54
2.3	Ion exchange in saline water	56
2.4	Biologically active ion exchange	57
2.5	Aim and scope of the research	60
3	Experimental materials and methods	61
3.1	Experimental materials	61
3.1.1	Material analysis	61
3.1.2	Material preparation	63
3.2	Experimental methods	64
3.2.1	Batch equilibrium studies without bacteria	64
3.2.2	Ammonia removal on biologically active materials	66
3.2.3	Kinetic studies	68
3.2.4	Column studies	70
3.2.5	Bacteria immobilization	76
3.2.6	Alkaline regeneration	77
3.3	Analytical methods	78
3.3.1	Ammonia measurements	78
3.3.2	Oxygen measurements	78
3.3.3	Metal cation measurements	79
3.3.4	pH measurements	79

3.3.5	Nitrite and nitrate analysing	79
3.3.6	Protein measurements	80
4	Results and discussion	81
4.1	Material analysing	81
4.1.1	Electron microscopy	81
4.1.2	XRF analysis	83
4.1.3	Surface area and pore size measurements	85
4.1.4	IR spectra	86
4.2	Batch equilibrium studies without bacteria	88
4.2.1	Fresh water	88
4.2.2	Saline water	102
4.3	Batch equilibrium studies with bacteria	107
4.3.1	Ammonia removal on biologically active materials in fresh water	107
4.3.2	Ammonia removal on biologically active materials in saline water	114
4.4	Kinetic studies.....	120
4.4.1	MN 500	120
4.4.2	Natural zeolites	126
4.5	Kinetic studies on biologically active materials	136
4.6	Column studies - fresh water	138
4.6.1	Column studies without bacteria	138
4.6.2	Column studies with bacteria	144
4.7	Column studies – saline water	155
4.7.1	Column studies without bacteria	155
4.7.2	Column studies with bacteria	157
5	Conclusions	159
5.1	Material analysing	159
5.2	Batch equilibrium studies without bacteria	159
5.2.1	Fresh water	159
5.2.2	Saline water	160
5.3	Batch equilibrium studies with bacteria	160

5.3.1	Fresh water160
5.3.2	Saline water161
5.4	Kinetic experiments161
5.5	Column studies161
5.5.1	Fresh water161
5.5.2	Saline water162
6	Future work163
7	References165
8	Appendices183

1 Introduction

It is not easy to tell when the environmental concern started to grow in our society. Activated sludge processing for sewage biological treatment, before discharging it into the receiving body, was used 100 years ago but this was not common practice and certainly was not regulated by the law. In the last 50 years, especially in the last 20, people have become aware of the fact that nature cannot cope and that we have to clean up waste produced. Legally, the solutions for the pollution problems started to develop in the 1970's when a number of laws were introduced regarding pollution discharge into the environment which industry was required to address: the Clean Air Act (CAA) of 1970, the Clean Water Act (CWA) of 1972 as well as establishing the Environmental Protection Agency (EPA) in 1970 in the United States. At the beginning of 1980s a sustainable approach started to grow and one of the major results of greater environmental awareness was the Pollution Prevention Act (PPA) from 1990. According to the guidance given in the PPA, "end-of-pipe-treatment" was the least desirable solution to potential environmental impact in any process design or any other planning. Therefore, it succeeded a number of other more acceptable solutions which together are called sustainable approach. This required a broader approach taking into account feedstocks, product design, life cycle assessment and final end-of-life considerations for a product (Anastas and Warner, 1998). Even though modern concepts of engineering and life in general are based on a sustainable approach which will eliminate pollutants at their source, some treatable waste is inevitably produced. Ammonia is one such unwanted product requiring removal from treated wastewater before it is released into a receiving body.

1.1 Wastewater treatment

Conventional wastewater treatment consists of a number of different processes that can be grouped together in four major steps:

- pre-treatment
- primary treatment
- secondary treatment

- tertiary treatment.

Figure 1.1 shows a flow chart of the process in municipal wastewater treatment systems (Kiely, 1997).

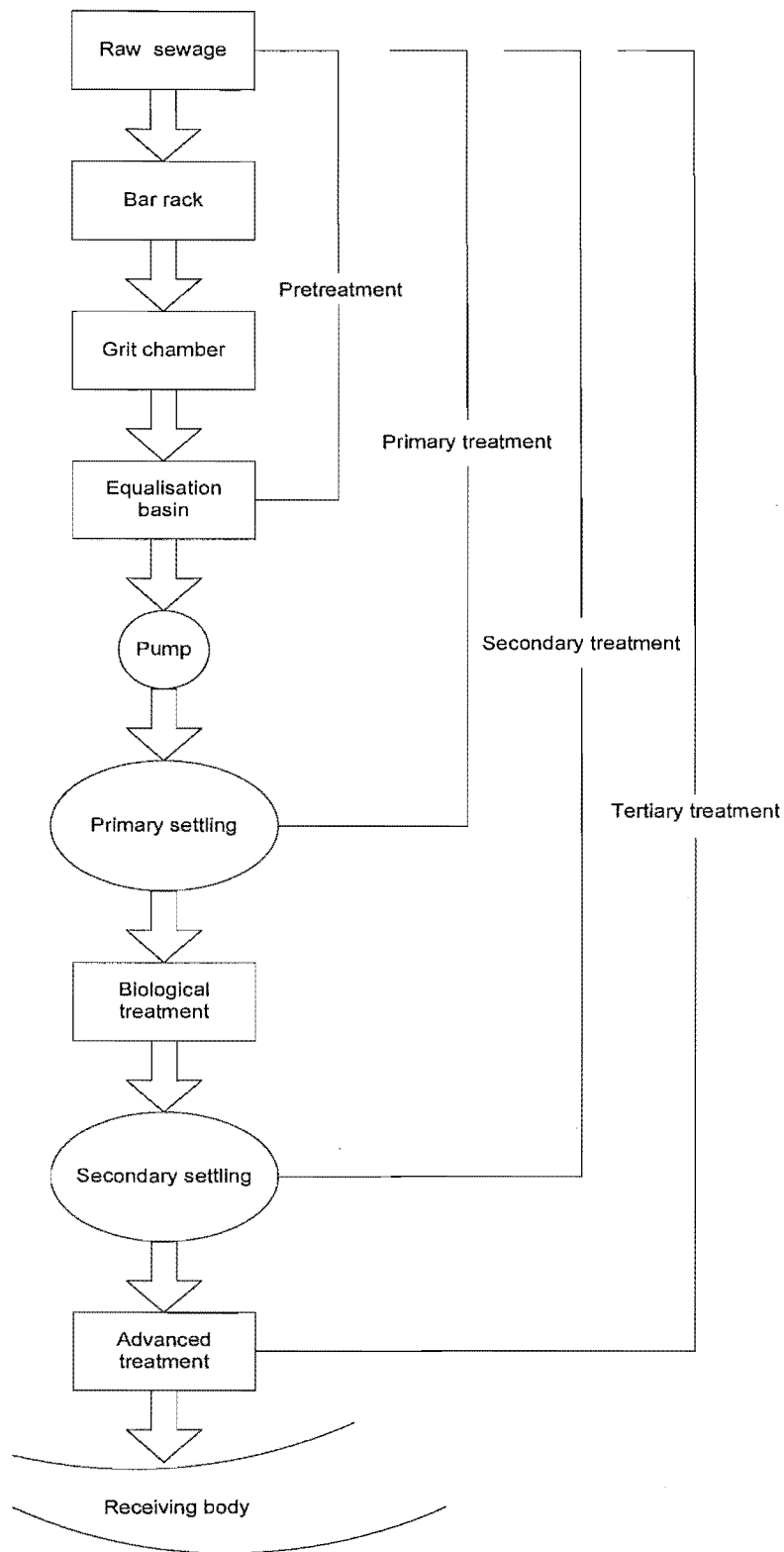


Figure 1.1 Flow chart of the common municipal wastewater treatment plant.

1.1.1 Pre-treatment

Pre-treatment is a preparation step and process units could be screens, a comminutor, a grit chamber and a flow equalization tank. The aim of the pre-treatment is to protect the wastewater treatment plant equipment (pumps and other mechanical devices) from mechanical damage by removing sizeable inorganic solids and to provide the constant flow rate during the process.

1.1.2 Primary treatment

Primary treatment is a part of the process where all settleable suspended solids (SS) are removed from the incoming wastewater by gravity sedimentation. Typical influent characteristics would show BOD (biological oxygen demand¹) values of approximately 300mg/l and suspended solids values of around 400mg/l (SS) (McKenzie and Cornwell, 1996). The potential success of a treatment achieved by primary treatment is as follows:

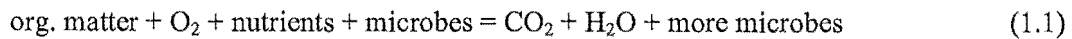
BOD	30-40% removed
SS	40-60% removed
organic nitrogen	10-20% removed
ammmoniacal nitrogen	0
total phosphorus	10% removed.

It is evident that the ammoniacal nitrogen stays in the water after primary treatment since it is dissolved in the water and does not settle out.

1.1.3 Secondary treatment

Secondary treatment processes convert more of the dissolved organic matter left after primary treatment into settleable biomass (sludge) through an aerobic biochemical process. The process can be simplified by the following equation:

¹ BOD is the amount of dissolved oxygen consumed by microorganisms for the biochemical oxidation of organic and inorganic matter .



The most commonly used types of biological wastewater treatment are: activated sludge, trickling filters or rotating biological contactors followed by the secondary settling tank. The degree of treatment achieved by the secondary treatment is as follows:

BOD	65-95% removed
SS	60-85% removed
organic nitrogen	10-20% removed
total nitrogen	10-25% removed
total phosphorus	10-15% removed.

It is noticeable that secondary treatment usually does not remove all of the phosphorus and nitrogen from the wastewater but usually it is sufficient to protect the water quality of most of the receiving waters into which the treated water is discharged. However, the activated sludge process can be modified so that the biological removal of nitrogen and phosphorus is encouraged. Nitrogenous compounds can be removed by nitrification followed by the denitrification, while the phosphorus can be removed by so called luxury uptake which is polyphosphate storage within the bacteria cells (Tchobanoglous and Schroeder, 1985). Keeping biomass longer in the reactor can improve growth of autotrophic organisms since nitrifying bacteria have a long generation time (at least 10-30hr) and lower growth rate compared to heterotrophic organisms. Sludge age of 20 days usually will allow maximum nitrogen removal (Orhon et al., 2000).

1.1.4 Tertiary treatment

If the secondary treatment had not been modified for the nitrogen and phosphorus removal and it becomes necessary to remove them, then the tertiary treatment process is introduced to achieve this before the effluent is discharged into the receiving water.

Nitrogenous compounds, again, can be removed by nitrification followed by either denitrification or ion exchange while phosphorus can be chemically precipitated as aluminium phosphate. Usually, the tertiary treatment process is expensive and requires a high degree of operational skills.

1.2 Nitrogen cycle

Nitrogen exists in many forms in the environment. Before it can be assimilated by higher plants and animals, nitrogen gas must be combined with oxygen or nitrogen to form organic nitrogen compounds, nitrate or ammonia. Figure 1.2 shows the major aspects of the nitrogen cycle.

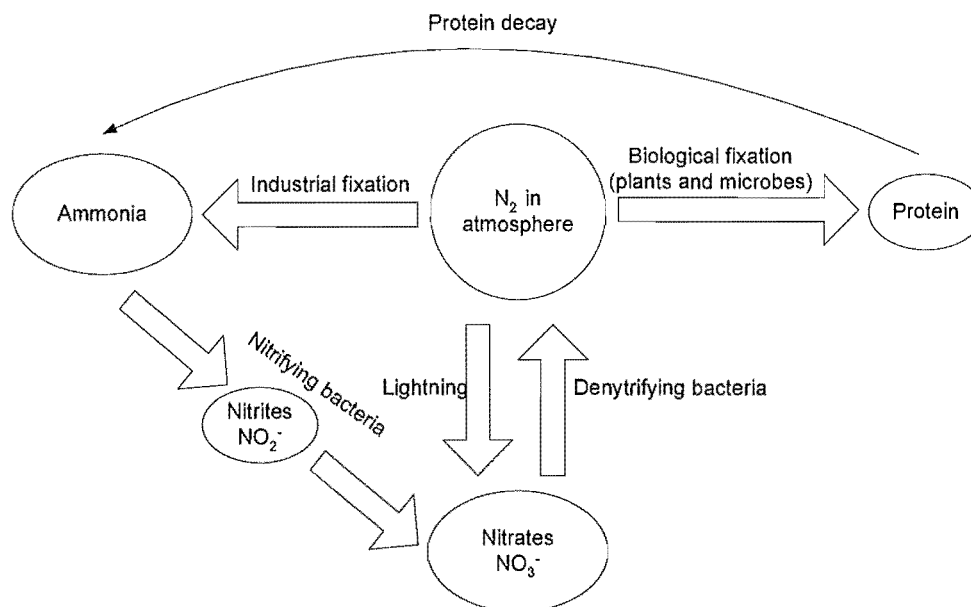


Figure 1.2 The nitrogen cycle

Four processes take place in the cycling of nitrogen through the biosphere:

- nitrogen fixation
- decay
- nitrification
- denitrification.

1.2.1 Nitrogen fixation

Most of the nitrogen fixation in the biosphere is achieved by one of the following processes:

- atmospheric fixation
- industrial fixation
- biological fixation.

Atmospheric fixation happens when energy from lightning enables the formation of nitrogen oxides, which dissolved in water and form nitrates.

Industrial fixation of nitrogen is achieved by combination of nitrogen and hydrogen at high temperature and pressure to form ammonia which can be used directly or used for further processes to form chemical products such as urea and ammonium nitrate.

Biological fixation is driven by bacteria alone or in a symbiotic relationship with certain plants. Ammonia is the first stable product of this process which is rapidly built into protein and other organic nitrogen compounds.

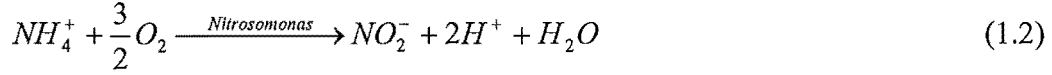
1.2.2 Decay

The proteins made in the nitrogen cycle enter the food chain. They are either incorporated into the structure of the organisms or returned to the environment as nitrogen organic compounds in excretions. Microorganisms of decay break down the organic molecules in excretions and dead organisms into ammonia.

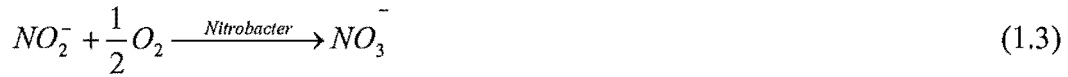
1.2.3 Nitrification

Nitrification is the natural biological process during which bacteria convert toxic ammoniacal nitrogen to less harmful nitrates. It is a two step process which requires the simultaneous presence of two bacterial groups that perform two reactions in series. The first reaction is oxidation of ammonium ion to nitrite and is driven by the group of bacteria known as *Nitrosomonas europaea* (Equation

1.2). This is the slower of the two reactions and thus can determine the kinetics of the overall process.

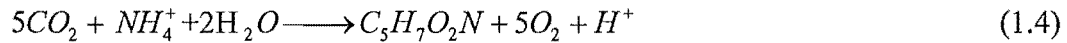


The second step is the conversion of nitrite to nitrate by *Nitrobacter winogradskyi*, which is given in Equation 1.3.

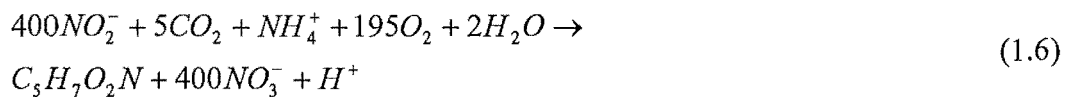
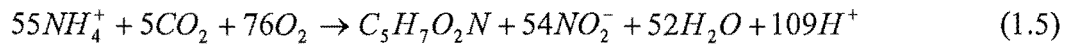


These two groups of autotrophic bacteria belong to a group of nitrifying bacteria. Nitrifying bacteria are widely spread in the environment and can be found in lakes, rivers, soil, oceans and brackish waters, where aerobic conditions and organic materials are available. Since the first step is slower, high nitrite concentrations are rarely found in the environment. This might happen if oxygen supply is limited.

Since some of the nitrogen is assimilated into bacterial protoplasm, with an empirical cell formulation of $C_5H_7O_2N$ the consumption reaction can be written as:



The resulting equations for ammonia and nitrite oxidation will be:



Ideally, the ammonia concentration will constantly decrease during the nitrification process while nitrates accumulate. The nitrite concentration will increase in the early stages of the reaction but should decline after certain level has been reached which indicates that the *Nitrobacter* population is fully functioning. Nitrogen transformation during nitrification in a non-inhibited system is given on the next figure.

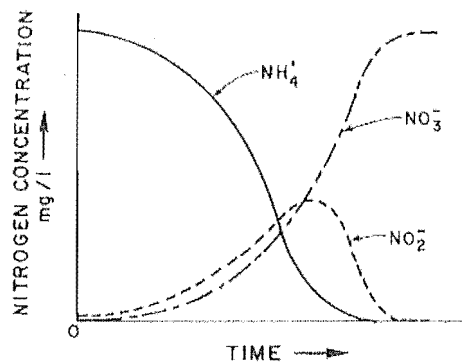


Figure 1.3 Nitrogen transformation during nitrification in non-inhibited system (Anthoniesen, 1976).

Nitrifying bacteria have a long generation time (at least 10-30hr). Growth rates of ammonia oxidizers (Equation 1.2) determine the volumes of the aerated tanks in the waste water treatment process. Low yield of cell mass per mass of substrate oxidized relative to most heterotrophic microorganisms has also been proven (Roger and Perry, 1972).

Verstraete and Alexander (1973) as well as Burell et al. (1998) stated that some heterotrophic organisms can carry out nitrification as well, but at a slower rate than autotrophic organisms.

1.2.3.1 Kinetics of biological processes

The life cycle of a bacterial population can be divided ideally into four stages.

The lag phase is the initial stage after bacteria have been inoculated into the substrate solution. Organisms experience an adaptation phase in order to adjust to

the new medium before they start to grow and multiply. The bacteria then begin to divide but before they reach the stage of geometric progression in population increase during the *exponential growth phase*, there is a phase called *accelerated growth*. At some point the bacteria population reaches a balance between reproduction and death rates. This phase is called the *stationary phase*. The substrate then becomes exhausted, which is usually followed by the production of toxic by-products, bacteria die faster than they multiply and the numbers decrease. This happens in the *death phase*. Figure 1.4 represents all four stages in the bacteria population life cycle.

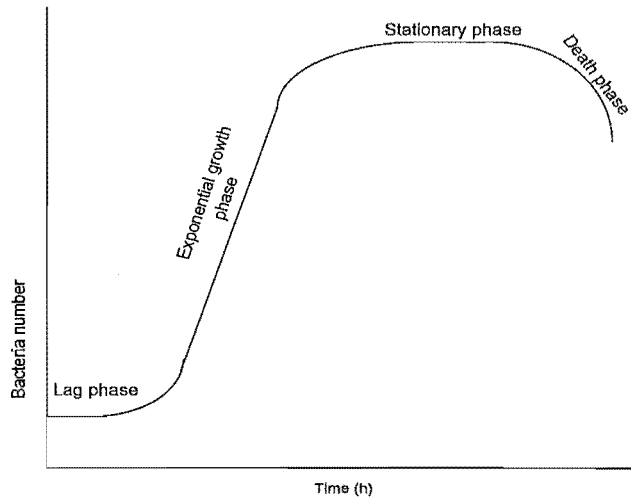


Figure 1.4 Bacteria growth curve.

The rate of food utilization and therefore the rate of biomass production can be related to the food compound that is in shortest supply, and the Monod equation (Davis and Cornwell, 1996) is used to describe the rate of growth, (Equation 1.7):

$$\mu = \frac{\mu_{\max} S}{K_s + S} \quad (1.7)$$

where:

- μ_{\max} - maximum growth rate constant (t^{-1});
- S - concentration of limiting food in substrate;
- K_s - half saturation constant and concentration of limiting food

when $\mu = 0.5\mu_m$, (t^{-1}).

The Monod equation assumes no inhibition, in which case the bacteria growth follows the hyperbolic function.

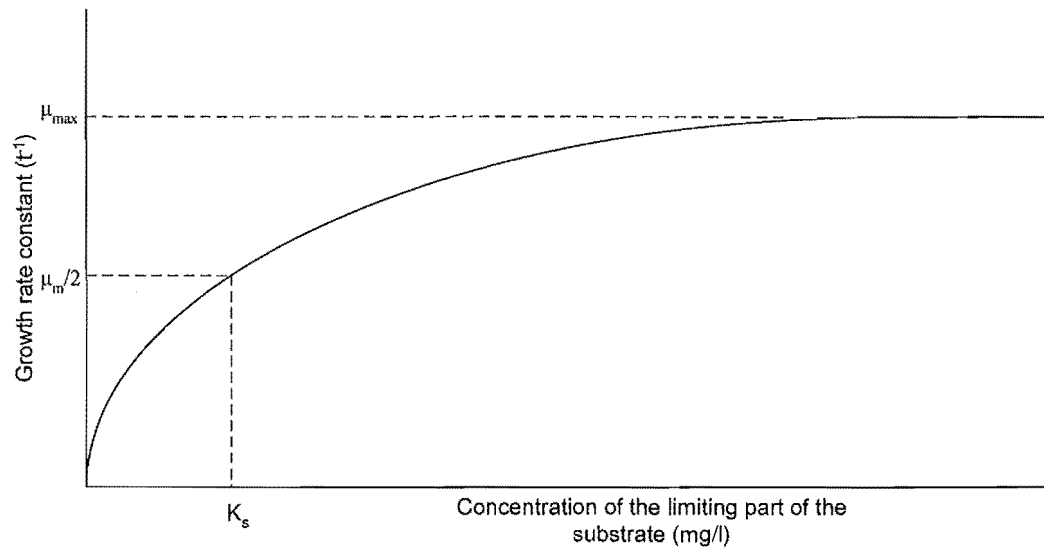
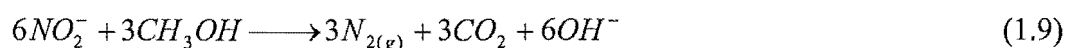
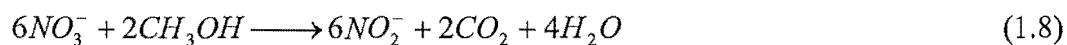


Figure 1.5 Monod curve for bacterial growth

1.2.4 Denitrification

Denitrification is a process that transforms nitrate to nitrogen. It can be presented by the following equations (Meade, 1974):



This biological process is driven by a variety of bacterial species such as *Pseudomonas* and *Bacillus* under anaerobic conditions. The organic source of energy may be glucose, ethanol or methanol and usually is added into the process, although in some cases the required organic source of energy might be available within the waste-water.

1.3 Ammonia

Before humans started to change the environment significantly, nature was able to maintain a normal nitrogen cycle. With increased nitrogen fixation in many

industrial or agricultural areas, ammonia started to accumulate. Nowadays ammoniacal-nitrogen is the nitrogenous compound most responsible for toxicity effects in aquatic life. Ammoniacal nitrogen is present in two forms when in water: ammonia (NH_3) or ammonium (NH_4^+). The equilibrium of these two forms can be presented with the following equations:



$$K = \frac{[\text{NH}_3][\text{H}^+]}{[\text{NH}_4^+]} \quad (1.11)$$

The equilibrium constant depends on temperature as can be seen in Figure 1.6.

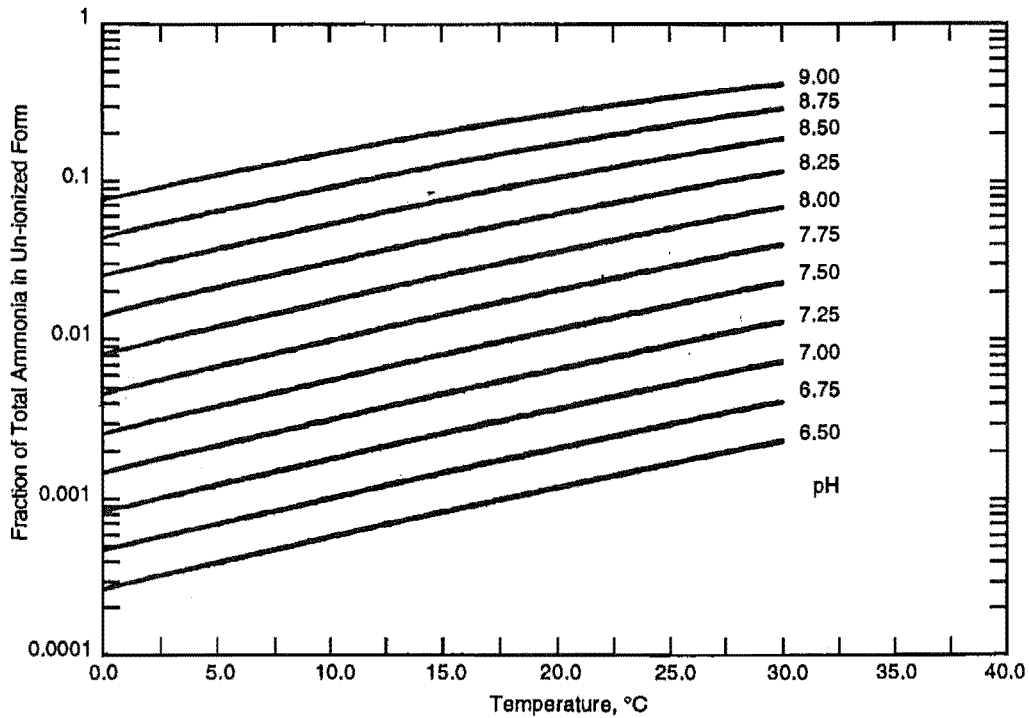


Figure 1.6 Fraction of unionized ammonia in the aqueous solution as a function of temperature and pH (USEPA, 1993).

The distribution of the two forms of ammonia at constant temperature can be represented by the following equation (USEPA, 1999):

$$f_{NH_3} = \frac{1}{1 + 10^{pK - pH}} \quad (1.12)$$

$$f_{NH_4^+} = \frac{1}{1 + 10^{pH - pK}}$$

The free ammonia concentration at a given pH and temperature can also be calculated by using Equation 1.13 (Surmacz - Gorska et al., 1997).

$$C_{NH_3} = \frac{17}{14} \cdot \frac{C_{N-NH_4^+} \cdot 10^{pH}}{e^{6344/T} + 10^{pH}} \quad (1.13)$$

where:

- C_{NH_3} - free ammonia concentration (mg/l);
- $C_{N-NH_4^+}$ - ammonium concentration expressed as (mg nitrogen/l);
- T - temperature (K).

The pH increase from 7.0 to 7.3 would double the concentration of unionized ammonia in the solution. The effect is not so drastic if pH values are higher than 8.5 (Dryden, 1984).

Table 1.1 shows the distribution of total ammoniacal nitrogen between the two forms. It gives the concentration of total ammonia at different pH values and temperatures which will lead to the unionized ammonia concentration of 0.025mg/l.

Table 1.1 Concentration of total ammonia which gives unionized ammonia concentration of 0.025 mg/l (Dryden, 1984)

Temperature	pH					
	7	7.5	8	8.5	9	9.5
5.0	19.6	6.3	2.0	0.7	0.2	0.09
10.0	13.4	4.3	1.4	0.5	0.2	0.07
15.0	9.1	2.9	0.9	0.3	0.1	0.05
20.0	6.3	2.0	0.7	0.2	0.1	0.04
25.0	4.4	1.4	0.5	0.2	0.7	0.04
30.0	3.1	1.0	0.3	0.1	0.6	0.04

Ionic strength also has an effect on speciation distribution but the effect is not significant in fresh water (Soderberg and Meade, 1991). At a given pH and temperature the concentration of unionized ammonia is approximately 40% less in seawater but the generally higher pH in saline water² moves the equilibrium towards the NH_4^+ form (Huguenin and Colt, 1989).

Distribution between the two forms is important since unionized ammonia is much more toxic than the ammonium ion. The higher toxicity of the neutral molecule may be explained by its ability to diffuse across the cell membranes of living organisms more easily than the ionised NH_4^+ form (USEPA, 1999). Even though the unionized form is more important some research has shown that ammonium ion can be harmful as well (Erikson, 1985; Wood, 1993), especially since it is usually present in higher concentrations than the neutral form.

1.3.1 Ammonia in the environment

Ammonia is the most commonly occurring nitrogenous pollutant in wastewater (McVeigh, 1999). Ammoniacal nitrogen reaches surface or underground water from sewage, agricultural and industrial sources. The industrial contexts of this problem include: oil refineries, coal gasification plants, slaughterhouses, dairy plants, distilleries, fertilizer plants, pharmaceutical plants, glass production plants and cellulose and paper manufacturing plants (Wiesmann, 1994). Due to sustainable engineering and strict legislations that control industrial effluents, sewage water is nowadays the major ammonia source in municipal wastewater systems.

The problem of ammonia removal is even more important in recirculation systems used in aquaculture. Intensive fish farming is based on usage of protein rich food (Lovel, 1989). The nitrogen fraction of the food on a dry basis can be 5-6.5% of which 70% remains in the pond either as uneaten food or fish excretion (Gross et al., 2003). While ammonia removal from wastewater is usually more important in long than in short time intervals due to the large volume of receiving water and

² Normal pH values in seawater are about 8.2 (Campbell and Wildberger, 1992).

dilution achieved, in recirculation systems permanent control of ammonia concentration is essential for fish survival. Nitrogen compounds in seawater also contribute to serious water pollution problems. Ammonia and other nitrogen compounds accumulate in seawater aquaria, aquacultural ponds and disposal sites. Ammonia levels in such facilities are strongly influenced by ammonia concentration in the feed water and by the production of ammonia by fish and other living organisms, which may be present.

1.3.2 Ammonia toxicity

Ammonia toxicity to fish and other aquatic animals is very significant and concentrations in the range 0.2mg/l to 0.5mg/l can be fatal (Wiesmann, 1994). Some of the problems that ammonia can cause are listed below:

- unionized ammonia is toxic to fish at very low concentrations (<0.5mg/l), (Huguenin and Colt, 1989);
- ammonia is oxidised by bacteria to nitrite and nitrate and this process can cause dissolved oxygen (DO) depletion and possible fish mortality. Nitrifying bacteria require 4.3mg of O₂ for every milligram of NH₃ converted into NO₃⁻. Dissolved oxygen levels vary between in 8-10mg/l in water and living organisms need at least 5mg/l (Jorgensen, 2002). Therefore, biological nitrification may cause oxygen depletion below acceptable levels. The nitrification reaction also produces H⁺ ions, which may cause a pH drop if the alkalinity of the water is not sufficient. High concentrations of nitrite and nitrate (>10mg/l-N) in drinking water cause methemoglobinemia in babies (blue baby syndrome) and furthers the formation of carcinogenic nitrosamines (Wiesmann, 1994). Nitrification in the receiving waters can cause biological problems as well by increasing the number of nitrifying bacteria;
- ammonia can fertilise a water course and cause eutrophication (growth of algae and weeds) which leads to serious water quality problems, such as unaacceptable taste and odour, and DO depletion. The recreational potential

and value in such situations will be much reduced (Tchobanoglous and Schroeder, 1985).

The guide levels for ammonia released into the receiving water vary in different parts of the world. The Environmental Protection Agency (USEPA) and the American Committee on Water Quality Criteria recommend a value of below 0.02mg/l N-NH₃ (Jorgensen, 2002; Dryden, 1984). The Council of the European Communities suggests a guide level of 0.05mg/l N-NH₃, with a maximum value of 0.5mg/l N-NH₃ (Woods, 1997). New Zealand standards for wastewater vary between 0.22 and 0.7mg/l N-NH₃ (Nguyen and Tanner, 1998).

1.3.3 Removal of ammonia

1.3.3.1 Biological removal

The classical solution to the problem of ammonia removal is nitrification, which is a component of biological waste treatment. It was already mentioned in Section 1.1.3 that secondary wastewater treatment usually will remove 10-25% of total nitrogen. This is most commonly achieved by applying an activated sludge process in which organic compounds containing carbon, nitrogen and phosphorus are broken down by different bacterial species into simple forms, leading to the production of more bacteria. After sedimentation, some of the cells are returned to the process so that a strong and active bacteria stream is always present in the reactor.

The other way to reduce ammoniacal nitrogen by up to 90% during secondary treatment is using a process which promotes nitrification by using fixed bacteria films. This can be a modified activated sludge process or an attached growth systems, such as a set of trickling filters (TF) or rotating biological contactors (RBC).

A Modified activated sludge process involves introduction of some anaerobic zones. The main result should be improved growth of nitrifying bacteria after carbon level was reduced and encouraging nitrifiers growth in the presence of

autotrophic, carbon oxidising organism which growth rate is ten times higher (Tchobanoglous and Schroeder, 1985).

Attached growth systems (TF or RBC) have an increased surface area available for bacteria growth. It has been proved in many circumstances that nitrifying organisms prefer being attached to a solid surface rather than swimming freely (Weatherley and McVeigh, 2000). The biofilms grow on packing (usually gravel, stone or some plastic material) and consume nutrients, including ammonia, from the passing solution.

Unfortunately, quite often biological systems are not reliable enough. Problems with biological ammonia removal include:

- the sensitivity of nitrifying bacteria to toxic shock which may be caused by sudden change in ammonia concentration or some compounds present in the wastewater;
- pH sensitivity;
- low dissolved oxygen concentration;
- low temperatures.

1.3.3.2 Ion exchange removal

An alternative to biological treatment is the physiochemical process of ion-exchange. The main principles of ion exchange are given in Section 1.4. The drawbacks of using ion-exchangers for ammonia removal are the following:

- the exchanger or adsorbent quickly becomes saturated with ammonia and chemical regeneration can prove expensive;
- when the ammonia concentration in the influent drops, desorption may occur from the adsorbent resulting in ammonia being discharged into the effluent.

When a biological process is combined with ion exchange some improvements may be obtained:

- the ion-exchanger responds to loading ammonia peaks;
- at low ammonia levels nitrifying bacteria serve to oxidise the desorbed ammonia;
- nitrifiers serve to extend the ion-exchanger's usage which results in less frequent regeneration;
- the ion-exchanger can serve as a solid surface to which bacteria can be attached, since it has been mentioned that nitrifying organisms prefer being attached to a solid surface.

1.3.3.3 Other methods for ammonia removal

Air stripping is a physical method which might be used at high pH values (10.8-11.5). Wastewater is trickled down through a packed bed while air is blown counter-currently, stripping the ammonia from the solution. The method is usually not economic for low ammonia concentrations of 25-60mg/l N-NH₃, usually found in sewage (Booker et al., 1996).

Break point chlorination is a process which might be used. Here high concentrations of active chlorine (hypochlorite, hypochlorous acid, and molecular chlorine), are used to completely oxidize ammonia to molecular nitrogen, with the active chlorine simultaneously reduced to chloride. The process is effective but has some drawbacks (Dryden, 1984): pH control is required; free chlorine produced during the treatment has to be removed since it is toxic to fish and toxic chlorinated hydrocarbons may be produced.

Ozonation converts ammonia to nitrates, but the rate of this reaction is very slow (Tanaka and Matsumura, 2003) and the cost of ozone regeneration makes the process expensive.

1.4 Ion-exchange

Ion-exchange is a phenomenon that can be described as an exchange of ions between a solid phase and a solution. Conventional ion-exchange materials are insoluble solids with a charged framework and mobile ions which neutralise the charge. In most cases, the crosslinked structure of the ion exchange material prevents them from dissolving either in water or in some other solvents. Ions are held to the charged functional groups on the surface of the material by electrostatic forces. Therefore, the strength of the bond varies in a way similar to the dissociation of weak and strong electrolytes. If the framework of the materials carries the negative charge then cations are available for exchange and the material is called cation exchanger while the carriers of the exchangeable anions are called anion exchangers; as given in equations 1.14 and 1.15.



where:

- X - insoluble matrix with negative charge
- Na^+ , NH_4^+ - counter ions
- Cl^- - co-ion



where:

- Y- insoluble matrix with positive charge
- OH^- , Cl^- - counter ions
- Na^+ - co-ion

Materials capable of both cation and anion exchange, depending on the conditions and ions present in the surrounding solution, are called amphoteric ion exchangers.

Ion-exchange is a stoichiometric process, which means that every ion removed from the solution has to be replaced by the ion or the group of ions with the same

amount of charge. All the time during the process the overall charge in the ion exchange matrix as well as in the surrounding solution has to be zero.

According to the origin and the structure, ion-exchange materials can be divided into:

- mineral ion exchange materials;
- synthetic inorganic ion exchange materials;
- ion-exchange resins
- ion-exchange coals and
- liquid ion exchangers (Helfferich, 1962).

Mineral ion exchangers are typically aluminium silicate materials with cation or anion exchange capabilities. Probably the best known and the most abundant representatives of this group of materials are zeolites. More about zeolites' structure will be given in Section 1.4.6. At the beginning of their production, *synthetic inorganic ion exchange materials* first were an attempt to make crystals similar to the natural zeolites. Nowadays, modern techniques enabled the production of materials which are a copy of the natural materials; however, their ion-exchange abilities are not of the major interest any more. Since the pore size can be adjusted to a certain degree during the synthesis, they serve as "molecular sieves" which can capture molecules smaller than the openings in the crystal framework (Christie et al., 2002). Some of the most common zeolites are analcite, chabazite, erionite, clinoptilolite, heulandite, laumontite and mordenite.

Ion-exchange resins are probably the most commercially used group of the ion-exchange materials. Hydrocarbon chains form a three-dimensional network (matrix) with cationic and anionic groups built in. The hydrophobic matrix makes them insoluble in water. Most of the properties of these materials depend on the structure and the degree of the crosslinking of the matrix as well as the nature and number of the fixed ionic groups.

Ion-exchange coals are natural coals with ion-exchange properties. Many forms of coal exhibit ion exchange behaviours (Helfferrich, 1962). However, they swell in the solution and are very sensitive to alkali influent, and so called “stabilization” is necessary before use.

Liquid ion exchangers have changed conventional opinion that ion-exchange materials must be insoluble solids. These materials are solutions of compounds with ionic groups in organic solvents such as kerosene, trichloroethylene, chloroform or xylene, which are not miscible with water.

1.4.1 Ion exchange equilibrium

Ion exchange is a reversible process and the system will reach equilibrium after a certain amount of time. The equilibrium stage can be characterized by the distribution of different counter ions between the ion exchanger and the solution. The aim of establishing different equilibria laws is to predict the behaviour of the ion exchanger.

Ion exchange equilibrium models have two main approaches:

- simple adsorption models and
- models that involve mass action.

Simple adsorption models describe ion-exchange equilibrium by isotherms. Ion-exchange isotherms usually represent distribution of the ion species of interest between the solid and the liquid phase.

The Langmuir and Freundlich adsorption isotherms are commonly used to follow the adsorption of variety of cations onto zeolites (Zhaohui, 1999). The study of the isotherms was out of the scope of this study. The Langmuir adsorption isotherm relates the liquid phase concentration to the solid phase concentration as shown in Equation 2.16.

$$Q_e = \frac{KbC_e}{1 + K C_e} ; \quad \frac{1}{Q_e} = \frac{1}{KbC_e} + \frac{1}{b} \quad (1.16)$$

- where:
- Q_e - concentration of adsorbate on the adsorbent (mg/g),
 - C_e - adsorbate liquid concentration (mg/l),
 - K - Langmuir constant (l/mg)
 - b - Langmuir adsorption capacity constant (mg/g).

When applying this adsorption model one assumes that:

- adsorption surface is homogeneous (all sites are equally available for adsorption);
- the adsorbate forms only one layer on the adsorbent surface (Langmuir, 1918).

If we assume that the adsorbent surface is heterogeneous then Freundlich equation could be used³ (Freundlich, 1907):

$$Q_e = kC_e^{1/n} ; \quad \log Q_e = \log k + 1/n \log C_e \quad (1.17)$$

- where:
- Q_e - concentration of adsorbate on the adsorbent (mg/g),
 - C_e - adsorbate liquid concentration (mg/l),
 - k - parameter in the Freundlich equation (l/g),
 - n - parameter in the Freundlich equation.

1.4.2 Ion exchange capacity

Capacity is one of the ion exchanger parameters used for material characterisation as well as process design calculations. According to the literature (Helfferich, 1962), there are a couple of capacity definitions:

³ In the whole work the expression *log* refers to *log₁₀*

Maximum capacity is the number of counter ions per specified amount of ion exchanger. *Sorption capacity* is the amount of solute taken by sorption instead of ion exchange. The *breakthrough capacity* is the value obtained in column experiments when capacity is calculated in the point when the breakthrough of the column starts.

The most common way of expressing capacity is the amount of ions taken up per milligram of ion exchanger. The amount of ions is expressed in milliequivalents (meq) to allow comparison of the uptake of the ions with different charges. Dependence of the mass concentration and milliequivalents is given in Appendix I.

A zeolite's capacity depends on the Si:Al ratio. The charge imbalance is greater if more aluminium is present which means that more cations are needed to neutralise the negative charge. Capacity also depends on the purity of the material, the ionic form in which material is present, pretreatment, particle size, storage conditions, competing cations and experimental procedure. Therefore, when reporting capacity data all experimental conditions should be reported for better comparison. Capacity is usually calculated on the basis of dry material which in the case of zeolites is not completely true since zeolites have water incorporated in their framework and dry material will still be hydrated (Knowlton and White, 1981). The amount of hydrated water varies between samples mined from the different sites, which gives an unequal number of ion exchange sites in the same mass of the material.

All mentioned factors that affect capacity data are reasons for the variety of data reported for zeolites' capacity which are given in Section 2.2.2.

1.4.3 Ion exchange selectivity

Preference for removal of one ion from the solution of mixed ions is called selectivity of the ion exchanger. Selectivity is an important parameter in terms of process efficiency and cost. Parameters that control selectivity among ion exchange materials are quite complex. Dryden (1984) gave the list of parameters

which are associated with selectivity of zeolites when exchanging cations. These are:

- cation charge;
- size of the ion;
- electrolyte concentration in the aqueous phase;
- cation hydration energy;
- zeolite or exchanger structure e.g. degree of crosslinking and
- heterogeneity.

Zeolites with a high Si/Al ratio and high water content will have affinity for cations with a large radius and low hydration energy. Table 1.2 gives data for zeolites used in this research (clinoptilolite and mordenite) with the heulandite, next in order of Si/Al ratio. High Si/Al ratio values show that both materials will favour ammonium ion for exchange.

Table 1.2 The Si/Al ration and water content of some natural zeolites (Dryden, 1984)

	Si/Al ratio	Water content (%)
Clinoptilolite	10.8	14
Mordenite	10	
Heulandite	5.6	

Natural zeolites have sieve properties due to their channel structure with uniform pore size. This means that cations larger than the pore radius will be excluded from the exchanger. However, most of the monovalent and polyvalent cations, including ammonium ion, have a radius small enough to enter the zeolite's framework. Some cations may pass the critical size for entering the pores when hydrated. In this case, the cation will be exchanged if the lattice forces of the zeolite are stronger than the hydration energy of the molecule (Helfferich, 1962).

When aqueous ion concentration is decreased zeolites become more selective for polyvalent cations (Dryden, 1984).

1.4.4 Ion exchange regeneration

1.4.4.1 Chemical regeneration

After a certain amount of solution has been passed through the packed bed of ion exchanger, all sites available for exchange become saturated. Regeneration is usually the most expensive part of the ion exchange process (Muraviev and Khamizov, 2004). In the process of ammonia removal, regeneration is usually done chemically with NaCl and NaOH solutions (Jorgensen, 2002). This so called alkaline regeneration has been used in this work.

Sodium chloride is a source of cations which will replace ammonium ion in occupied sites and high pH value will transform greater fraction of total ammonia in unionized form. The disappearance of ammonium ions from solution will shift the equilibrium towards releasing more ammonium ions from ion exchanger sites. Furthermore, unionized molecules will not be held by the negatively charged ion exchanger framework and this will enhance the regeneration process.

However, some literature data indicate that exposing zeolites to NaOH solution could cause mass losses (Section 2.2.2). The amount of water for washing will also increase when a high pH is applied, to lower the pH and to dilute the regeneration effluent which will have high salt concentration. Ammonia from the regeneration solution can cause environmental problems.

To reduce costs of regeneration, the solution can be reused after released ammonia has been removed. However, the calcium concentration of the regeneration solution increases after each run. Since calcium reduces zeolite capacity by 50% (Dryden, 1984) it should be removed together with ammonia before reusing the solution.

1.4.4.2 Biological regeneration

Biological regeneration of saturated ion exchanger is based on nitrification, described in Section 1.2.3. It can be performed as a separate process, when

bacteria are introduced into ammonium rich spent regenerant after chemical regeneration is finished (Semmens et al., 1977a, 1977b, Semmens and Porter, 1979). Once nitrification is established, a bacteria rich suspension could be introduced into the exhausted bed to improve the regeneration process.

1.4.4.3 Thermal regeneration

Thermal regeneration is a method suitable for zeolites and not for polymeric ion exchange materials. The method is based on heating the material to high temperatures (300-600°C) when all NH_4^+ adsorbed by the material is replaced by H^+ ions by releasing NH_3 molecules at applied temperatures (Tsitsishvili et al., 1992). The method is not completely effective since other cations, like Ca^{2+} , Mg^{2+} and K^+ are not displaced.

1.4.5 Kinetics of the ion exchange

Knowledge of the kinetics of the ion exchange is important for process design since number of process parameters are influenced by the rate of the removal of ions from solution to the solid phase. A slower exchange rate will require a longer contact time to achieve maximum breakthrough capacity and vice versa. A better contact can be obtained by reducing either particle size of the material or flow rate of the feeding solution. Knowing process kinetics and diffusion parameters will enable the optimisation of the process in the best possible way. The ion exchange process could be described as occurring in three stages:

- diffusion of the counter ions through the bulk solution to the edge of the boundary layer film surrounding the ion-exchange particle;
- diffusion of counter ions through the boundary layer film (film diffusion);
- internal diffusion of the counter ions within the ion exchanger particle (particle diffusion).

In the bulk solution, significant agitation can balance any concentration differences (Helfferich, 1962), and therefore, in a well stirred batch system the kinetics of ion-exchange are largely determined by liquid film diffusion in the

vicinity of the solid/liquid interface and/or by particle diffusion inside the particle. If particle diffusion is rate controlling then exchange flux is:

- proportional to concentration of fixed charges and interdiffusion coefficient in the particle;
- inversely proportional to particle radius and
- independent of the film thickness, solution concentration and diffusion coefficient in the film.

If however, film diffusion is the rate limiting step then flux is:

- proportional to solution concentration and interdiffusion coefficient;
- inversely proportional to film thickness and
- independent of fixed charged concentration, interdiffusion coefficient in the particle and particle radius.

1.4.5.1 Modelling of the ion exchange kinetics

Two theoretical models from the literature are reviewed briefly. The first one is the *External Mass Transfer Model* introduced by Furasawa and Smith (1973) and applied to many systems in order to model adsorption processes. Since adsorption isotherms describe many ion exchange equilibria with good accuracy, we expected that this model could also be applicable to our system since it uses parameters from the Langmuir adsorption isotherm. On the assumption that good mixing provided uniform ammonia concentration through the vessel, Furasawa and Smith correlated the external mass transfer coefficient with the change in liquid phase concentration with time, according to the following expression:

$$\ln \left[\frac{C_t}{C_0} - \frac{1}{1 + m_s K} \right] = \ln \left[\frac{m_s K}{1 + m_s K} \right] + \left[\frac{-1 + m_s K}{m_s K} k_f S_s t \right] \quad (1.18)$$

$$m_s = \frac{M}{V} \quad \text{and} \quad S_s = \frac{6m_s}{d_p \rho_p} \quad (1.19)$$

where: - d_p - particle diameter (cm)

- K - Langmuir constant (l/g)

- k_f - mass transfer coefficient between liquid and outer surface of particles (m/s)

- M - mass of ion exchanger (g)

- m_s - concentration of particle in the free liquid (g/l)

- S_s - specific surface area available for mass transfer (cm^{-1})

- t - time (s)

- V - volume of the particle free liquid (cm^3)

- ρ_p - particle true density (g/cm^3)

- C_0 - initial solute concentration (mg/l)

- C_t - liquid phase concentration at time t (mg/l)

Equation 1.18 assumes that most of the diffusional resistance lies in the liquid phase surrounding the particles. For values of t close to zero, the plot of the left side of the equation versus time will yield a straight line and hence the value for k_f can be obtained from the slope of the graph.

The second model tested assumes that most of the diffusional resistance lies in the solid phase and is based on Fick's law (Equation 1.20). This approach and the method of application has been successfully adopted for adsorption processes (McKay et al., 1983).

$$\frac{\partial C}{\partial t} = D \frac{\partial^2 C}{\partial X^2} \quad (1.20)$$

To apply the single resistance intraparticle diffusion model the following assumptions were made:

- solute concentration is uniform and equals zero in the particle at $t = 0$;
- diffusion is radial with no concentration variation in the angular direction;

- the external mass transfer resistance is significant only in the early stages of the process and
- for ion-exchange, D is the intraparticle diffusion coefficient, based on the approach of Turner et al. (1965) and is a function of the self-diffusion coefficients of the exchanging counter ions.

To test the experimental rate data against the time we used the approach reported by McKay et al. (1983). He described the internal diffusion in the particle by an internal diffusion parameter, k_d . Under particle diffusion control led conditions the value of k_d should reflect the actual diffusion coefficient and could be determined by fitting each set of rate data as solid phase concentration versus time to Equation 1.21, extracting k_d from the slope:

$$k_d = \frac{1}{t^{0.5}} Q_t \quad (1.21)$$

where:

- Q_t - solid phase concentration at the particle (mg/g)
- k_d - mass transfer coefficient within the particle (mg/gmin^{0.5})
- t - time (min)

1.4.6 Natural zeolites

Since the first massive deposits of zeolites were discovered in the 1950s in the U.S.A. (Sherman, 1978), more than forty countries reported new findings (Mumpton, 1976). Details of New Zealand deposits are presented in Figure 1.7.

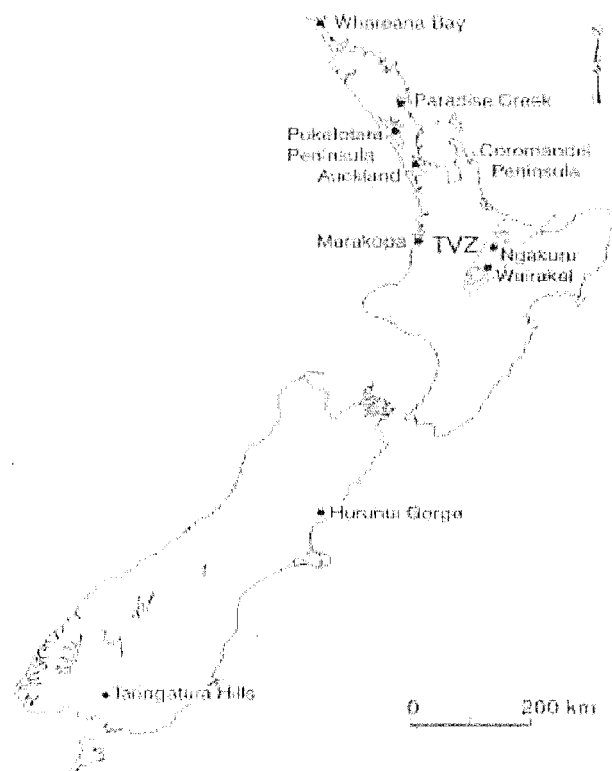


Figure 1.7 New Zealand zeolite deposits (Christie et al, 2002)

Zeolites are hydrated aluminosilicates which possess a three dimensional framework structure. This structure is formed by AlO_4 and SiO_4 tetrahedra which are connected by sharing oxygen atoms and water molecules occupying open cavities. Dehydration is reversible and mostly occurs at temperatures below 400°C (Bish and Ming, 2001). The zeolites' crystal framework remains stable after dehydration with uniform molecular-sized channels which makes them natural molecular sieves. The tetrahedral building block theoretically can be combined into infinitely different framework structures. However, around 40 are found in nature and some of the zeolitic structures are given in Figure 1.8.

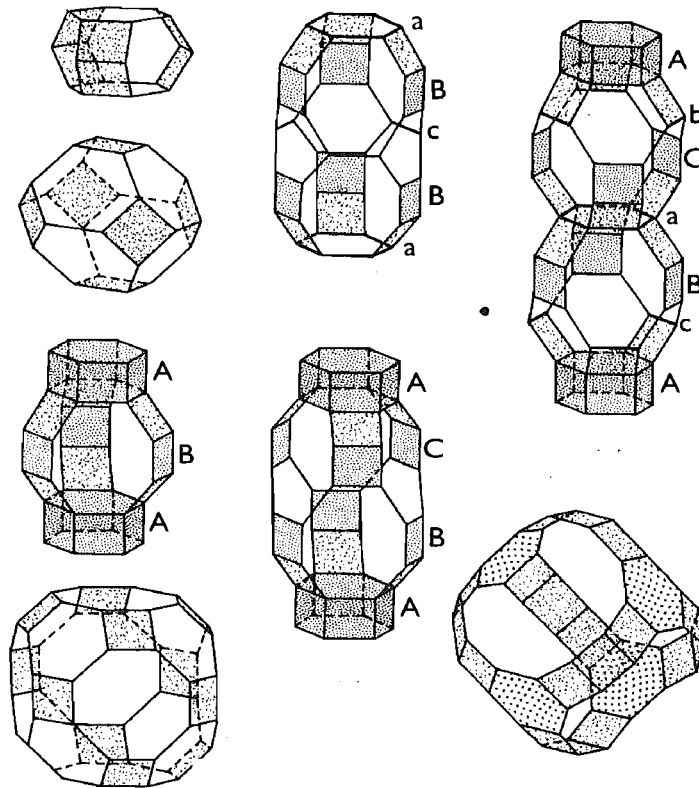


Figure 1.8 Some of the zeolitic structures (Tsitsishvili et al., 1992)

The replacement of quadrivalent silicon by trivalent aluminium creates a negative charge that has to be balanced by exchangeable cations, mainly Na^+ , K^+ , Ca^{++} and Mg^{++} . The compositions of exchangeable cations in clinoptilolite and mordenite are given in Figure 1.9.

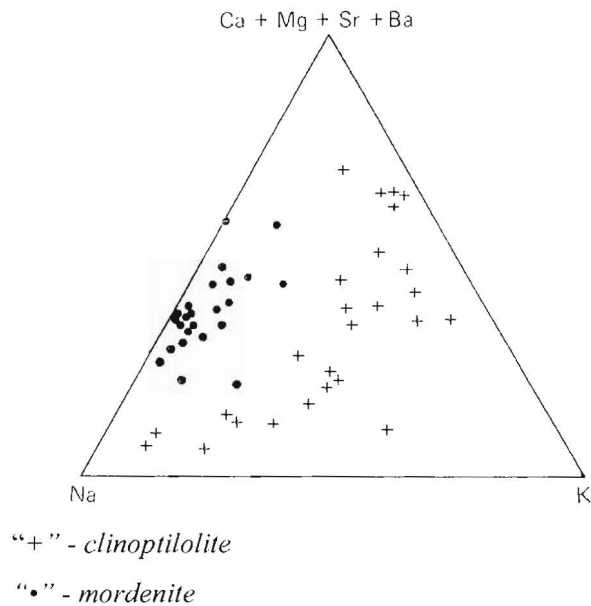


Figure 1.9 Distribution of exchangeable cations in mordenite and clinoptilolite (Tsitsishvili et al, 1992)

Zeolites are soft but abrasive materials and undergo partial decomposition in acidic or basic solution. Their usage is therefore limited to a quite narrow pH range around neutral value. Clinoptilolite and mordenite belong to a group of silica rich natural zeolites. Therefore, they have a lower capacity than other zeolites (see Section 1.4), but are more stable in solution at lower pH value compared with aluminium rich zeolites.

Natural zeolites are coarse sandy like materials with clinoptilolite being more brittle than mordenite. Photographs of both materials are shown below.

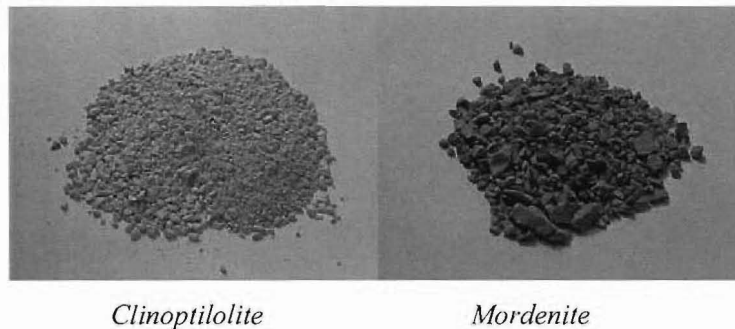


Figure 1.10 Natural zeolites

1.4.6.1 Clinoptilolite

Clinoptilolite is a silica rich member of the heulandite group of zeolites. This is probably the most widely distributed mineral in nature. According to Dryden (1984) at least three prerequisites have to be met for zeolite to be classified as a clinoptilolite:

- polymorphism should not be manifested;
- Si/Al ratio should be greater than four and
- $(\text{Na} + \text{K})/(\text{Ca} + \text{Mg} + \text{Sr} + \text{Ba})$ ratio should be greater than one.

The structure of clinoptilolite is given in Figure 1.11 while the molecular formula is $(\text{Na}, \text{K}, \text{Ca})_6(\text{Si}, \text{Al})_{36}\text{O}_{72} \cdot 20\text{H}_2\text{O}$ (Christie et al., 2002).

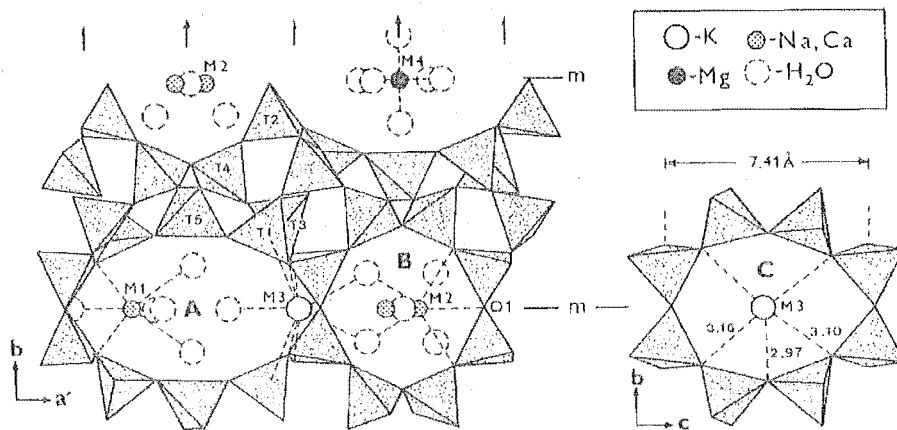


Figure 1.11 Structure of the clinoptilolite (Tsitsishvili et al., 1992)

The three dimensional channel system consists of ten and eight membered channels marked as *A*, *B* (parallel) and *C* (along). Sites M1 and M2 are occupied by calcium and sodium while potassium and magnesium occupy sites M3 and M4 respectively. Approximate channel sizes are: A: 4.4 x 7.2Å, B: 4.1 x 4.7Å and C: 4.0 x 5.5Å (Aguilar-Armenta et al., 2001).

1.4.6.2 Mordenite

Mordenite is another zeolite widely distributed in nature (Tsitsishvili, 1992). Large deposits of mordenite are present in the oceans and alkaline saline lakes. In contrast to clinoptilolite, the Si/Al ratio does not vary too much among mordenite from different deposits and is in the range 4.5-5.5. Figure 1.9 shows that exchangeable cation composition also varies less, compared to clinoptilolite.

Sodium and calcium are presented in higher amounts than magnesium and potassium. Mordenite's molecular formula is $\text{Na}_8(\text{Al}_8\text{Si}_{40}\text{O}_{96}) \cdot 24\text{H}_2\text{O}$ (Mumpton and Fishman, 1977) while the structure is given in the next figure.

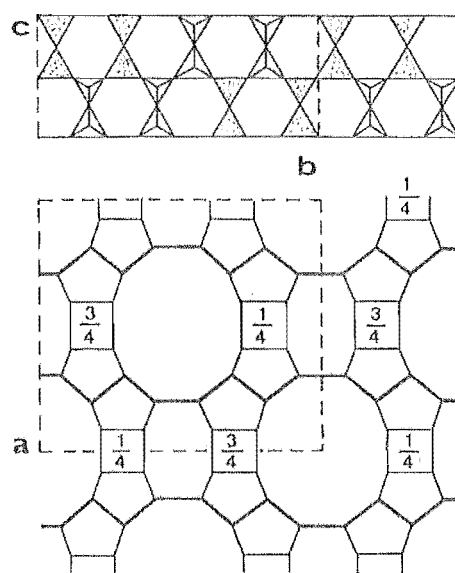


Figure 1.12 Structure of the mordenite (Tsitsishvili et al., 1992)

Aluminium and silicon tetrahedra are combined in a way such that twelve and compressed eight membered channels are formed along the c axis. Larger channels are often called main channels with reported sizes of $6.69 \times 7.05 \text{ \AA}$ while smaller channels have dimensions of $4.82 \times 3.97 \text{ \AA}$ (Webster et al., 1999) and are known as side pockets. Mordenite is capable of adsorption of the cations with a radius less than 0.42 nm in diameter (Tsitsihvili et al., 1992). Since the ionic

diameter of ammonium ion is 0.29nm (Dreyden, 1984), it can easily pass through the channels within the crystals.

1.4.7 Products of zeolitic nature

Products of a zeolitic nature have been developed by the Zeolite Research Group from the University of Cadiz, Spain (Lopez-Alcala et al., 1998). Among other materials, a Cuban natural zeolite mined in Tasajeras (Cuba) has been used as a base product which was modified to obtain products (Mg.NZ and ZZ), which were then applied for ammonia removal from saline water (Rodriguez-Fernandez et al., 2003). Major components of Cuban zeolite are: clinoptilolite (70%), amorphite (15%), quartz (10%) and mordenite (5%). In order to modify it, the base product was saturated with ammonium ion and heated to 450°C so that as many cations as possible were removed and zeolite in hydrogen form was obtained. Finally, the forms with Mg (Mg.NZ) or Zn (ZZ) were obtained by treatment with concentrated solution (0.6M) of Mg^{2+} or Zn^{2+} (Lopez-Alcala and Lopez-Ruiz, 2001).

Another base product was ceramic waste which was exposed to a strong alkaline medium at a temperature of 95°C for 8 hours in an open reactor with stirring. The final product was named Zecer 56 (Lopez-Alcala and Lopez-Ruiz, 2001). Chemical compositions of base products as well as the derived products are given in the Table 1.3 with a note that due to the variations in the zeolite's chemical composition, values for the composition of the final products will also vary. It was observed that the Si/Al ratio did not change much during the preparation procedure for ZZ since the initial and final product have values of 4.73 and 4.70 respectively. In the case of the Zecer 56, the Si/Al ratio increased from 5.6 in the initial product to the value of 6.21 in the final one.

Table 1.3 Chemical composition of base material and the derived products
(Lopez-Alcala et al., 1998)

	CaO	Fe ₂ O ₃	K ₂ O	Na ₂ O	MgO	SiO ₂	Al ₂ O ₃	ZnO	Si/Al
Cuban zeolite	3.32	1.82	1.12	1.45	0.71	63.27	11.78		4.73
ZZ	1.57	1.97	1.28	1.06	0.23	65.12	12.21	2.66	4.70
Ceramic residues		0.3				54.0	8.5		5.60
Zecer 56		0.2				52.2	7.4		6.21

Photographs of used PZN are given in the next figure.

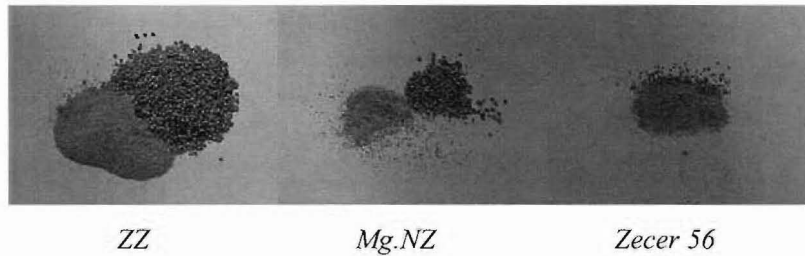


Figure 1.13 Products of zeolitic nature

1.4.8 Synthetic ion exchanger, Purolite MN 500

Purolite MN 500 is a macronet, a new generation of synthetic ion exchangers which have styrene as a base building unit. Their hypercrosslinked structure was discovered by Davankov and Tsyurupa in 1969 while commercial development was done by the Purolite company in 1993 (Street and Sweetland, 1997). Due to the very high internal surface area in the range 800-1100m²/g (Jorgensen, 2002), macronets are used mainly for adsorption. However, purolite MN 500 has the capacity to function like an ion exchanger too (Dale et al., 2000). The possession of sulphonic acid groups places MN 500 as a strong acid cation exchanger. Like other macronets, MN 500 contains macropores (800-950Å), which enable faster diffusion through the bead, as well as micropores (15 Å) so that the high surface area and high capacity can also be observed. A photograph of the MN 500 is shown in Figure 1.14.



Figure 1.14 Macronet, MN 500

1.5 Bacteria adhesion

The formation of a biofilm on the surface happens as a result of a number of physical, chemical and biological processes occurring simultaneously. Those are: cell and particle transport to the surface, cell adhesion, biofilm growth by cell multiplication and extracellular products formation, biofilm detachment and substrate and product transport to and from the biofilm (Picioreanu et al., 2000). The adhesion of the bacteria to the surface depends on the characteristics of bacteria and the surface, as well as on the parameters of the surrounding environment (Richardson et al., 2000). However, all the factors mentioned could be expressed through the charge and hydrophobicity properties of the two surfaces involved: the bacterial surface and the surface of the immobilising medium respectively. Therefore, it is likely that any coating of the surfaces will have impact onto bacteria adhesion. The charge and hydrophobicity of the surface can be quantified by the double layer theory and surface free energy. Specific surface area could be important but only in the case when the diameter of the pores is big enough to host the bacteria. Bacteria adhesion is reversible and Rijnaarts et al. (1995) reported that the reversibility could be controlled by the ionic strength adjustment.

1.6 Saline water

Salinity is one of the water parameters which can have a significant influent on the type of the organisms present in the water body. According to *Wikipedia* (2004), water is classified as saline if the content of salt is 3-5% salt by volume. Salinity of most lakes and rivers is less than 0.05% which defines them as fresh or

sweet water. Traditionally, salinity is expressed in parts per thousand (‰ or ppt), which means grams of salt per litre of water. The next table gives classification of saline waters according to the salt level.

Table 1.4 Water classification based on salt level (*Wikipedia*, 2004)

Salinity range (‰)	Type of water
36-40	Metahaline seas
30-35	Euhaline seas
0.5-29	Brackish seas

2 Literature review

2.1 Nitrification

Nitrification is a biological process that requires certain conditions. The growth rates of bacteria depend on:

- substrate ammonia concentration;
- temperature;
- pH;
- oxygen concentration;
- microbial composition of the growing environment;
- chemicals other than ammonia present in the solution;
- surface available for bacteria growth.

In most cases researchers agree that nitrification kinetics can be described by using the Monod equation (Equation 2.1), explained in the Section 1.2.3.1 of this work (Metcalf and Eddy, 1979; USEPA, 1993).

$$\mu = \frac{\mu_{\max} S}{K_s + S} \quad (2.1)$$

where:

- μ_{\max} – maximum growth rate constant (t^{-1});
- S – concentration of limiting food in substrate;
- K_s – half saturation constant and concentration of limiting food when $\mu = 0.5\mu_{\max}$, (mg/l).

However, Rozich and Castens (1986) argued that due to the substrate inhibition (Section 2.1.1) the Monod equation does not model ammonia removal rates. They suggested using the Haldane equation instead:

$$\mu = \frac{\mu_{\max} S}{K_s + S + \frac{S^2}{K_i}} \quad (2.2)$$

where: - K_i – inhibition constant (mg/l).

According to this model, there is a reduction in the nitrification rate after the peak is reached due to high ammonia concentrations.

The selection of the appropriate model for a specific system should be based on the initial ammonia concentration which can cause substrate inhibition (Section 2.1.1).

2.1.1 Substrate ammonia concentration

Literature conclusions about substrate inhibition of nitrification are quite different. It is likely that free ammonia rather than ammonium ion is the substrate for *Nitrosomonas* (Groeneweg et al., 1994). Free ammonia concentrations can have an inhibitory effect on *Nitrosomonas* growth if greater than 8mg/l. Surmacz-Gorska et al. (1997) reported that free ammonia in the concentration range of 1-6 mg/l inhibited *Nitrobacter* function and also led to shorter nitrification and build up of nitrites while Mauret et al. (1996) noticed the same behaviour but in the range of 6.6-8.9mg/l N-NH₃. Chudoba et al. (1976) reported inhibitory effects of ammonium ion above concentrations of 2mg/l, whereas McVeigh (1999) employed ammonium inlet concentrations of 30mg/l N-NH₄⁺ without any inhibitory effect reported and neither did Tanaka and Dunn (1982) when using extreme concentrations of 200mg/l N-NH₄⁺. However, excess ammonia has been used to inhibit nitrification in the BOD test (Siddigi et al., 1967). Ammonium chloride was applied at the extremely high concentration of 1400mg/l N-NH₄⁺ to completely suppress nitrification in the 5 and 20 day BOD tests. Ford and Churchwell (1980) stated that total ammonia concentrations above 70mg/l are not only inhibitory but also toxic to nitrifying bacteria since the system is not able to recover even when the concentration is reduced to an acceptable level. On the other hand, nutrient deprivation was not fatal to the bacteria which were able to operate at 70% of initial capacity within 48 hours of ammonia reintroduction. This

was observed after a period of 8 days without ammonia present in feeding solution (Bower and Turner, 1983).

Research about the nitrification on clinoptilolite indicate that the process can be inhibited by the retention of NH_4^+ on the sites where the nitrifying bacteria can not reach it (Weber et al., 1983) if the initial ammonia concentration is not high enough.

After summarising all available literature data, we chose to apply a maximum inlet ammonia concentration of 40mg/l N- NH_4^+ with a maximum pH of 7.5 to avoid high free ammonia concentrations. Since no inhibition was expected the Monod equation was chosen to model bacteria growth.

2.1.2 pH role in nitrification process

At the ammonia concentrations usually found in waste water, the optimal pH is more important for the nitrification process than the initial ammonia concentration. Even though it is more likely that free ammonia rather than ammonium ion is the key substrate for *Nitrosomonas*, nitrification is a process that prefers slightly, alkaline conditions. During *Nitrosomonas* activity hydrogen ion is constantly produced (Equation 1.2). The hydrogen ion produced will be neutralized by bicarbonate ions according to the following equation:



A combination of the carbon dioxide which is produced during the reaction and the reduction in bicarbonate concentration, will result in a decrease of pH. The theoretical value of required alkalinity based on Equation 2.3 is approximately 7.13mg of bicarbonate expressed as the CaCO_3 equivalent for 1mg N- NH_3 oxidized (Haug and McCarty, 1972). Sherrad (1976) argues that this value is not correct and that required alkalinity is determined by influent and effluent bacteria concentration, the amount of organic chemicals and concentration of nitrogen and phosphorus. Mauret et al. (1996) found that the pH increase from 7-8.5 increased

nitrification by 24%. A further pH increase led to process inhibition probably due to high free ammonia concentrations which inhibited *Nitrobacter* growth. Groneweg et al (1994) obtained best ammonia oxidation when the pH was between 7.5 and 8 with some bacterial activity up to a pH value of 11. This finding indicates that nitrifying bacteria are able to survive during a relatively short period of increased pH in the system but do not have ability to adjust to live in such conditions for extended periods. Adam and Eckenfelder (1977) reported an optimum pH range for nitrification of 7.8-8.3 and it was observed that bacteria had the ability to adapt to even lower pH values. This ability is also indicated by work of Odell et al. (1996) who observed nitrification at pH 6.6. Since many other factors contribute to bacteria activity, nitrification has been observed across a wide pH range. However, best results were usually obtained around the value of 7.5.

In many cases the required alkalinity could be achieved by adding potassium chloride (Gross et al. 2003) sodium bicarbonate (McVeigh, 1999) or sodium carbonate (Woods, 1997). Adams and Eckenfelder (1977) recommended using sodium hydroxide or potassium hydroxide for high and low-strength ammonia wastewaters respectively. In the current work, sodium bicarbonate was used to maintain desired pH values.

2.1.3 Temperature effect on nitrification

Since nitrification is a process driven by mesophilic bacteria, temperature plays an important role in the process. Together with pH, temperature control has a higher impact on process efficiency than initial ammonia concentration (Woods, 1997). Low temperature, which slows down the bacteria metabolism is one of the major causes for water treatment plants to fail in terms of ammonia removal. Even drinking water treatment plants may encounter problems if incoming water is exposed to temperature change. Low nitrification rates in streams during the winter can cause an increase in ammonia inlet concentration from 0.05mg/l during summer to 4.2mg/l during cold months which puts higher demands on plant design (Uhl and Gimbel, 2000). Apart from physiological effects, higher

temperatures will also improve nitrification by shifting the equilibrium between the two ammoniacal nitrogen forms towards the unionised form (Figure 1.6), since it is more likely that NH_3 , rather than NH_4^+ is *Nitrosomonas* substrate. Adams and Eckenfelder (1977) suggest that the optimum temperature range is 28-32°C with nitrification significantly reduced at temperatures below 12°C and suppressed at values below 5°C.

Groeneweg et al. (1994) reported the importance of temperature preadaptation of nitrifiers. For bacteria cultivated at 20°C and 30°C they obtained a linear relationship between the ammonia oxidation rate and the temperature in the temperature range of 10-20°C and 10-30°C respectively. This indicates that maintaining the temperature during the process is as important for process efficiency as choosing the optimum range.

2.1.4 Oxygen concentration

According to metabolic activity, nitrification bacteria are aerobic organisms, which means that oxygen is the source of electrons in their metabolic processes. Again, the literature results vary in terms of recommended dissolved oxygen (DO) concentration for best nitrification results. The stoichiometric oxygen consumption to convert 1kg NH_4^+ to NO_3^- during the nitrification (based on Equations 1.2 and 1.3) is 4.57kg of oxygen per kg of oxidised N- NH_4^+ . Equations 1.5 and 1.6 indicate that some oxygen will be introduced into the process together with inorganic carbon which reduces pure oxygen requirements to the value of 4.26kg O_2 (Bryant et al., 1996). Most of this oxygen is utilized in the first step of the process (ammonia oxidation to nitrite); approximately 3.2g of oxygen is consumed by *Nitrosomonas*. Adams and Eckenfelder (1977) argue that oxygen requirements might be even lower due to the use of ammonia for cellular synthesis as well as due to losses caused by air stripping at higher pH values (pH =8) usually applied in the nitrification process. They suggest a reduced value for oxygen requirements from 4.57kg to 3.90kg of oxygen per kg of oxidised N- NH_4^+ . On the other hand, Ng et al. (1996) reported that oxygen consumption in their reactor was higher than the predicted value of 4.6 kg. This was before maximum

efficiency was established. They attribute this finding to the initial lower ammonia loadings and therefore DO was used for cell maintenance activities instead of chemical ammonia oxidation.

According to USEPA recommendations nitrification can be limited if dissolved oxygen (DO) concentration is within the range of 0.5-2.5mg/l (USEPA, 2000). When dissolved oxygen concentration drops below 1mg/l, de-nitrification can occur due to the anoxic conditions. Semmens et al. (1997a) found that the nitrification rate was unaffected by the DO concentration only when the DO concentration was greater than 6mg/l. Below this value the reduction in rate was significant and reached only 33% of maximum effectiveness when the DO concentration was reduced to 2mg/l.

2.1.5 Role of the surface in the nitrification process

Nitrifying bacteria show a preference for surface attachment, colonising solid surfaces, rather than remaining in free suspension. This is proved for both fresh and marine environments (Haug and McCarty, 1972), as well as for nitrification in soil. The efficiency of nitrification in trickling filters is also proved to depend on filter media type (Lekang and Kleppe, 2000). According to the literature this can be due to either purely mechanical reasons when growth on the surface enables the formation of more stable biofilms, or due to the combined physiochemical processes which together improve bacteria growth. Fry (1955) reported that enhanced nitrification in the soil was obtained only when the added material had an ammonia adsorption ability as well. Increase of the surface area available for bacteria growth alone appeared to have little effect. This work also concluded that bacteria live on the surface of soil particles around sites which adsorb ammonia. When this area is saturated then further growth is dependent on death cell replacement. Vieira et al. (2001) reported that in the case of kaolin particles, nitrification was improved mostly due to the release of certain ions which served as nutrients for the bacteria. In their experiment, ammonia oxidation was enhanced to a greater degree by kaolin particles than in the case of nitrite oxidation. Vandevivere et al. (1998) immobilized Cu(0), Cu(I) and Cu(II) on

chelating resins which were added to a nitrifying reactor and the presence of these ions significantly reduced nitrification inhibition in industrial wastewater. Catalan-Sakairi et al. (1997) reported that oxygen diffusion plays a significant part in effectiveness of any particular growth medium. A four fold reduction in loading rate was observed when using cellulose instead of polyester carriers and this was attributed to limited oxygen diffusion.

There are several methods for microbial inoculation onto a solid surface. Entrapment microbial cell immobilization (EMCI) assumes the direct capture of the cells into the matrix of polymeric carriers (Yang et al., 1994). Most common are attachment methods where the support material is either soaked in a bacteria-rich solution or the solution is slowly pumped through the packed material allowing bacteria to colonise the surface of the particles.

2.1.6 Other influencing factors on nitrification

Biological nitrogen removal is the most common way to reduce nitrogen levels in municipal wastewater. The process is usually part of the secondary treatment in the form of an activated sludge process or some attached growth process (trickling filters or rotating biological contactors). Since municipal wastewater does not normally contain chemicals that can cause bacterial inhibition, control of ammonia inlet and organic carbon usually will prevent any failures if physical parameters are in an acceptable range. However, industrial wastewater is a mixture of different chemical elements and compounds each of which may have a different effect on the nitrification process. Since biological ammonia oxidation is a two stage process driven by a different group of micro organisms, the same elements or compounds may improve one process while inhibiting or having no influence on the other process. Hockenbury and Grady (1977) reported that dodecylamine, aniline and n-methylaniline inhibited *Nitrosomonas* activity by 50% when present in concentrations less than 1mg/l. At the same time no effect on nitrite oxidation was observed. Their research concluded that organics containing sulphur or nitrogen are usually inhibitory to nitrification. This is confirmed by Adams and Eckenfelder (1977) who also reported that thiourea

(which contains sulphur), together with heavy metals, cyanides, halogenated compounds, phenols, mercaptans and guanidines causes significant nitrification inhibition. Organic carbon present in the wastewater can enhance the growth of heterotrophic bacteria and suppress the nitrification process. Fdz-Polanco et al. (2000) reported that a nitrification reactor resisted organic carbon loading up to a value of 200mgCOD¹/l without losing 100% efficiency. Higher COD values severely inhibited the growth of nitrifying organisms. Some organics on the other hand, proved to improve the process. Semmens et al., (1977a) introduced bacteria rich regenerant solution into zeolite beds and concluded that humic acid and phenol not only did not inhibit nitrification but in fact promoted some improvement.

Much research has been done to find a way of reducing the inhibitory effect of organic chemicals on nitrification. Powdered Activated Carbon Treatment (PACT) involves the addition of activated carbon which will remove organics from the solution (Lankford et al., 1988; Kochany and Lugowski, 1998). A similar effect can be achieved using Fenton's reagent² (Kochany and Lugowski, 1998). In the case of nitrification in the activated sludge process, longer retention time (usually 40 days) may allow biodegradation of toxic organics by other bacteria populations present (Vandevivere et al., 1998).

Inorganic ions also can have a different influence on nitrification. Chromium (Cr³⁺) was found to reduce the maximum growth rate of nitrifying bacteria by 25-30% when present at a concentration of 3mg/l (Orhon et al., 2000). However, in the case of copper, initial addition was shown to increase nitrification but continued use led to inhibition (Barber and Stuckey, 2000). High ionic strength can also inhibit the growth of nitrifying bacteria which may cause problems,

¹ Chemical Oxygen Demand (COD) is defined as the amount of specified oxidant that reacts with a sample under controlled conditions. The quantity of oxygen consumed is expressed in terms of its oxygen equivalent: mg/L of O₂

² Fenton's Reagent is a solution of hydrogen peroxide and an iron catalyst that is used to oxidize mainly organic contaminants of wastewater.

particularly if the process is applied to ammonia removal in saline wastewater (Catalan-Sakairi et al., 1997). No literature data could be found about the effect of Ca^{2+} , Mg^{2+} or K^{+} ions on nitrification.

Product inhibition is another phenomenon which might occur during the biological ammonia oxidation. As explained in Section 1.2.3, nitrites are a product of *Nitrosomonas* activity and are first produced in the nitrification process. Some researchers reported a toxic effect of nitrites which are produced, on nitrification (Gross et al., 2003). Chen et al. (1988) suggested a safe level of 0.36mg/l NO_2^- in water. On the other hand, Anthoniesen et al. (1976) argue that unionized nitrous acid (HNO_2), rather than nitrites, causes *Nitrobacter* inhibition. To overcome the problem of nitrite inhibition it is important to achieve complete nitrification so that oxidation of ammonia to nitrates is obtained. Usually, high enough oxygen concentration will eliminate a problem of nitrite accumulation.

The optimum pH and temperature, discussed in Sections 2.1.2 and 2.1.3 respectively, are not the only physical parameters required for good biological activity within the reactor. Nitrifying bacteria are sensitive to UV, visual and fluorescent light, which means that nitrification tends to occur in the darker parts of the reactor (Wolfe and Lieu, 2001). Therefore, protection from light will improve process efficiency.

2.1.7 Nitrification in saline water

Nitrogen compounds that accumulate in seawater aquaria and waste disposal sites cause the same problems associated with this type of pollution of fresh water. Indirect threats to living organisms are algal growth and oxygen depletion while a high concentration of nitrogen compounds can be fatal to aquatic animals. The nitrogen cycle presented in Section 1.2 includes nitrification in oceans (Hovanec and DeLong, 1996) which has been used to establish nitrification filters in marine aquaria for ammonia removal. There is a general assumption that ammonia and nitrite biological oxidation in saline water is driven by the same bacterial species responsible for the nitrification in soil and fresh water that were explained in

Section 1.2.3. Shan and Obbard (2003) used a culture of nitrifying bacteria from saline water to successfully establish a nitrifying biofilter for fresh water treatment without allowing any time for bacteria to adapt to the non-saline medium while Gross et al. (2003) used a culture of enriched nitrifiers from soil to start filters for recirculating saline water aquaria. Since the same bacterial species carry out the process in both media, the optimum pH and temperature for the nitrification in the saline medium are in the range reported for the fresh water (Jones and Hood, 1980). However, the bacterial activity in the saline medium is found to be low due to free ammonia, nitrite ions and high ionic strength inhibition. Even though nitrification has been observed in the water with a salinity range from 2g/l (Gross et al., 2003) to 30g/l (Bower and Turner, 1983), reported values for growth yield in saline water are 0.06-0.1mg cells/mg N oxidized whereas it can go up to 0.20mg cells/mg N oxidized for fresh water media (Catalan-Sakairi et al., 1997). Dincer and Kargi (1999) carried out research into salt inhibition of nitrification and reported that above salt concentrations of 20g/l inhibition was significant. Slow growth may be one of the reasons that required alkalinity for nitrification in saline media is well below the theoretical value of 7.13mg of bicarbonate as CaCO_3 for 1mg N-NH_3 oxidized (Haug and McCarty, 1972). Catalan-Sakairi et al. (1997) reported a value of 4.6mg while Furukawa et al. (1993) obtained a value of 4.1mg of bicarbonate as CaCO_3 for 1mg N-NH_3 oxidized. Due to the high salt concentration in the saline media, sodium bicarbonate can be added up to maximum concentration of 5g/l without precipitation (Catalan-Sakairi et al., (1997). In wastewaters containing ammonia the following process occurs:



which increases the carbonate concentration in the solution, perhaps causing calcium and magnesium carbonate precipitation. Due to the restricted amount of applied bicarbonate for pH control, ammonium loading for saline media becomes restricted as well.

2.2 Ion Exchange

2.2.1 Removal of ammonia by ion exchange

Ion exchange, like many industrial physiochemical processes was introduced into industry in the middle of the last century. The removal of ammonia by ion exchange has received attention in the 1970s, since this was a time when awareness of pollution problems increased in the form of Clean Air Act and Clean Water Act (Section 1). Natural zeolites, such as clinoptilolite and mordenite, have been widely used since then as they are materials with a great affinity for ammonium ions (Booker et al., 1996; Dryden, 1984; Gurdeep and Prasad, 1997; Klieve and Semmens, 1980; McVeigh, 1999; Nguyen and Tanner, 1998). Polymeric macronet exchangers (Purolite) have been recently introduced as materials with a huge available surface area (Dale et al., 2000) and have been used in some research for ammonia removal (Jorgensen and Weatherley, 2003).

Ion exchange efficiency for ammonia removal depends on pH, since the NH_4^+ form is removed. Section 2.3 gives the distribution between two forms at different temperatures and pH values. Dryden (1984) gives pH values for different temperatures at which the amount of both forms in solution is equal. These are presented in the Table 2.1.

Table 2.1 pH values for equal distribution between ionized and unionized ammonia form on different temperatures (Dryden, 1984)

temperature (°C)	pH
5	9.90
10	9.73
15	9.56
20	9.40
25	9.25
30	9.09

At lower pH values than those given in the table, a more ionized form will be present in the solution and will be available for ion exchange at a given temperature. Figure 1.6 indicates that when the pH is less than 7.5 the fraction of the unionized form is lower than 0.01 regardless of the temperature. Sheng and

Chang (1996) highly recommended a pH value below 7 for ion exchange ammonia removal. Njoroge and Mwamachi (2004) investigated temperature influence on the ammonium ion adsorption rate. They found that ammonia adsorption onto zeolites is an endothermic process with 71.2% and 82.4% efficiency removal at the temperatures 14°C and 25°C respectively, for the 5mg/l initial ammonia concentration.

Due to the high cation concentration in brackish water and therefore the short ion exchanger running life before regenerations has to be performed, ion exchange alone is not suitable for ammonia removal from this environment.

2.2.2 Ion exchange capacity

In Section 1.4.2 it was pointed out that the ion exchange capacity is dependent on many factors. A great deal of research has been carried out on the uptake of ammonia onto clinoptilolite. There are also some data about the uptake capacity of mordenite, another natural zeolite used in this research. However, purolite is a new material and few data on capacity for ammonia removal are available.

Klieve and Semmens (1979) showed that capacity data for clinoptilolite vary with the different measurement techniques employed. Different experimental conditions can therefore be a reason for different literature data about ion exchange capacity. Natural zeolites often have a different capacity even when mined from the same deposit but from different locations in that deposit. A list of capacity data for clinoptilolite and mordenite obtained by different researchers is given in the Tables 2.2 and 2.3.

Table 2.2 Literature capacity data for clinoptilolite

Author	Capacity (meq NH_4^+ /g)
Ames (1967)	1.81
Skudder (1976)	2.1
Dryden (1987)*	2.16
Booker et al. (1996)*	1.5
Nguyen and Tanner (1998)	0.66
McVeigh (1999)*	1.76
Jorgensen and Weatherley (2001)*	1.61

* material was pretreated to obtain particles in sodium form

Table 2.3 Literature capacity data for mordenite

Author	Maximum CEC* (meq NH_4^+ /g)	Capacity (meq NH_4^+ /g)
Mumpton (1976)	2.29	
Tsitsishvili (1985)	1.36	
Klieve and Semmens (1980)		1.80
Nguyen and Tanner (1998)		0.59

*) Cation exchange capacity

Tables 2.2 and 2.3 show that ammonium capacity values lie in the range 0.66-2.16meq/g for clinoptilolite and 0.59-1.80meq/g for mordenite. Together with other factors, ion exchange capacity is also dependent on solution concentration of removed ions. The increase of the ammonium concentration in the feed solution from 14 to 70mg/l N-NH_4^+ increased the clinoptilolite capacity from 0.47 to 0.95meq NH_4^+ /g (Weatherley and McVeigh, 2000) due to the shift of the equilibrium between solid and liquid phase. Work by Singh and Prasad (1997) showed that the smaller the particle size of the zeolite the higher is the capacity due to the greater surface area available for ion exchange. They reduced particle size of synthetic zeolite from range 1-1.7mm to 0.5-1mm and improved capacity from 12.33mg NH_4^+ /g to 16.36mg NH_4^+ /g. Nguyen and Tanner (1998) obtained even better improvement. They increased breakthrough capacity 2 to 4 times by reducing the particle size from 2-2.83mm. The better uptake capacity for smaller particles obtained in the batch experiments could also be explained by structural modification that has occurred during comminution of larger particles to smaller,

which caused changes in access to available sites. The breakthrough capacity is influenced by the larger specific area of smaller particles, but also by lower liquid phase mass transfer coefficient of smaller particles due to the less free liquid volume. The mass transfer will affect the shape of the breakthrough curve and hence the overall breakthrough capacity. Pretreatment of ion exchangers might also have a significant influence on capacity data. While pretreatment with mineral acids will reduce capacity due to dealumination (Watanabe et al., 2003), alkali as well as heat treatment are observed to improve zeolite's capacity (Dryden and Weatherley, 1987). Chemical pretreatment which gives the homoionic form of material has been shown to improve ion exchange capacity (Koon and Kaufman, 1975). The sodium form achieved highest ammonia capacity for zeolites (Booker et al., 1996) probably due to the high selectivity for NH_4^+ over Na^+ ion (Jorgensen, 2002). Since the selectivity for NH_4^+ over Na^+ is even higher for MN 500 (4.3 compared to 2.7, obtained for clinoptilolite) it can be expected that chemical pretreatment will improve capacity of this exchanger as well. Jorgensen and Weatherley (2003) carried out research on the influence of organic acids and proteins on ammonia uptake onto clinoptilolite and purolite, which are some of the ion exchangers used in our research. They concluded that some organics increased the capacity of ion exchangers probably due to the ability to reduce the surface tension of the aqueous phase enabling the aqueous phase to reach macropores of the exchanger and therefore better mass transfer. Further consideration of the effects of exchanger structure can be found in Section 1.4.6.

2.2.3 Ion exchange selectivity

Even though natural zeolites have a relatively low capacity due to the low Al/Si ratio, their high affinity for ammonium ions, regardless of the material's origin has been proved by many researchers (Metropoulos et al., 1993, Papadopoulos et al., 1996, Conney et al., 1999). Much research has been done on zeolite selectivity. Most workers agree that clinoptilolite has a high affinity for potassium ions relative to ammonium, calcium, and magnesium.³ However, there is some

³ Calcium, magnesium and potassium are observed since those ions are present in high concentration in waste water.

uncertainty on the selectivity between calcium, sodium and magnesium ions exchanging on to clinoptilolite. Ames (1963) as well as Dryden and Weatherley (1987a) determined a higher affinity for sodium relative to calcium and magnesium ($K^+ > NH_4^+ > Na^+ > Ca^{2+} > Mg^{2+}$), whereas Skudder (1976) suggested calcium exhibited a higher affinity compared to both sodium and magnesium ($K^+ > NH_4^+ > Ca^{2+} > Na^+ > Mg^{2+}$).

Watanabe et al. (2003) found that the order of preference of ammonium ion for exchangeable cations on mordenite from Japan was $Na^+ > K^+ > Ca^{2+} > Mg^{2+}$.

No literature data could be found about selectivity of purolite, the synthetic ion exchanger used in this research.

2.2.4 Ion exchange kinetics

The kinetics of ammonia removal by natural zeolites have been studied in a number of researches carried out. Most of the papers applied some of the adsorption isotherms to model the rate of the ammonia removal from the solution (Kithome et al., 1998; Weber, 1983; Nguyen and Tanner, 1998). Major conclusions are that the reduction in particle size will increase the removal rate (Woods, 1977; Njoroge and Mwamachi, 2004) and that the process will be accelerated by increasing the flow rate (Dimova et al., 1999). On the other hand, in terms of the influence of initial ammonia concentration on the process kinetics a general conclusion cannot be reached. While some researchers claim that process kinetics will be improved by increasing initial ammonia concentration (Woods, 1977), Njoroge and Mwamachi (2004) as well as Kithome et al. (1998) state the opposite. In correlation with physiochemical properties of ammonia explained in Section 1.3 and the fact that the process of removing it by ion exchange is endothermic (Section 2.2.1), higher temperatures as well as a pH below 7 will accelerate the process (Lin and Wu, 1996). Lower pH value will ensure that all ammonia in the solution is in NH_4^+ form available for ion exchange. Jorgensen (2002) compared the rate of ammonia removal onto zeolite,

(clinoptilolite) and synthetic ion exchangers (Purolite MN 500 and Dowex 50w-x8) and concluded that uptake onto synthetic materials was faster.

However, this type of research does not answer the dilemma of whether particle or film diffusion controls the uptake rate (see Section 1.4.5). Another type of ion exchange kinetics research involves applying models that correlate the rate of removal with the particle diameter or square particle diameter. In the first case, mass transfer will be controlled by film diffusion while in the latter case particle diffusion will control the process (Liberti and Helfferich, 1983). Booker et al. (1996) assumed that uptake onto clinoptilolite is controlled by particle diffusion. They applied Vermeulen's approximation to obtain values of diffusion coefficients in the range of 3.21×10^{-12} - $3.49 \times 10^{-12} \text{ m}^2/\text{s}$ for initial ammonia concentration of $25 \text{ mgN-NH}_4^+/\text{l}$ and particle size in the range of 0.6-1.2mm. No data could be found about diffusion parameters for ammonia removal onto mordenite and a synthetic ion exchanger used in our research, Purolite MN 500.

2.2.5 Ion exchange regeneration

2.2.5.1 Chemical regeneration

Literature data show that alkaline regeneration carried out by using a mixture of sodium hydroxide and sodium chloride solution was the most effective in clearing occupied sites after ammonia removal (Koon and Kaufman, 1975; Booker et al., 1996; Jorgensen, 2002). No significant improvement in regeneration efficiency was noticed after increasing the pH to more than 12.5 (Koon and Kaufman, 1975; McVeigh, 1999) and sodium chloride concentration above the value of 12g/l (Koon and Kaufman, 1975). McVeigh (1999) also reported that pH of 7 regeneration was extremely slow. However, it was already mentioned in Section 1.4.4.1 that there were some problems associated with alkaline regeneration. Some literature data demonstrated that zeolites chemical structures can be damaged when they are exposed to NaOH solution. Barrer et al. (1967) reported a 70% loss of clinoptilolite capacity when exposed to 20% NaOH solution for two days. Koon and Kaufman (1975) found that when the pH of the regeneration solution was 11.5, 12.0 and 12.5, clinoptilolite lost 0.25%, 0.35% and 0.55% of

weight respectively. Semmens and Porter (1979) reported that Ca^{++} and Mg^{++} , removed from the wastewater while removing ammonia, are displaced later from the zeolite due to the slower diffusion of these cations. Higher cation concentration in the solution caused by this “late elution” changes the equilibrium, and ammonium ion is recaptured by the zeolite. On the other hand, Booker et al. (1996) reported no capacity loss after using the alkaline method for natural zeolites’ regeneration. Jorgensen (2002) used the alkaline method for purolite’s regeneration (synthetic material used in our research), after using it for ammonia removal in terrestrial water. Again, no capacity loss or structure damage due to high pH values (pH=12.5) was reported.

2.2.5.2 Biological regeneration

Biological regeneration of exhausted ion exchanger is based on the ammonia oxidation by bacteria, described in Chapter 1.2.3. McVeigh (1999) performed the biological regeneration of an exhausted bed. After the ammonia saturation, a packed bed of exchanger was treated with a high bacteria population solution obtained from an existing, preadapted culture. In the McVeigh’s study the culture was obtained from an established Rotating Biological Contactor running with inlet ammonia concentration, oxygen concentration and pH values 55mg/l, 9.5mg/l and 8.0 respectively. The outlet ammonia concentration was 14mg/l, and the oxygen level was 0mg/l with an obvious alkalinity drop and a huge increase in nitrate concentration. Even though the nitrification was taking place in the bed it was not enough to regenerate the zeolite completely. Fragmentary regeneration was proved by using the regenerated bed for ammonia removal when a significant capacity drop was reported. Insufficient regeneration might be attributed to the lack of oxygen as well as to the fact that biological regeneration will displace only ammonium ions, leaving sites occupied by other cations unavailable for further exchange.

Semmens et al. (1977a, 1977b) have performed biological regeneration of clinoptilolite in a column and operated as a separate process. In order to perform biological regeneration as a separate process, bacteria was introduced into

ammonium-rich spent regenerant after chemical regeneration was finished. The nitrification within the column was slower and it took a longer time to perform the biological regeneration compared to chemical regeneration. The comparison of the breakthrough curves of the columns, which were regenerated biologically or chemically, revealed a better uptake capacity of chemically regenerated material. This phenomenon was attributed to the incomplete removal of calcium and magnesium during biological regeneration. The nitrification rate, and not the release of ammonium ions, proved to be the rate limiting step for the biological regeneration of the column.

No literature data were found about mordenite or purolite being biologically regenerated. However, instead of regeneration, ammonium saturated zeolite may be used as a fertiliser in the agriculture industry. Ming and Allen (2001) successfully applied ammonium saturated mordenite with 1mg/g of N-NH_4^+ as a fertiliser at an application rate of 5kg/m².

2.3 Ion exchange in saline water

High salt concentration in saline water significantly reduces the efficiency of the ion exchange process for ammonia removal in saline water (Koon and Kaufman, 1975; Lin and Wu, 1996). Even though high selectivity of zeolites for ammonia has been reported (Section 2.2.3), high concentrations of Ca^{2+} , Mg^{2+} , K^+ and Na^+ in saline water reduce the life time of the material rapidly making process uneconomic. Briggs and Funge-Smith (1996) reported that a salinity of 5g/l reduced the ammonia removal efficiency of clinoptilolite by ten times compared to the performance in the fresh water. Increased salinity further reduced the capacity, leading to failure to adsorb ammonia at 20g/l salinity with an initial ammonia concentration of 4-11mg/l. They also argued that due to a high concentration of Ca^{2+} ions, irreversible adsorption might occur, causing incomplete regeneration of exhausted material.

On the other hand, some researchers claim that zeolite performance in saline water might be improved by modifying them so that decationization is achieved (Lopez-

Alcala et al., 1998). With an initial ammonia concentration of 10mg/l NH_4^+ they achieved up to 39.2% and 20% removal at salinities 1.75g/l and 3.5g/l respectively (Rodriguez Fernandez et al., 2003). Some of these materials were chosen for our research and more about the structure can be found in Section 1.4.7.

2.4 *Biologically active ion exchange*

Since biological removal and ion exchange are the most common ways to remove ammonia from wastewater, combining the two of them might be a way to improve the process overall. In Section 2.1.1 it was indicated that nitrifying bacteria are very sensitive to any sudden, extreme changes in the ammonia inlet concentration. Kruner and Rosenthal (1983) reported that increasing the total ammonia concentration to the 1-1.8mg/l reduced nitrification to 40% compared to the value when the ammonia concentration was 0.15-1mg/l. This latter observation was made in the case of nitrification in trickling filters filled with plastic material without any ammonia adsorption capability. This research confirmed a necessity to solve the problem of a sudden increase in ammonia concentration which can inhibit bacteria. Section 2.1.5 emphasized benefits of bacterial growth when they are attached to the surface. Sand, plastic media and activated carbon as well as some ion exchange materials are all possible supports for bacteria growth. Most of the natural surfaces, including the nitrifying bacteria, are negatively charged (van Loosdrecht et al., 1987). Preston and Alleman (1994) suggested that negatively charged nitrifying bacteria are electrostatically bound on a zeolite crystal surface. Richardson et al. (2000) concluded that adhesion of bacteria onto sand was improved by coating the sand with iron, but this was reduced after organic matter was adsorbed onto sand. The same author emphasized that the surface charge was more important than hydrophobicity in the process of bacteria adhesion onto quartz sand. Generally, hydrophobic cells adhere to a greater extent than hydrophilic cells (van Loosdrecht et al., 1987a).

The majority of research so far in the area of biologically active ion exchange was done using wastewater from a secondary effluent or some other waste water with an already established population of nitrifying bacteria. An ion exchanger might

be added into the suspended growth reactor where nitrification already occurred (Sims and Little, 1973), or it could be introduced into the process in the form of packed beds (McVeigh, 1999; Chung et al., 2003). A simple addition to the reactor does not allow regeneration of the exhausted material, which means that if saturation happens, instead of combined ion exchange and nitrification only the latter will occur. Cooper and Williams (1990) compared the costs of two possible ways to run the process and concluded that for a projected plant life time of 30 years it was 13% cheaper to install and run a biological bed (BB) than to extend an activated sludge plant. They did not allow costs for regeneration of exhausted material and assumed that the biological process would be enough. Yang (1997) immobilized zeolite particles together with nitrifying bacteria in sodium alginate pellets to improve ammonia transfer to the entrapped bacteria. However, the entrapped method did not show good results since it took two days to establish nitrification in the batch reactor due to slow oxygen and ammonia transfer through the pellets and it was effective only for initial ammonia concentrations above 50mg/l. When the biological process was initiated, a high ammonia/oxygen ratio within the pellets inhibited *Nitrobacter* and limited nitrification to the first step only so that final product was nitrite instead of nitrate.

Belser-Baykal et al. (1994) introduced ion exchanger into an already established biological nitrifying filter in the form of a packed bed and obtained better results in resolving the problem of the occurrence of sudden ammonia peaks. This compared favourably with the use of a biofilter alone or to an ion exchange column alone. This experiment proved that the established colony of nitrifying bacteria takes time to reduce the ammonia peak in the influent concentration and that ion exchange can serve as a buffer during that time. This research also indicated one of the problems associated with biologically active ion exchange as follows. In order to inoculate bacteria, the ion exchanger had to be in contact with bacteria rich medium long enough so that a good biofilm is established. In some research this period was up to 2 months (Gross et al., 2003; Haug and McCarty, 1972). During that time all cations which compete with ammonium ions for available sites will be removed as well, reducing ion exchange capacity

significantly. Therefore, when using ion exchange materials as carriers, it is necessary to reduce the time for establishing biofilters as much as possible so that the exchange capacity of the material is retained. The review in Section 2.1.6 showed that some materials can improve nitrification by adsorbing toxic organics from wastewater. According to Jorgensen (2002) zeolites exhibit poor adsorption ability in the case of organic acids and proteins, therefore can not be attributed this improvement.

One of the problems that can occur when ion exchange is biologically activated in the form of packed beds is a drop in oxygen concentration in columns which was reported by McVeigh (1999). After passing the bacteria rich solution through the clinoptilolite exhausted column the outlet DO concentration was zero. Lahav and Green (1998) also stated that oxygen concentration was a limiting parameter for the nitrification rate within the packed column of the zeolite. In both researches, maximum oxygen inlet concentration was achieved by either agitation or aeration. However, oxygen is not easily dissolved in wastewater. More than 70% of oxygen blown into an activated sludge system for wastewater treatment is lost to the atmosphere (WERF, 2002). In addition, air must be compressed to overcome the hydrostatic pressure and the back pressure of the aerators. A more economical way for aeration of the biological reactors is membrane aeration (Kanokwaree and Doran, 1998). The problem of oxygen depletion within the biologically active ion exchange column could be solved by in-column membrane aeration, since the conventional aerators would create bubbles which would significantly reduce the mass transfer from solution to the ion exchange material. Kuhlman (1987) successfully performed bubble free aeration with a silicone tubing oxygenation system for his reactor with animal cell cultures.

Some authors stated that the biological process within the packed bed could cause fouling of the material and a backwashing procedure was suggested in order to prevent this (Semmens and Porter, 1979). On the other hand, Lahav and Green (1998) stated that even the thickest biofilm did not have any influence either on zeolite's removal capacity nor on the process kinetics.

Nitrification in saline water was reviewed in Section 2.1.7 when it was pointed out that, as in a fresh medium, bacterial growth is promoted when the bacteria are attached to a solid surface rather than in free suspension. The materials most often used like biofilter carriers for non-fresh media were polyester or cellulose (Catalan-Sakairi et al., 1996, 1997; Gross et al., 2003).

No data could have been found about biological activation of materials with ion exchange properties for ammonia removal in saline water.

2.5 Aim and scope of the research

Literature review revealed that clinoptilolite was the only natural material which has been used as biologically active ion exchange material. All the other materials used as bacterial carriers did not have any ammonia adsorption abilities and were used only as a solid support to improve the bio filter growth.

Pre aeration of the combined system exhibited some disadvantages which caused oxygen to be the limiting factor for the combined process.

Based on the reported, the major aims of the research were to try to find more natural materials for biological activation for fresh and saline media as well as to try to design a system with better aeration which however would not disturb ion exchange process on the materials.

3 Experimental materials and methods

3.1 *Experimental materials*

The materials used in this research were the natural zeolites, clinoptilolite and mordenite for adsorption in fresh water, as well as a product of a zeolitic nature (PZN) and the synthetic ion exchanger Purolite MN 500 for application in saline water. More about the structure of the materials used can be found in Section 1.4.

3.1.1 Material analysis

3.1.1.1 Electron microscopy

A visible analysis of the surface of the materials used was carried out using a JSM-6100 Electron Scanning Microscope, JOEL USA at the Electron Microscope Laboratory, Department of Mechanical Engineering, University of Canterbury. In order to prevent charging which affects the image clarity, sample particles were put on a layer of epoxy resin on a circular aluminium disk. After 24 hours of drying, particles were coated with a fine layer of carbon followed by a fine layer of gold. Prepared disks were then exposed to an evaporated alloy which condensed on the surface of the material. Each prepared sample was placed in the vacuum chamber of the microscope and exposed to the focused electron beam. The magnification used, and the value of the accelerating voltage for each sample are indicated on each image (Figures 4.1 and 4.2).

3.1.1.2 XRF analysis

The chemical composition of the materials used was obtained using a PW2400 X-Ray Fluorescence Spectrophotometer (XRF), Philips Holland at the Geochemistry Laboratory, Department of Geological Sciences, University of Canterbury. The method is based on quantifying major compounds present in the samples by electron bombarding and initiating X-ray emission. The X-ray images which were obtained were then divided into separate groups and each group indicated the presence of one specific compound in the sample. Due to the high temperatures applied during the procedure (1000°C) some volatile compounds are lost such as

carbon, carbonate or hydrated water which is marked as LOI (Loss on Ignition). For all samples LOI was less than 1%.

3.1.1.3 Surface area and pore size measurements

The surface area and pore size data were obtained using a surface area and pore size analyser, Nova 4200e, from Quantachrom Instruments UK, at the Queen's University of Belfast, UK. (Figure 3.1).

All samples were degassed for at least 12 hours at an elevated temperature (250°C). This preparation ensured that the surface of the material was free from any volatiles adsorbed during the storage of the sample. Adsorption isotherms were obtained by dosing nitrogen onto the adsorbent contained within a bath of liquid nitrogen at 77K.



Figure 3.1 Surface area and pore size analyser, Nova 4200e

3.1.1.4 Particle density measurements

The particle densities of the zeolites and of the products of zeolitic nature were measured by applying the following procedure (Schoeman, 1986). The material was washed, dried at 65°C for 24h and placed in a dessicator to maintain constant weight. 5g of material was then placed in a measuring cylinder containing water. Air bubbles were removed by tapping and the change of the water volume in the cylinder was recorded. Each result is a mean value of three repeated measurements.

3.1.1.5 IR spectra

Fourier Transformation Infra Red (FTIR) spectra of the materials were recorded on a FT/IR-200E single beam Fourier transform infra-red spectrophotometer, Jasco Japan at the Agricultural and Life Sciences Division, Lincoln University. Samples were prepared as follows: each material was preground with a mortar and pestle and mixed with paraffin oil to get a fine suspension. A drop of suspension containing each sample was placed between sodium chloride plates in a sample chamber and was exposed to a monochromatic infra red radiation. Spectra were recorded in the range from 650-4600cm⁻¹.

3.1.2 Material preparation

Prior to use, clinoptilolite and mordenite were crushed in a jaw crusher “Retsch BB 50” and classified to a size range of 0.5-0.71mm, 0.71-1.0mm and 1.0-1.4mm by using a set of Endecott’s laboratory test sieves. Sieves were placed in order with the base pan at the bottom and clamped onto a sieve shaker (Fritsch, Laborgeratebau) for 30 minutes. The particle size for the each set of the experiments is given together with the results. Materials were then washed to remove any fines and other undesirable material. In order to avoid comminution, washing was achieved by soaking the zeolite in deionised water for 24 hours with regular gentle agitation. The materials were then soaked successively in a series of batches of sodium chloride solution (1M) for periods of approximately 7 days in order to ensure complete conditioning into the sodium form. The materials were washed to remove excess NaCl until a negative reaction for chlorides with AgNO₃ was achieved and dried at 65°C for 24 hours. Preconditioned material was kept in a desiccator to maintain constant weight.

MN 500, ZZ and Mg.NZ were prepared by following the same procedure with the only difference being that crushing was not performed since the material was already in the range 0.5-2mm. MN500 was dried at a slightly lower temperature (30°C).

The Zecer 56 was already in sodium form since the modification process included contact with concentrated NaOH solution. Therefore the preparation procedure included only sieving to obtain particle size classification and washing to remove any impurities.

3.2 Experimental methods

3.2.1 Batch equilibrium studies without bacteria

All experiments were done in a laboratory with the temperature maintained at 22°C. The study of the effect of temperature on the combined process was out of the scope of this study. Every point shown on the equilibrium graph is the mean value of the 3 samples measurements.

3.2.1.1 Fresh water

To obtain the desired N-NH_4^+ (ammonium nitrogen) concentration, a stock NH_4Cl solution having 0.5mg N-NH_4^+ /ml was made and was diluted in 100ml volumetric flasks.

The equilibration procedure adopted was as follows: 0.5g samples of material were continuously shaken on an orbital shaker with 50 ml aliquots of ammonium chloride solution in deionised water, having concentrations in the range 0-200mg/L N-NH_4^+ . In preliminary measurements, ammonia levels were measured daily over a period of up to 7 days to establish the time required for equilibrium to be reached. For further experiments, three samples for each concentration were shaken two days longer than preliminary experiments indicated. Samples were then filtered using Whatman ammonia free analytical filter paper No 5 to prevent any traces of material from reaching the sample since material contained ammonium ion removed from solution which would be released during the analytical procedure of ammonia measurements (Section 3.3.1) reducing the accuracy of the experimental results. The ammonium ion concentrations in the aqueous phase at equilibrium were measured and the solid phase concentrations determined by mass balance. Detailed calculation is given in Appendix II.

In order to establish the extent to which the presence of potassium, calcium and magnesium ions in solution influenced ammonium ion uptake, further equilibration experiments were conducted. These were designed to determine the effect of each individual ion alone upon ammonium ion uptake. The starting solutions were dosed with the appropriate metal cation at a concentration of 40mg/l. Stock solutions of $\text{MgCl}_2 \cdot 6\text{H}_2\text{O}$, $\text{CaCl}_2 \cdot 2\text{H}_2\text{O}$ and KCl were made containing 200mg/l of Mg^{2+} , Ca^{2+} and K^{+} respectively and 2ml of solution was added in each 100ml volumetric flask containing different volumes of ammonia stock solution and diluted with deionized water. Equilibration was then repeated as already explained.

Since at temperatures of 20°C and pH in the range 7-7.5, less than 0.01% of total ammonia solution is in unionized form (Figure 1.6), we maintained the pH value in this range to be sure that all ammonia was available for ion exchange. The optimum pH value for bacteria growth is within the same range; therefore, the effect of pH on adsorption process was not investigated since this was the only possible pH range for the combined process. Usually, the pH of the solution was already in the desired range; however, saturated sodium bicarbonate solution was used to adjust pH when it was needed.

3.2.1.2 Saline water

Equilibrium studies were done following the same procedure given for experiments in fresh water, using saline water as the medium. Artificial seawater was prepared according to the composition shown in Table 3.1 (WPCF, 1975):

Table 3.1 Artificial sea water

Compound in order of addition	mg/l
NaF	3
SrCl ₂ ·6H ₂ O	20
H ₃ BO ₃	30
KBr	100
KCl	700
CaCl ₂ ·2H ₂ O	1470
Na ₂ SO ₄	4000
MgCl ₂ ·6H ₂ O	10780
NaCl	23500
Na ₂ SiO ₃ ·9H ₂ O	20
Na ₄ EDTA	1
NaHCO ₃	200

In order to establish the extent to which potassium, calcium and magnesium interfere with ammonia removal, the concentrations of these metals were measured by Ion Exchange Chromatography before and after the ion exchange equilibration for each N-NH₄⁺ concentration, since mentioned cations were already present in the saline medium. The analytical procedure is explained in Section 3.3.3.

3.2.2 Ammonia removal on biologically active materials

The experiments in this area were designed to study the suitability of the ion exchangers for bacteria growth and to measure the capacity of the ion exchange materials for the ammonium uptake in the presence of nitrifying organisms.

To investigate the suitability of the ion exchange materials as a support for the bacteria growth, the following procedure was applied: 3g of each of the materials were saturated with ammonium ion by placing them in 300ml of ammonium chloride solution in deionised water (C=200mg/l N-NH₄⁺) and shaking them on an orbital shaker for seven days. The ammonium solution was replaced each day. The materials were then washed, dried and placed in 2 litre conical flasks together with 500ml of bacteria broth and 50ml of bacterial seed. Bacterial seed was obtained by taking a sample from the municipal wastewater treatment plant and enriching the ammonia oxidisers by adding the broth for the growth of the nitrifying organisms that was made according to the procedure explained in

Appendix III. Subcultures were prepared by the inoculation of 50ml of a fully grown enriched culture into 500ml of fresh broth. Instead of ion exchange material, one flask was charged with 3g of CaCO_3 , which is commonly used as a support for a bacteria growth. Flasks on the shaker were kept at a constant temperature, aerated and protected from the light with aluminium foil. Two samples from each flask were taken daily for 19 days and were analysed for nitrites, nitrates and ammonium ion to follow ammonia depletion and bacteria growth on different materials and in different media (terrestrial and saline water). Results presented are the mean value of the two measured samples. Even though more than two samples would improve reliability of the presented results, only two were taken so that the initial volume of the solution was not reduced too much during the experiment. Flasks were weighed every day before and after sampling, and the deionised water was added as make-up before sampling for losses due to evaporation during the 24 hours periods between sampling.

The capacity of the material to remove ammonia from synthetic wastewater with the presence of nitrifying bacteria was measured as follows. 0.5g of the ammonia free material was placed in a 100ml conical flask with 50ml of ammonia solution in deionised water with concentrations ranging from 10-200mg/l N-NH_4^+ . Ammonia solutions were made in a sterile broth. In each flask, 1ml of the bacteria seed was added and the flasks were placed on an orbital shaker (with the speed adjusted to 200rpm). After the seed was added, artificial aeration was introduced to improve the nitrification process in the flasks and each flask was coated with aluminium foil to exclude light. In order to compare adsorption on biologically active and non-active materials, the flasks with the same ammonia concentration were prepared, in which 1ml of sterile seed was added, and put them under the same conditions on the orbital shaker. In that way, we had the same medium for adsorption, however, bacteria were not present. Each day the pH was checked and adjusted to a level of 7.5 by adding sodium bicarbonate solution. To make up for evaporated water, sterile water was added when it was necessary. After 13 days of shaking at a constant temperature of 22°C, samples were filtered into the 50ml volumetric flasks and each sample was filled up to 50ml with sterile water.

Ammonia concentrations were measured in each flask. The ammonia concentration was also measured in the seed solution and this value was used in the calculation (the initial ammonia concentrations were therefore slightly increased).

To determine the extent to which bacterial colonies influenced ammonia adsorption (not overall removal), material in each flask was washed and shaken with 1% potassium chloride solution to release all adsorbed ammonia, which was then measured. Adsorption on biologically active and bacteria free materials was compared.

For experiments in the saline medium the same procedure was followed with the only difference being that the broth in artificial sea water was used like a growth medium for nitrifying organisms. The broth in saline water was prepared according to the procedure explained in Appendix III. To avoid an adaptation period in saline water, the seed solution of nitrifying bacteria was obtained by the enrichment of ammonia oxidisers in saline broth using a sample taken from a waste water treatment plant. The enrichment process lasted at least 2 weeks prior to the experiment.

3.2.3 Kinetic studies

To carry out the kinetic studies the apparatus outlined in Figure 3.2 was used.

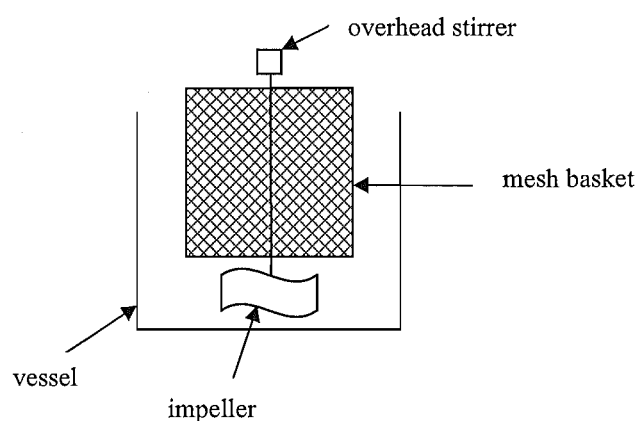


Figure 3.2 Apparatus for kinetics experiments

The batch ion exchange unit was based on the design of McKay (O'Connor, 1995) for the batch adsorption rate experiments. It comprised a 4 litre vessel equipped with a 500 μ m mesh basket which was immersed in the solution. The impeller was located below the lower level of the basket with the drive shaft located centrally such that the particles were protected from crushing by the action of the impeller blades. An overhead stirrer-drive provided good mixing in the range 500-2000rpm. The mixing speed over 500rpm was used since the turbulence provided better movement of particles within the basket. The ammonia solution (NH_4Cl in deionised water) was placed in the vessel and ion exchange resin placed in the immersed mesh basket. Samples of the solution were taken at recorded time intervals and ammonium ion concentration was measured according to the procedure given in Section 3.3.1. The parameter studies included: particle size (0.7-1.4mm, mixing speed (500-2000rpm); initial ammonia concentration (50-150mg/l) and mass of the ion exchanger (1.5-6g). Volume of the free liquid was always 3 litre and the mass of the material never exceeded 6g. In that way, a high ratio of *volume of the free liquid/mass of material* was maintained and decrease in the volume due to the sampling could have been neglected.

The results were correlated using two theoretical models from the literature explained in the Section 1.4.5.1. Values for the diffusion coefficients are mean values obtained from the three repeated experiments.

Similar kinetic experiments were conducted using materials on which bacteria were growing to investigate whether bacteria film on the surface would obstruct mass transfer of ammonia onto the ion exchange particles. Prior to kinetic experiments, bacteria rich and low ammonia concentration solution (N-NH_4^+ concentration was below 0.5mg/l) was pumped through the column packed with material for 5 days with a speed of 0.5BV/h. Reduction in the protein concentration in the solution prior and after the column confirmed microbial attachment onto the materials. The analytical procedure is explained in Section 3.3.6. Since the column adsorbed many of the cations present in the growing solution, to be able to compare the results with bacteria free material the same

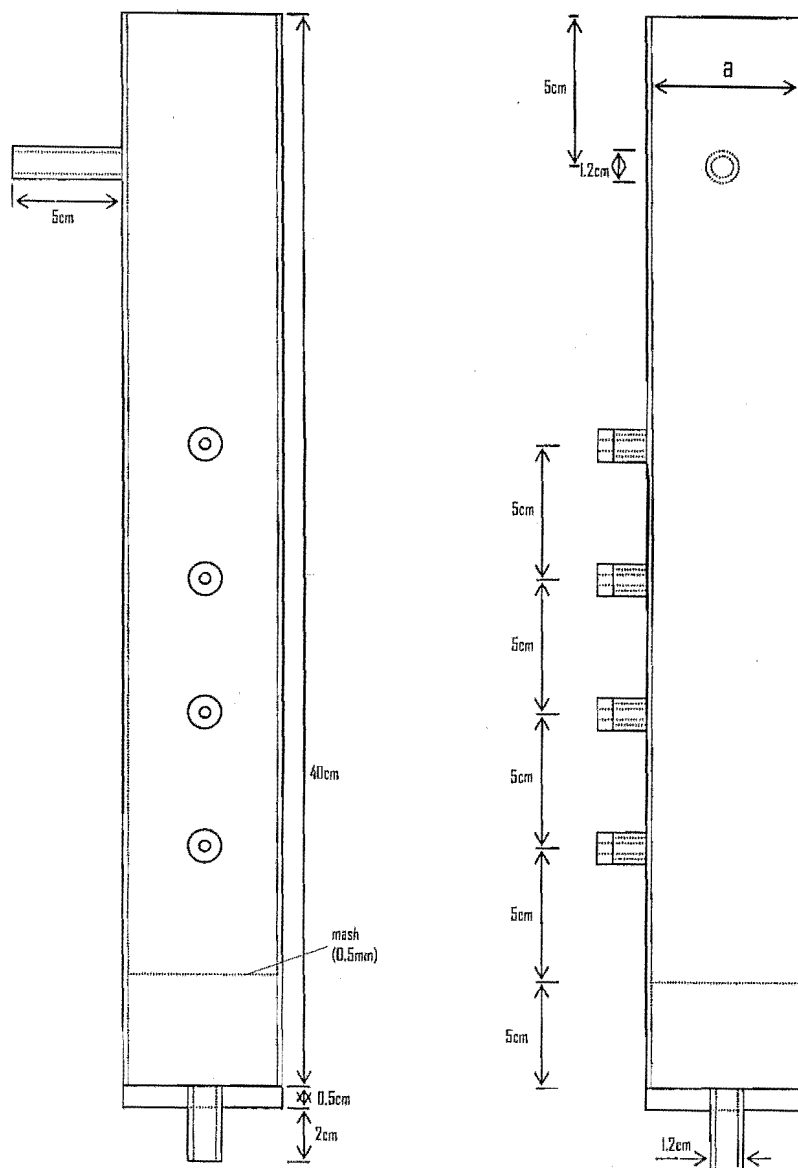
solution was autoclaved and pumped through another column with the same speed. Any water evaporated during autoclaving was replaced with deionised water. The solution containing bacteria was aerated with an aquarium aeration pump prior to the introduction into the column to provide conditions for bacteria to attach and grow on the surface of the material. After 5 days, the material from each of the columns was taken and dried for 24 hours on 29°C. Material was immediately used for the kinetic experiments which were carried out following the procedure already explained.

3.2.4 Column studies

3.2.4.1 Design of the columns

Column studies were performed using two types of columns. The design of the first one (which also was the basis for the design of the second type of columns) is presented in the Figure 3.3 and was commonly used in previous experiments in this area (McVeigh, 1999; Jorgensen, 2002).

The other one was a new design (Figure 3.4), with the main purpose being to improve aeration within the bed so that the nitrification is not limited by the oxygen concentration. The only difference is that a mesh cylinder goes through the middle of the column with peroxide-cured silicon tubing around it which is air permeable. The air permeability of the tubing was $7961 \times 10^{10} \text{ cm}^3 \text{ sec}^{-1} \text{ cm}^{-2} \text{ cmHg}^{-1}$ (Cole-Palmer, 2005). The internal and external tubing diameters were 2.4 and 4mm respectively. The tubing was clipped on the end which is at the bottom of the column and compressed air was introduced at the other end which is at the top of the column (Figure 3.5b). Ion exchange material was packed around the cylinder as well as through it since the top circle side remained open. Each column had four sampling points which were covered by silicon rubber septum and a bolt. The bolt had a hole big enough so that syringe needle was able to pass through. If not indicated differently, samples were taken from the point first from the top.



a - internal diameter varied and was 3cm or 1.4cm (indicated in the experimental results).

Figure 3.3 Basic column design (Jorgensen, 2002)

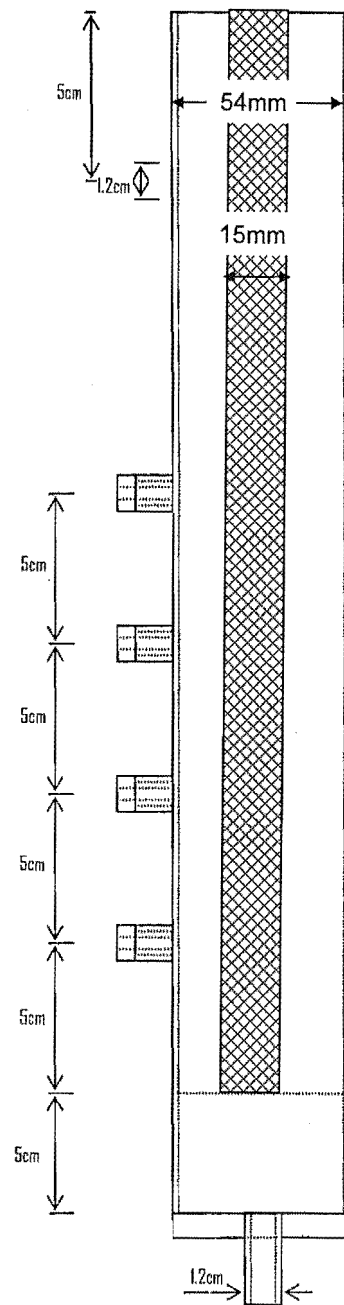
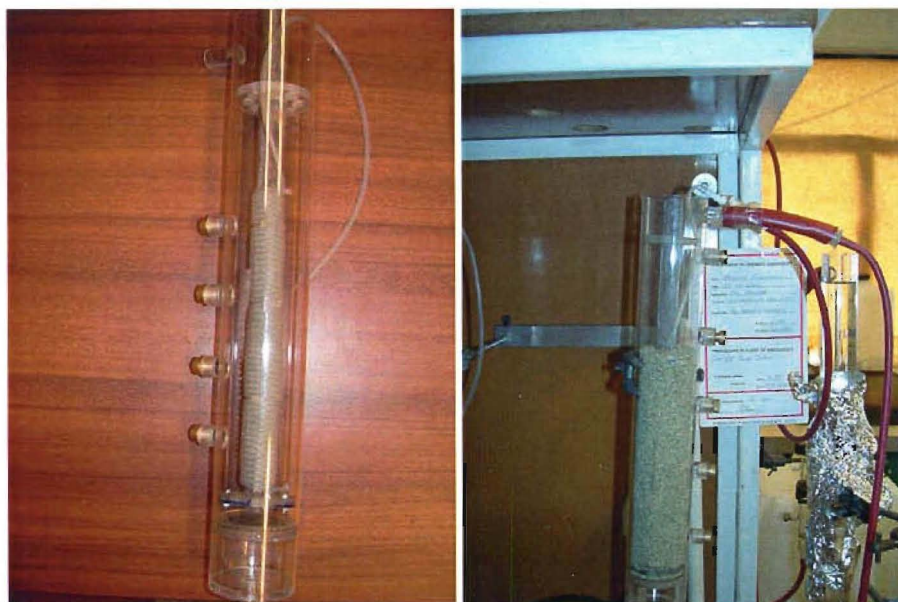


Figure 3.4 New column design



a)

b)

Figure 3.5 Photographs of the new design columns for improved aeration

Columns were built into a lab scale plant designed and built for this purpose. The design as well as the photo of the plant is given in the Figures 3.6 and 3.7 respectively.

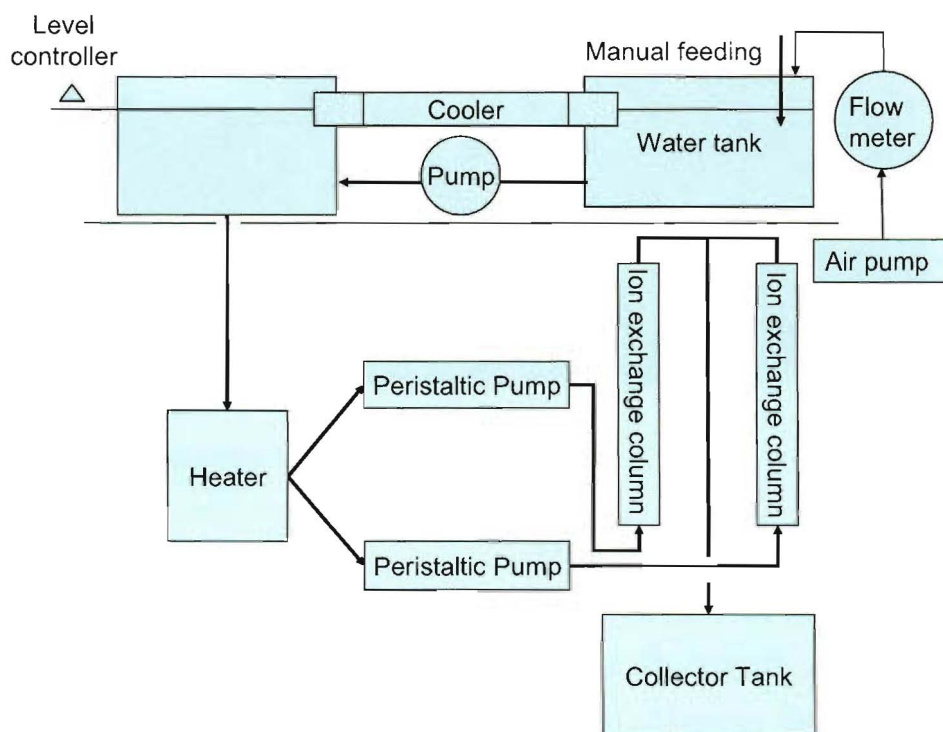


Figure 3.6 Lab scale plant design

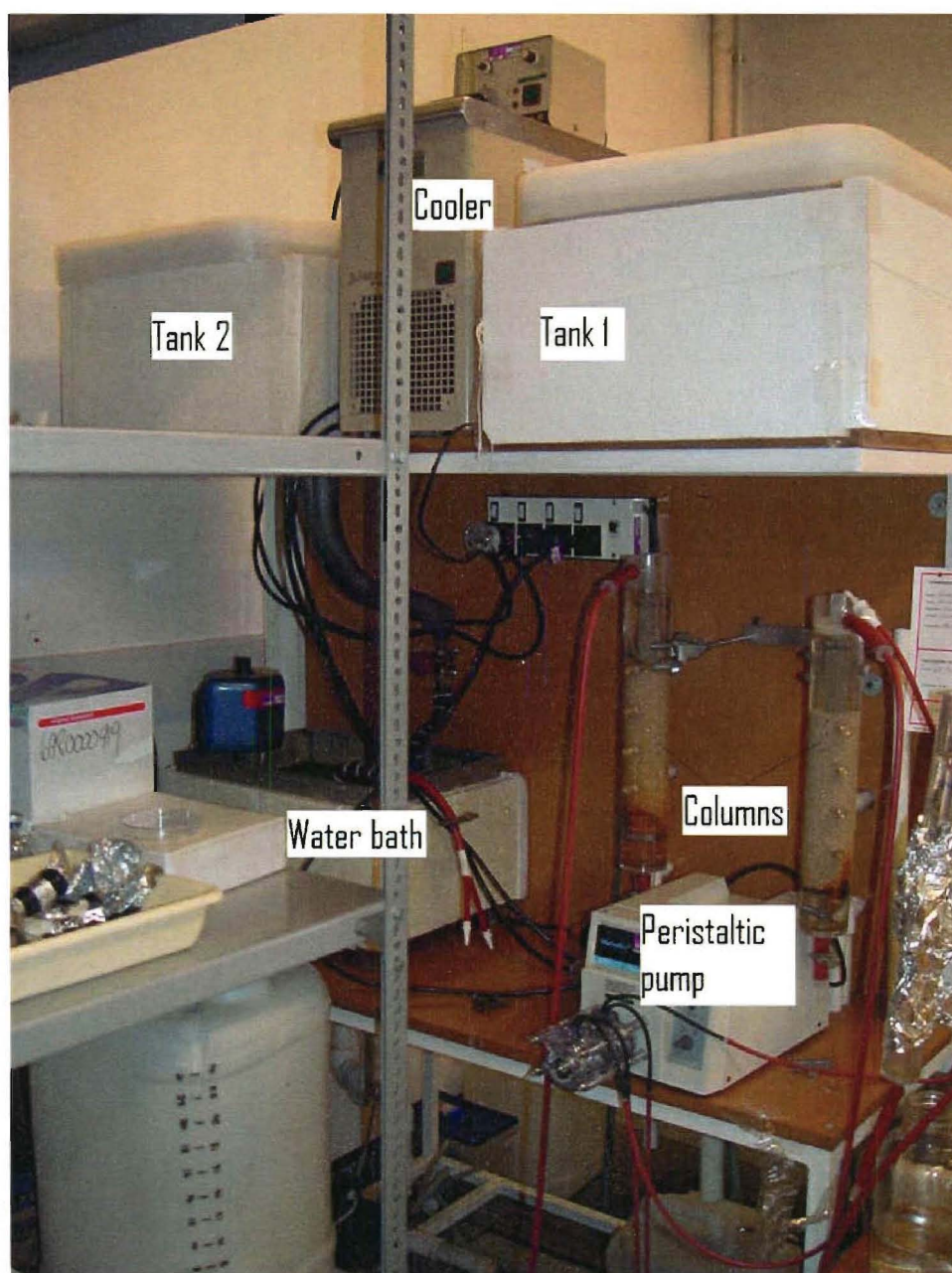


Figure 3.7 Lab scale plant for waste water treatment

3.2.4.2 Service procedure

Prior to the packing, the ion exchange materials were pretreated according to the procedure given in the Section 3.1.2. Each time, material was packed up to the 20cm height so that the last sampling point was at the top of the packing. The bed volume varied according to the variations in the internal diameter of the columns.

To prevent air bubbles being trapped within the column, water was pumped through it prior to exchanger material being added. Wet exchanger was then added. In all experiments solution was pumped upflow to minimise channelling. The feed solution was regularly added from the 5 litre vessel in which the ammonia concentration was adjusted by adding different amounts of standard ammonium chloride solution which contained 0.5mg of N-NH₄Cl in 1ml of solution. The desired flow was maintained by using Watson-Marlow and Cole-Palmer peristaltic pumps. Pumps were calibrated prior to use and regularly checked during the experiments due to the change in flow caused by the tubing damage.

In the column experiments carried out three types of fresh water were used: deionised water, water from the Salmon Fish Farm, Trents Road, Yaldhurst and water from the creek at the University of Canterbury campus. Chemical composition of the water being used is given in Table 3.2. Water analysing was done at the Canterbury Health Laboratories.

Table 3.2 Composition of the water used in the experiment

	Salmon	
(mg/l)	fish farm	Creek water
	water	
<i>Na</i> ⁺	8	7
<i>K</i> ⁺	2.19	0.9
<i>Ca</i> ⁺⁺	22.4	18.8
<i>Mg</i> ⁺⁺	2.4	2.2
<i>TOC</i> *	13.94	4.08
<i>N-NH</i> ₄ ⁺	0.97**	0.02

* total organic carbon

** sampling point was just before the biofilter, when the ammonia level was the highest

For the experiments that involved saline water, artificial sea water of different degree of salinity was used. Variations in salinity were obtained by diluting sea water already made according to the procedure given above Section 4.2.1.2).

In all cases, the level of ammonia was too low for the purpose of our research and was increased by making solutions of the desired concentration in the 5 litre

vessel following already described procedure. The inlet ammonia concentration varied between 5 and 150mg/l N-NH_4^+ depending on the experiment.

When experiments with bacteria were carried out the feed solution was added to the first tank (see Figure 3.7). Air was introduced either in the first tank using an aquarium air pump type JUN, ACO-5502 with a maximum output of 3dm³/min, or directly into the columns in the way already explained in Section 3.2.4.1. The second tank was introduced to allow air bubbles to settle so that mass transfer within the column was not inhibited. It was automatically fed by the pump which was activated when the level fell below the set value. Solutions in both tanks were maintained at 5°C by the cooler (Julabo type circulator, F10-C). In this way, any biological activity was prevented before the solution reached the columns. Solution was then passed through the water bath warmed to a constant temperature of 20°C. Literature data show that the rate of nitrification stays at 90% of the optimum value over the temperature range 15-30°C (McVeigh, 1998). Peristaltic pumps provided a constant flow through the columns.

Experiments on non-biologically active materials were done in the same way with the only difference being that aeration was not present if both columns did not involve bacterial activity.

By using the described equipment we were able to vary the air supply into the process, the internal diameter of the column, the flow rate of the water treated, the particle size of the material used, the temperature and the inlet ammonia concentration. Detailed parameters for each experimental run will be given together with the results presented. The term “Bed Volume” (BV) in our study always refers to the volume of the empty column (without packed material).

3.2.5 Bacteria immobilization

One of the problems associated with biologically active ion exchange is establishing the growth of a biofilm on the material without losing too much of its adsorption capacity. Sections 1.5 and 2.4 give more details regarding this problem.

It has been found that the entrapment method was ineffective, since the rate of oxygen diffusion to the central part of solid particles becomes rate limiting (Catalan-Sakairi, 1997). The adsorption method allows bacteria to grow on the surface of the particles so that oxygen and substrate are easily available, and has been effectively used in a number of researches (Woods, 1997; McVeigh, 1999). However, the problem with this technique is that oxygen concentration becomes a limiting factor when applied within a packed bed. By introducing the columns with a new design as explained in Section 3.2.4, this drawback could be eliminated. Another challenge was to find the optimum volume of bacteria rich solution which was to be passed through the column so that bacteria colonies could be established on the surface without losing too much of the ion exchange capacity. Therefore, in order to obtain biologically active columns, we opted for passing 48BV of bacteria rich and low ammonia concentration (N-NH_4^+ concentration was below 0.5mg/l) solution with the speed of 0.5BV/h, through the packed bed prior to use. The temperature of solution was maintained at 22°C. The solution was obtained by the enrichment method previously described and aerated with an aquarium pump. The column was coated with aluminium foil to protect bacteria from light and it was continuously aerated at the rate of 70cm³air/min. The protein concentration in the solution was checked before and after the solution went through the column to ensure that the column retained biomass, which would be indicated by the reduction in the protein concentration after passing the solution through the column.

3.2.6 Alkaline regeneration

When the materials became saturated with the ammonium ions, the feed solution was stopped. The columns were then washed with 10BV of deionised water at the same speed that feed solution was pumped. To regenerate the columns, alkaline regeneration was carried out (see Section 1.4.4.1). The solution for regeneration was NaCl (10g/l) and NaOH (1.2g/l) in deionised water with a pH of 12. To increase pH from 12-12.9 the NaOH concentration should be increased from 1.2-10.6g/l (McVeigh, 1999) which would make the whole process too expensive. Therefore, even though a pH slightly higher than 12 might slightly improve

regeneration we opted for a more economical solution which is more likely to be used in practice. 20BV of regenerant solution was then passed through the exhausted column at half the flow rate that the feed solution was pumped. The column was washed with 10BV of deionised water and used again.

3.3 Analytical methods

3.3.1 Ammonia measurements

Ammonia analyses in solution were conducted using an ion selective electrode (Orion 95-12) and separate checks were made in a number of cases using the conventional Nesslerisation technique (Eaton et al., 1995). The ammonia probe measures N-NH_3 only but the method used measures total ammoniacal nitrogen in the solution (N-NH_3 and N-NH_4^+). The probe consisted of an outer body with an ammonia selective membrane at the bottom and an inner electrode body with a sensing element. The principles of the method are as follows. Before measurement, an ionic strength adjustor containing 5M NaOH and colour indicator, was added to each sample. In this way the pH in samples was always above 11.5 so that all ammonia was in unionized form. Ammonia from the solution diffuses through the selective membrane until concentrations on the both sides of the membrane are equal. In the inner body, ammonia reacts with the internal filling solution to form NH_4^+ and OH^- ions. The latter are then detected and measured by a pH meter Orion EA940. The equipment uncertainty during the ammonia measurements was $\pm 2\%$ according to the manufacturer (Thermo Orion, 1997). Samples were either analysed immediately after being taken, or preserved with 1 drop of 1M HCl and refrigerated for up to 7 days. Results are given in mg/l N-NH_4^+ .

3.3.2 Oxygen measurements

Dissolved oxygen concentrations were measured by using an oxygen probe (YCI model 5739, Yellow Spring Instruments, USA) with a temperature probe built in, attached to a meter YCI model 57. Prior to each measurement the probe was calibrated at two points. The first calibration point was 0mg/l and the second one was the saturation oxygen concentration for the given temperature. The list of

maximum oxygen concentrations at different temperatures is given on the back of the meter with resolutions 0.01mg/l and 0.1°C respectively. Deionised water was saturated with oxygen by bubbling air through it for 5 minutes. The resolution of the oxygen readings was 0.1 or 0.01mg/l depending on the type of the experiment. Dissolved oxygen was measured immediately after the samples were taken. Accuracy of the measurements was $\pm 2\%$.

3.3.3 Metal cation measurements

Metal cations (K^+ , Mg^{2+} , Ca^{2+}) were analyzed using a Waters Non-Suppressed Ion Exchange Chromatograph, Millipore Corp, USA with Waters Baseline 810 software and an Alltech universal cation column with 3mM methane sulfonic acid as an eluent, at the Agricultural and Life Sciences Division, Lincoln University. The results are given in mg/l or meq/l of cations measured. The accuracy of the measurements was $\pm 5\%$.

3.3.4 pH measurements

Measurements of pH were done using a Hanna meter model pH211 with the glass-body combination pH probe, HI 1131B which had a temperature probe included. The meter was calibrated prior to each measurement by using Hanna buffer solutions pH=4.01 and pH=7.01. The resolution was 0.01 pH units.

3.3.5 Nitrite and nitrate analysis

Nitrite and nitrate were accurately determined on a Hach DR/2000 Spectrophotometer following the procedure given in the Hach water analysis handbook. Different NitraVer, Hach, USA reagent powder pillows were used depending on the ion measured and the range of the obtained results. All results are given in mg/l $N-NO_2^-$ or $N-NO_3^-$. The accuracy of the measurements was $\pm 6\%$.

For a quick check during the experiment prior to the accurate measurements Merckoquant nitrite and nitrate test strips were used. They provided us with the information as to whether nitrites and nitrates were present at all and how much to dilute samples so that the results fit into the range of the applied method.

Samples were either analysed immediately after been taken, or preserved with 1 drop of 1M HCl and refrigerated for up to 7 days.

3.3.6 Protein measurements

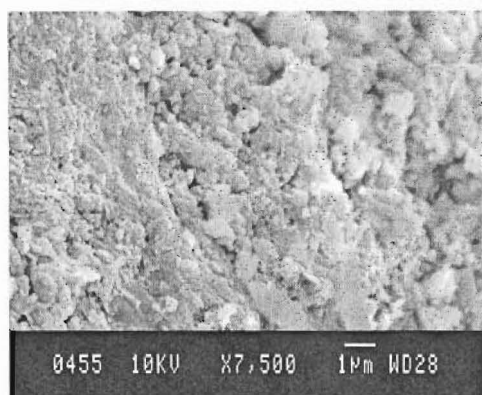
Protein measurements were carried out using a Sigma protein kit by applying the following procedure. 2ml of sample solution was mixed with 2ml of Lowry Reagent Solution. After 20 minutes, 1ml of Folin and Coicalteu's Phenol Reagent Solution was added and mixture was left for 30 minutes. Samples were then transferred to a cuvette and the absorbance was measured. Calibration was done with protein standards.

4 Results and discussion

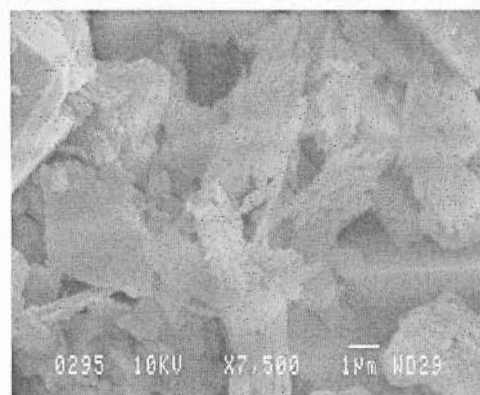
4.1 Material analysing

4.1.1 Electron microscopy

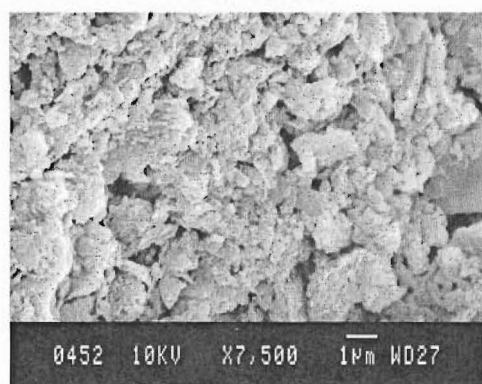
Scanning electron microscopic pictures of materials used in this research are given in Figures 4.1 and 4.2. All photos were taken with the same magnification (7,500) for better comparison. Due to the size reduction, figures are given as the 4,000 magnification. The surface of the natural zeolites looks different even though the same magnification was used. The clinoptilolite's crystals form is noticeable on the electron microscope photos, while surfaces of the mordenite and the ZZ look similar even though ZZ was obtained by modifying the Cuban zeolite which contained 70% of clinoptilolite and only 5% of mordenite (see section 1.4.7). It is likely that the original structure of the Cuban zeolite was affected by the pretreatment process which involved heating at 450°C.



Mordenite



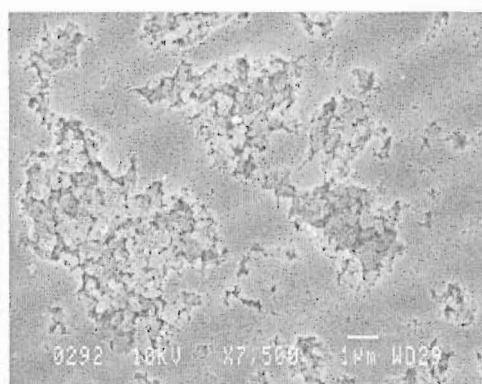
Clinoptilolite



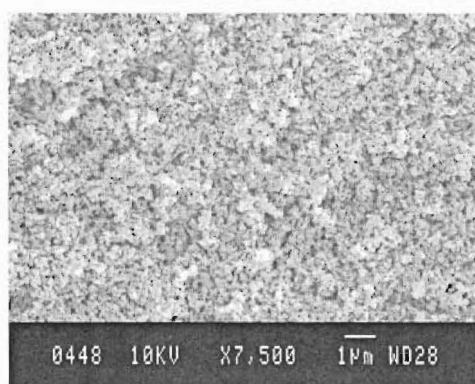
ZZ

Figure 4.1 Surface photographs of zeolites and ZZ, used in this research

The surface of the Purolite particle (Figure 4.2) does not show significant porosity but the image of the broken particle reveals the presence of the micropores and macropores of this synthetic resin. The synthetic Purolite was more uniform than the natural materials in Figure 4.1.



Purolite MN 500 (unbroken particle)



Purolite MN 500 (broken particle)

Figure 4.2 Surface photographs of the purolite MN 500

4.1.2 XRF analysis

The chemical composition of the clinoptilolite and mordenite is given in Tables 4.1 and 4.2 ("New Zealand"), together with the compositions of clinoptilolite and mordenite mined in different parts of the world. After calculating the Si/Al ratio from available data it can be seen that the Si/Al ratio for New Zealand clinoptilolite and mordenite is 4.78 and 5.46 respectively. The value for clinoptilolite is in the lower range among the other materials while the Si/Al ratio in the mordenite is not only the highest among the given materials but also is on the upper side of the range given in the literature (Si/Al = 4.5-5.5, Tsitsishvili et al., 1992). This could indicate a higher capacity for clinoptilolite and a lower value for mordenite, as silica rich material (see Section 1.4.2). The manganese concentration in New Zealand clinoptilolite is high compared to samples from other parts of the world. Together with phosphorus and titanium, this metal is present in small amounts probably due to the adsorption from the saline environment during the formation of the zeolite (McVeigh, 1999).

Table 4.1 Chemical composition of clinoptilolite mined on the different sites (taken from Dryden 1984, except data for the New Zealand type)

(%)	New Zealand	Japan	Hungary	Georgia	U.S.A. (California)
SiO ₂	70.75	81.03	75.89	68.04	71.01
Al ₂ O ₃	13.04	11.70	12.74	14.40	12.09
K ₂ O	3.64	3.94	6.04	1.30	1.70
Fe ₂ O ₃	2.08	1.51	1.75	3.99	1.05
CaO	1.93	2.46	1.40	6.99	3.85
Na ₂ O	1.83	0.99	0.19	2.22	6.09
MgO	0.41	0.57	0.20	2.00	0.54
TiO ₂	0.18	0.02	0.43		0.41
MnO	0.14	0.09	0.01		0.02
P ₂ O ₅	0.04				0.00
CO ₂					3.25
LOI*	5.05				
Si/Al	4.78	6.00	5.16	4.09	5.09
Total	99.08	102.30	98.70	98.40	

*) *Loss of ignition* - weight loss from the sample due to the loss of carbon, carbonate, hydrated water or other volatile compounds which are driven off at 1000°C

Table 4.2 Chemical composition of mordenite mined on the different sites (taken from Tsitsishvili et al., 1992 except data for the New Zealand type)

(%)	New Zealand	Bulgaria	Cuba	Azerbaijan	Hungary
SiO ₂	65.82	65.93	65.00	64.94	67.58
Al ₂ O ₃	10.60	10.80	11.24	11.81	14.41
K ₂ O	0.66	2.31	0.70	0.64	4.60
Fe ₂ O ₃	3.04	1.10	1.56	2.37	1.48
CaO	6.14	3.47	4.13	4.06	1.26
Na ₂ O	2.07	2.02	1.86	2.33	1.20
MgO	0.56	0.48	0.39	0.95	0.18
TiO ₂	0.29				
MnO	0.07				
P ₂ O ₅	0.07				
FeO			0.27	0.21	
H ₂ O		13.77	13.31	12.94	8.97
LOI*	10.16				
Si/Al	5.46	5.37	5.09	4.84	4.13
Total	99.48	99.88	98.46	100.25	99.68

*) *Loss of ignition* - weight loss from the sample due to the loss of carbon, carbonate, hydrated water or other volatile compounds which are driven off at 1000°C

Table 4.3 gives composition data for the ZZ and is compared with the data for New Zealand clinoptilolite and mordenite.

Table 4.3 Chemical composition of zeolites used in this research

(%)	ZZ	Clinoptilolite	Mordenite
SiO ₂	67.45	70.75	65.82
Al ₂ O ₃	11.34	13.04	10.60
K ₂ O	1.18	3.64	0.66
Fe ₂ O ₃	2.10	2.08	3.04
CaO	3.01	1.93	6.14
Na ₂ O	1.93	1.83	2.07
MgO	0.35	0.41	0.56
TiO ₂	0.30	0.18	0.29
MnO	0.04	0.14	0.07
P ₂ O ₅	0.06	0.04	0.07
FeO			
H ₂ O			
Zn	3.00		
LOI*	8.47	5.05	10.16
Si/Al	5.24	4.78	5.46
Total	99.23	99.08	99.48

*) *Loss of ignition* - weight loss from the sample due to the loss of carbon, carbonate, hydrated water or other volatile compounds which are driven off at 1000°C

The Si/Al ratio for ZZ is 5.24 which is higher than for New Zealand clinoptilolite but lower than the value for mordenite. In Section 1.4.7 there is a value of 4.70 for the Si/Al ratio reported in the literature. However, this is perhaps unsurprising since the value of Si/Al ratio for Cuban zeolite from which the ZZ was synthesised is also low, and the ratio is unlikely to change during the modification process (Section 1.4.7). Table 4.3 also confirms the previous finding that high silica clinoptilolite is enriched with potassium and that mordenite contains calcium and sodium in higher amounts than potassium and magnesium, as exchangeable cations (Tsitsishvili et al., 1992).

4.1.3 Surface area and pore size measurements

Results obtained for surface area and pore size analysis are given in Table 4.4 together with the values obtained for particle density.

Table 4.4 Surface properties and density of the materials used in this work

	Clinoptilolite	Mordenite	ZZ	MN 500
Particle density (g/cm³)	2.1	2.2	2.8	1.04*
Surface area, multipoint BET (m²/g)	117.7	14.54	81.07	339.8
Total pore volume (cm³/g) **	0.123	0.035	0.065	0.254
Average pore radius (nm)	2.092	4.894	2.617	1.492

*) The Purolite Company, 1999

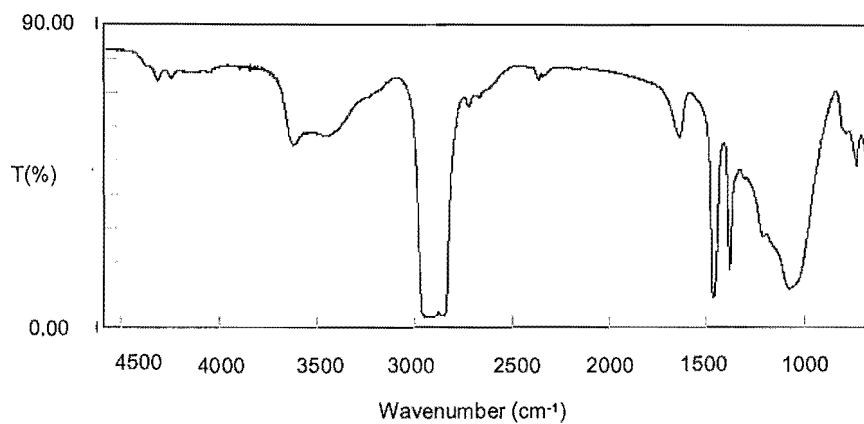
**) For pores with a radius less than 66.49nm, 75.17nm, 68.17nm and 66.17nm; at $P/P_0=0.985343$, 0.987065, 0.985712 and 0.985273; for clinoptilolite, mordenite, ZZ and MN 500 respectively

As expected, the synthetic ion exchange media (MN 500) possesses a much higher surface area than zeolites or a product of zeolitic nature. Among zeolites, clinoptilolite exhibited the highest surface area and pore volume. This is still low compared to the reported surface area of clinoptilolite from other parts of the world which is within the range of 172-340m²/g (Nguyen and Tanner, 1998; McVeigh, 1999) but higher than the value reported for New Zealand zeolite of

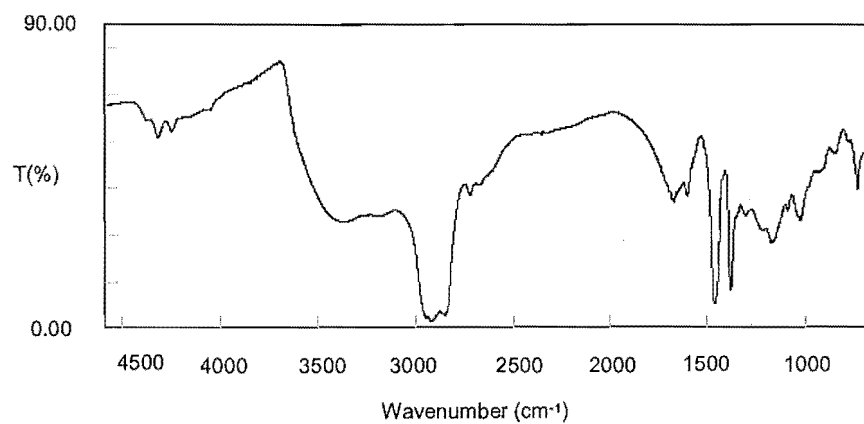
40m²/g (Nguyen and Tanner, 1998). However, differences are expected since the structure and therefore surface area properties vary greatly among even the same type of zeolites which originate from different deposits. Mordenite had the smallest surface parameters among the zeolites, with an unexpectedly low surface area of 14.54m²/g, compared to clinoptilolite. This is lower than the surface area for peat (35m²/g) and in the same range as the value for lignite (13.5m²/g), (McVeigh, 1999). The value reported in the literature for New Zealand mordenite (25.5-30.1m²/g, Nguyen and Tanner, 1998) is also higher than the one obtained here. The average pore radius was the greatest for mordenite and the smallest for MN 500.

4.1.4 IR spectra

Fourier Transformation Infra Red (FTIR) spectra of clinoptilolite and mordenite are given in Figure 4.3. Absorption bands at 2900, 1380 and 1460cm⁻¹ appear on every spectra and they belong to the paraffin oil that was used for making the suspension. Both, clinoptilolite and mordenite are significantly hydrated and show spectra with strong water absorption bands in the 3500 and 1640cm⁻¹ regions. On both spectra the regions of major absorption are 1060-1030, 650-550 and 470-440cm⁻¹. According to the structural scheme described by Breck (1974), based on the secondary building unit (SBU), clinoptilolite and mordenite belong to group 7 where the SBU is a complex unit compressing ten interlinked Al-Si tetrahedra. Although the spectra of clinoptilolite and mordenite are generally very similar they show differences in detail. There are differences in the region 1000-640cm⁻¹ where the metal-oxygen bands are. Bands at 2513 and 1794cm⁻¹ in the mordenite spectrum can predict a slightly more complex structure of this mineral when compared to clinoptilolite. A band at 1074cm⁻¹ in the clinoptilolite spectrum distinguishes clinoptilolite from heulandite. In the heulandite spectrum, this band is shifted to 1035cm⁻¹.



a)



b)

Figure 4.3 FTIR spectra of clinoptilolite (a) and mordenite (b)

IR spectra of synthetic ion exchanger MN 500 is given in Figure 5.4.

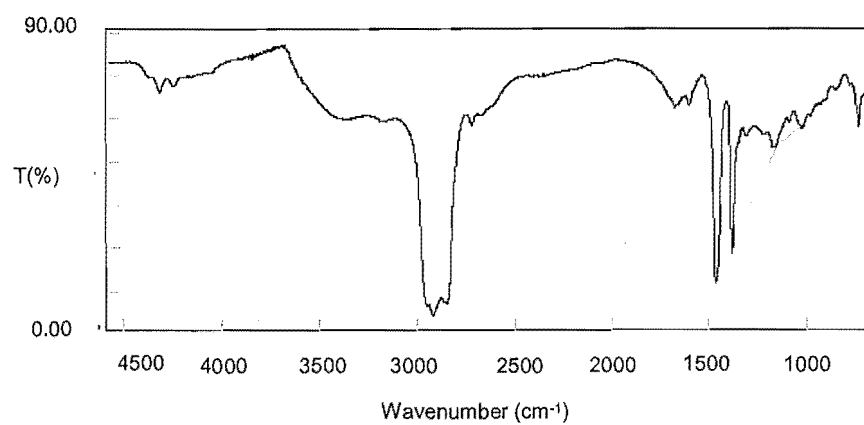


Figure 4.4 FTIR spectra of MN 500

Bands in the region $900\text{-}700\text{cm}^{-1}$ (maximum in the spectra at 722cm^{-1}) indicate some kind of aromatic substitution. Three major peaks at 2924, 1460 and 1377cm^{-1} can be attributed to alkanes present in the side chains, and not to the major aromatic ring in polystyrene. Due to hypercrosslinkage in MN 500, bands from C=C and C-H vibrations in the aromatic ring are probably not noticeable since their number is much smaller compared to the vibrations from the groups present in the substituents.

4.2 Batch equilibrium studies without bacteria

4.2.1 Fresh water

4.2.1.1 The uptake capacity

Section 1.4.2 of this work deals with theoretical information about ion exchange capacity. Since there are different approaches and definitions, for capacity we elected to take the one in which capacity is defined as the number of millimoles of counter ion equivalent per gram of material (McVeigh, 1999). Ammonia concentration, either in the solution or on the solid material is always given in mg N-NH_4^+ if not stated differently.

Experiments in this area were done following the procedure given in Section 3.2.1 of this work. The scope of the experimental work was confined to the determination of the equilibrium uptake behaviour of ammonium ions onto clinoptilolite, mordenite and MN 500 in the presence of chloride ions. During all experimental work the pH was maintained at a value of less than 7.5. It was assumed that all ammonia existed in the ionic form and was available for ion-exchange. The uptake of fully ionized ammonium ions from aqueous solutions in the concentration range 0–200mg/l onto different materials was compared. Preliminary experiments were carried out to determine how long it takes for equilibrium to be reached so that enough contact time was allowed for each material. Figures 4.5-4.7 show the decrease of ammonia concentration from the solution containing different materials.

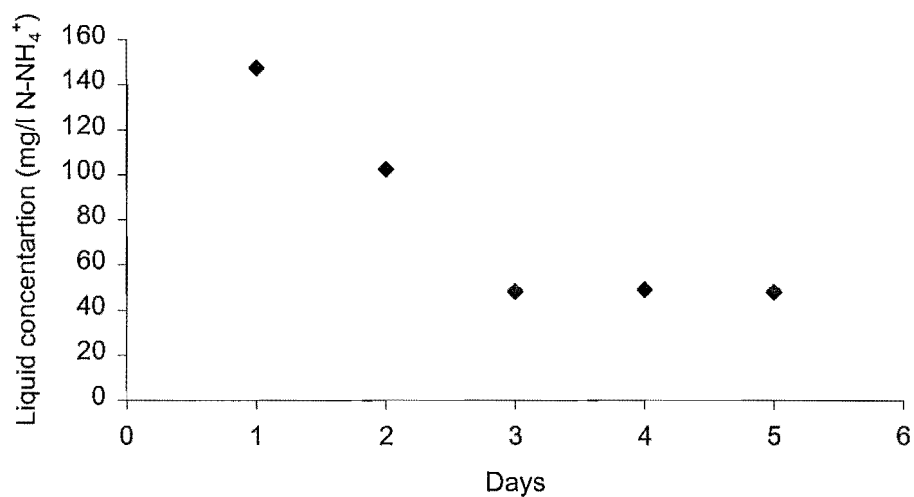


Figure 4.5 Reduction of ammonia concentration over a five day period in 50ml of solution and 0.5g of clinoptilolite ($T=22^{\circ}\text{C}$, particle size range 0.75-1.00mm, initial ammonia concentration: 200mg/l N-NH_4^+).

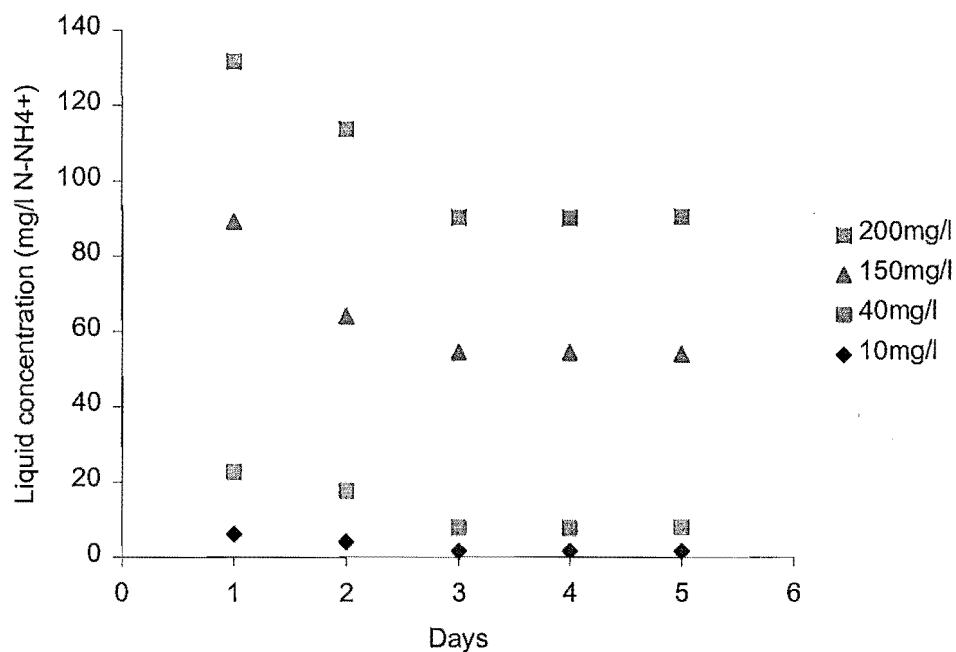


Figure 4.6 Reduction of ammonia concentration over a five day period for different initial ammonia concentrations in 50ml of solution and 0.5g of mordenite ($T=22^{\circ}\text{C}$, particle size range 0.75-1.00mm).

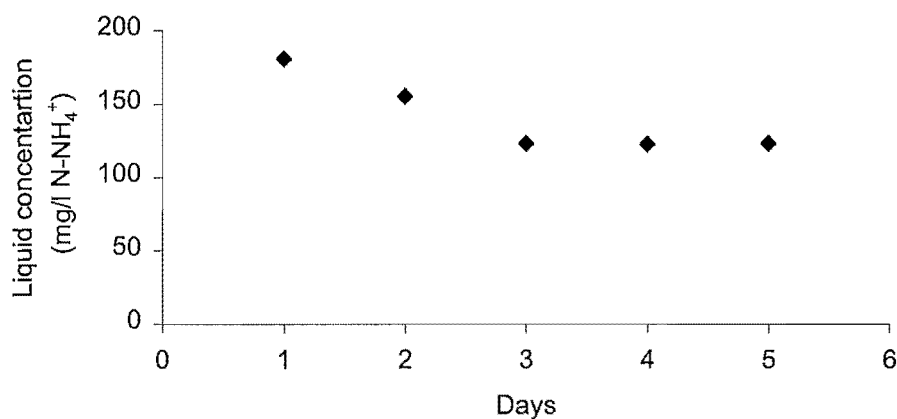


Figure 4.7 Reduction of ammonia concentration over a five day period in 50ml of solution and 0.5g of MN 500 (T=22°C, particle size range 0.75-1.00mm, initial ammonia concentration: 200mg/l N-NH₄⁺).

It can be concluded that for all the materials equilibrium was achieved after 3 days.

Jorgensen (2002) reported that in his research it took 4 days for clinoptilolite and MN 500 to reach equilibrium. However, samples were only agitated by hand four times per day compared with our research in which kinetics were assumed to be improved by placing samples on an orbital shaker at a low speed. Intensive shaking would crush the particles.

The uptake capacities after seven days contact for all materials are given in the next table.

Table 4.5 Uptake data for ammonium ion onto clinoptilolite, mordenite and MN 500.

Init.amm. (N-NH ₄ ⁺ mg/l)	Capacity for different initial conc. (meq/g)		
	<i>Clinoptilolite</i>	<i>Mordenite</i>	<i>MN 500</i>
10	0.07	0.07	0.07
40	0.26	0.24	0.26
70	0.42	0.42	0.43
90	0.49	0.52	0.54
150	0.62	0.72	0.79
200	0.66	0.80	0.96

From results presented in the Table 4.5 one can notice that the MN 500 exhibited the highest capacity in the whole range of ammonium ion concentrations. When compared with clinoptilolite, mordenite showed better removal of ammonia for initial liquid concentrations greater than 80mg/l N-NH₄⁺. This is perhaps contrary to expectations given that the internal surface areas for clinoptilolite are greater than those measured for mordenite. However, it might be that clinoptilolite possesses a great number of micropores with radii less than the radius of the ammonium cation; results obtained and presented in Table 4.4 had only average pore size radii of the materials. Comparison of the data with other similar published results reveals some interesting differences. Our results agree with the one from Jorgensen (2002), who found that MN 500 has higher ammonia capacity compared to clinoptilolite. Comparison of the ammonium ion uptake onto clinoptilolite with that measured by Nguyen and Tanner (1998) showed uptake in our case to be 0.66 meq/g comparing with 0.4 meq/g. This is a surprising result given that the starting concentration employed by Nguyen and Tanner was significantly higher than in our case. However, the ratio of mass of exchanger to the volume of solution phase was higher in their case leading to a lower solution phase equilibrium concentration. Another possible factor is that the equilibration time of 17 hours reported in their paper may have been insufficient to ensure complete equilibration. Results of Jorgenson and Weatherley (2001) for ammonium ion uptake onto commercially available clinoptilolite from the Hector deposit, obtained at the same solution phase starting conditions as the current

work, showed a significantly higher ammonium ion uptake of 1.61meq/g. A possible explanation for this is that the clinoptilolite for the commercial market would probably be pre-screened and pre-treated to yield an optimal performance by removing inert components. McVeigh (1999) determined ammonium ion capacity using column exchange with commercial clinoptilolite. He reported a capacity of 1.76meq/g for the uptake in the column. However, in a column, the zeolite will come to equilibrium with the feed solution ammonium concentration which will force more ions into the structure and the apparent capacity obtained might be higher since in batch experiments the concentration decreases with time. This result, as with Jorgensen's data, suggests a higher performance of commercial clinoptilolite.

The only comparison we have for New Zealand mordenite is in the data of Nguyen and Tanner (1998) who reported an ammonium ion uptake value of 0.59meq/g, which again is significantly lower than the values obtained here (see Table 4.5) even at the considerably lower starting concentrations reported here.

4.2.1.1 Other cation influence on the uptake capacity

In the case of water to be treated prior to recycle and end-use, in addition to removal of ammonia, there may be a requirement that the overall ionic composition of species other than ammonium ion be maintained. For example, in the case of recycled fish farm water, and in the case of "bottled" drinking water, a balance of ionic composition is an essential water quality criterion. Another major factor is that significant uptake of ions other than ammonia will reduce the effective uptake capacity for ammonium ions and thus the economics of the process. Therefore, it is essential to determine the extent to which cations other than ammonium will be removed during the process. The cations chosen for this study were typical of those found in many natural waters and in water used in industrial recycle operations, and included potassium, calcium and magnesium. Experiments were done following the procedure explained in Section 3.2.1 of this work. These were confined to determination of the effect of each individual ion on ammonium ion uptake. The starting solutions were dosed with the appropriate

metal cation at a concentration of 40mg/l and equilibration in the presence of ammonium ions repeated as before. Equivalent concentrations for each metal were as follows: 1.0meq K/l, 2.0meq Ca/l and 3.3meq Mg/l. The ammonium ion concentrations in the aqueous phase at equilibrium were measured as before, and the solid phase concentrations determined by mass balance. The uptake data are presented in Tables 4.6 and 4.8 where the percentage of ammonium ions removed in each case is shown as a function of starting concentration, and Figures 4.8-4.10. However, in order to quantify the selectivity behavior of the materials, the units of concentration were expressed in milliequivalents per gram for the exchanger phase.

Table 4.6 Uptake data for ammonium ion onto clinoptilolite in the presence of magnesium, calcium and potassium ions

Init. N- NH ₄ ⁺ (mg/l)	Percentage of removed ammonia				Capacity for different conc. (meq/g)			
	NH ₄ ⁺ only	Mg	Ca	K	NH ₄ ⁺ only	Mg	Ca	K
10	98.82	94.73	93.66	95.95	0.07	0.07	0.07	0.07
40	92.37	86.68	84.78	89.25	0.26	0.28	0.24	0.26
70	83.61	79.45	75.65	80.18	0.42	0.40	0.38	0.40
90	75.97	71.76	68.50	71.30	0.49	0.46	0.44	0.46
150	57.45	54.43	50.40	52.17	0.62	0.58	0.54	0.56
200	46.28	42.69	40.09	41.99	0.66	0.61	0.57	0.60

When plotted in these units, the results for the clinoptilolite show that in each case there is a small but significant reduction in the equilibrium uptake of ammonium ions in the presence of the other ion. Overall, the effect of the three metal ions upon percentage uptake is small. The effect is greatest for calcium ion and least for magnesium ion. Since the equivalent concentration for magnesium ion is the biggest for the applied mass concentration, we can conclude that this metal has the smallest effect upon ammonium uptake. For 40mg/l mass concentration, calcium interferes with ammonium uptake more than potassium. This could be due to the fact that calcium equivalent concentration is twice that of potassium (40mg/l equals 2.0meq Ca/l and 1.0meq K/l) since most workers agree that clinoptilolite has a high affinity for potassium ions relative to ammonium, calcium, and magnesium. McVeigh (1999) measured ammonium ion capacity in column

exchange using commercial clinoptilolite. The effect of the presence of magnesium, calcium and potassium upon ammonium ion uptake was determined and his data are shown in Table. 4.7.

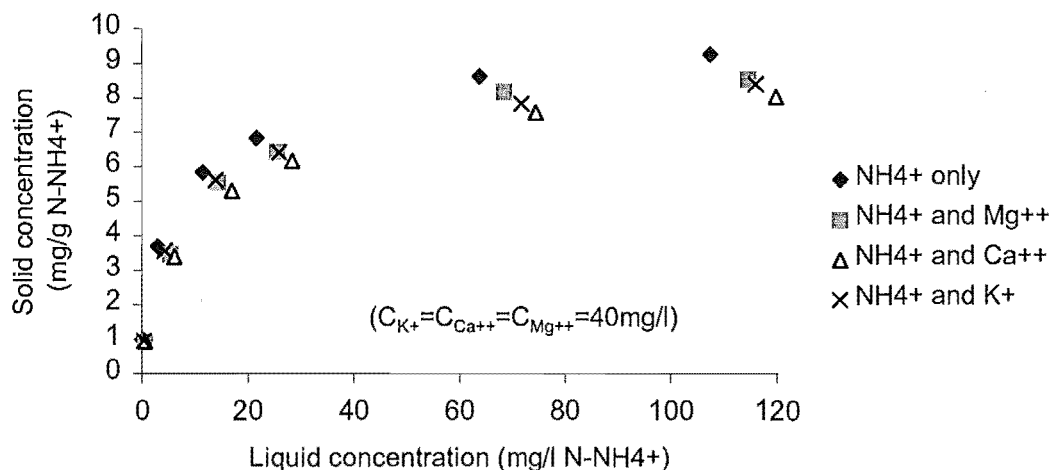


Figure 4.8 Ammonium ion uptake clinoptilolite in the Na^+ form, in the presence of magnesium, calcium and potassium ions

Table 4.7 Ammonium ion uptake onto clinoptilolite in the presence of calcium, magnesium and potassium ion at 40mg/l (McVeigh, 1999)

Solution tested	Clinoptilolite capacities
NH_4^+ only	1.76 meq/g
$\text{NH}_4^+ - \text{Ca}^{++}$	1.58 meq/g
$\text{NH}_4^+ - \text{Mg}^{++}$	1.65 meq/g
$\text{NH}_4^+ - \text{K}^+$	1.38 meq/g

Although the conditions of McVeigh's experiments were different from those described here, they provide an interesting comparison. Column contact would ensure complete displacement of the sodium ions initially present on the exchanger and this would influence the overall equilibrium uptake of both the counter-ions from the aqueous phase. The effect of the metal ions suggests an order of preference $\text{K}^+ > \text{Ca}^{++} > \text{Mg}^{++}$ since the ammonium ion uptake shows the greatest reduction in the presence of the potassium ion for the initial metal concentrations of 40mg/L. These contrast with our data, where the order of

preference appears to be $\text{Ca}^{++} > \text{K}^{+} > \text{Mg}^{++}$ for the same initial metal concentrations; the explanation for this cannot be concluded.

Table 4.8 Uptake data for ammonium ion onto mordenite in the presence of magnesium, calcium and potassium ions

Init. N-NH ₄ ⁺ (mg/l)	Percentage of removed ammonia				Capacity for different conc. (meq/g)			
	NH ₄ ⁺ only	Mg	Ca	K	NH ₄ ⁺ only	Mg	Ca	K
10	92.28	92.24	91.80	86.29	0.07	0.07	0.07	0.06
40	85.09	83.26	84.78	82.10	0.24	0.24	0.25	0.23
70	82.97	81.77	75.65	80.73	0.42	0.41	0.40	0.40
90	80.50	79.74	68.50	77.56	0.52	0.51	0.50	0.50
150	67.14	64.38	50.40	64.98	0.72	0.69	0.69	0.70
200	55.71	55.14	40.09	53.59	0.80	0.79	0.78	0.77

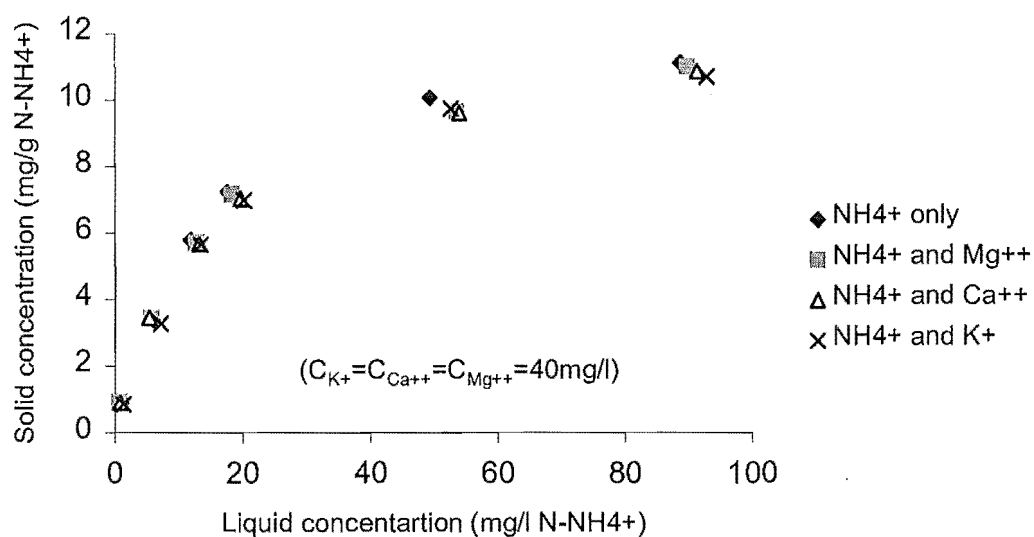


Figure 4.9 Ammonium ion uptake onto mordenite in the presence of magnesium, calcium and potassium ions

The influence of other cations on ammonia removal is smaller for mordenite than for clinoptilolite. The differences in the data obtained are within the limits of uncertainty so that any conclusion in terms of selectivity will not be reliable.

However, results obtained for the uptake onto MN 500 given in the following table and in Figure 4.10 give clear indication that the order of preference was $Mg^{++} > Ca^{++} > K^{+}$. The order of concentration of metal ions in the solution expressed in the meq/g was the same, 3.3, 2 and 1 meq/g for Mg^{++} , Ca^{++} and K^{+} respectively. We can conclude that compared to clinoptilolite, the effect of other cations on ammonia removal onto MN 500 is consistently greater across the whole range of the initial concentrations. The reduction by 8.58% of the amount of ammonia removed was obtained for MN 500 compared to the value of 6.19% for clinoptilolite for the 200mg/l initial $N-NH_4^{+}$ concentration.

Table 4.9 Uptake data for ammonium ion onto MN 500 in the presence of magnesium, calcium and potassium ions

Init. $N-NH_4^{+}$ (mg/l)	Percentage of removed ammonia				Capacity for different conc. (meq/g)			
	NH_4^{+} only	Mg	Ca	K	NH_4^{+} only	Mg	Ca	K
10	96.80	88.56	91.59	93.87	0.07	0.06	0.07	0.07
40	92.13	84.03	86.92	89.50	0.26	0.24	0.25	0.26
70	86.97	78.26	81.70	84.34	0.43	0.39	0.41	0.42
90	83.36	74.78	78.25	81.01	0.54	0.48	0.50	0.52
150	73.41	64.82	68.42	71.42	0.79	0.69	0.73	0.77
200	67.12	58.54	61.58	64.67	0.96	0.84	0.88	0.92

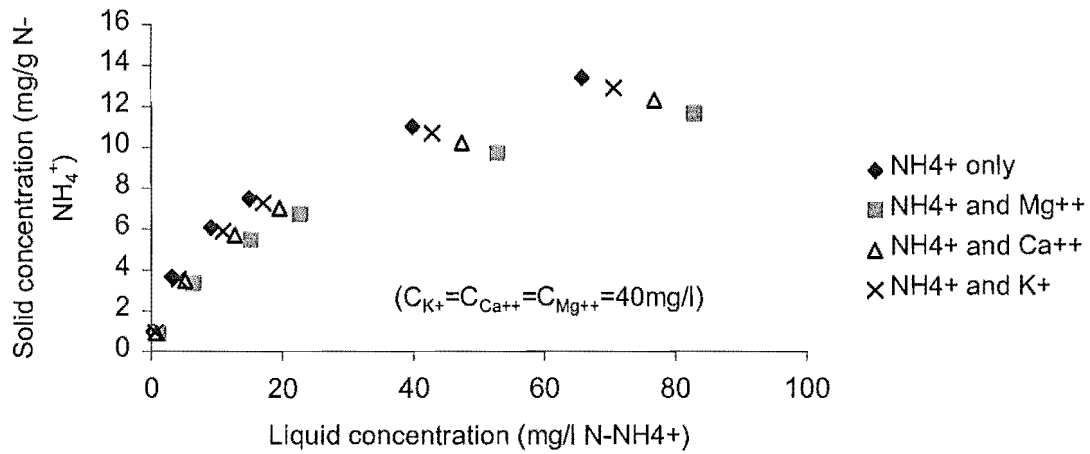


Figure 4.10 Ammonium ion uptake onto MN 500 in the presence of magnesium, calcium and potassium ions

4.2.1.3 Modelling of the uptake data

The equilibrium data obtained (relationship between solution phase ammonia concentration and ion-exchanger phase concentration) were compared with the Langmuir and Freundlich models. Rearranging the Langmuir equation (Section 1.4.1) gives equation 4.1, which is linear.

$$\frac{1}{Q_e} = \frac{1}{KbC_e} + \frac{1}{b} \quad (4.1)$$

where:

- Q_e - concentration of adsorbate on the adsorbent (mg/g),
- C_e - adsorbate liquid concentration (mg/l),
- K - Langmuir constant (l/mg)
- b - Langmuir adsorption capacity constant (mg/g).

After equilibrium was reached, C_e was measured, Q_e was calculated by mass balance and the coefficients K and b can thus be determined by plotting $1/C_e$ v $1/Q_e$ (see Appendix II).

The Freundlich isotherm can also be presented by the linear equation

$$\log Q_e = \log k + 1/n \log C_e \quad (4.2)$$

where: - k – parameter in the Freundlich equation (l/g),

- n – parameter in the Freundlich equation.

Hence the coefficients k and n can be calculated by plotting $\log Q_e$ against $\log C_e$. Knowing the coefficients and using experimental data for C_e , the Langmuir and Freundlich theoretical Q_e can be calculated. The detail calculation is given in Appendix II. The model fit obtained for clinoptilolite, mordenite and MN 500 without other cations present in the solution are given in the Figures 4.11, 4.12 and 4.13 respectively. Tables 4.10-4.12 show the calculated isotherm parameters for the given isotherms, as well as for the adsorption when interfering metal ions were present in the solution.

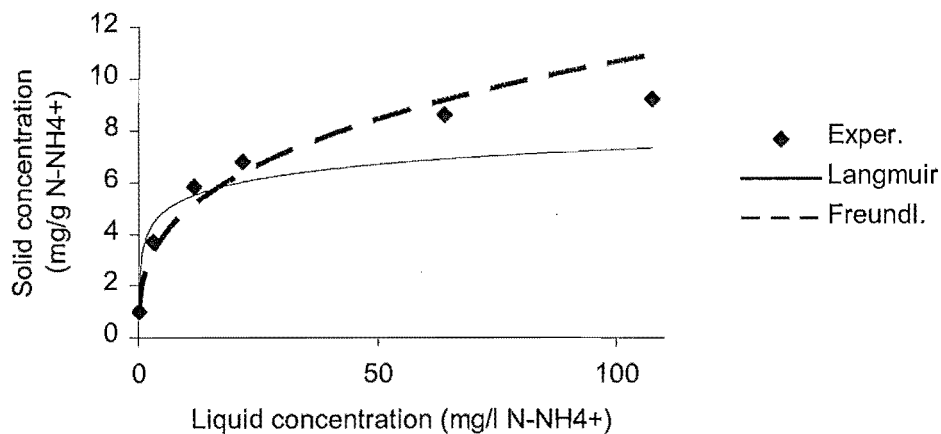


Figure 4.11 Equilibrium isotherm data for ammonium uptake onto clinoptilolite fitted to the Langmuir and the Freundlich adsorption models

Table 4.10 Values for the Langmuir and Freundlich coefficients for the clinoptilolite $C_{N-NH_4^+} = 10-200\text{mg/l}$, particle size: 0.7-1mm

Langmuir parameter	NH_4^+ only	Mg	Ca	K
b	6.588	7.123	6.821	6.920
K	1.493	0.289	0.249	0.405
r^2	0.982	0.993	0.994	0.994
Freundlich parameter				
k	2.270	1.496	1.365	1.675
$1/n$	0.336	0.415	0.414	0.382
r^2	0.978	0.951	0.951	0.944

For the adsorption onto clinoptilolite, in all cases the Langmuir model provides a slightly more consistent fit to the data compared with the Freundlich. At lower concentrations (up to $70\text{mg/l } N-NH_4^+$) the fit is satisfactory in both cases. At higher concentrations neither model provides an accurate fit.

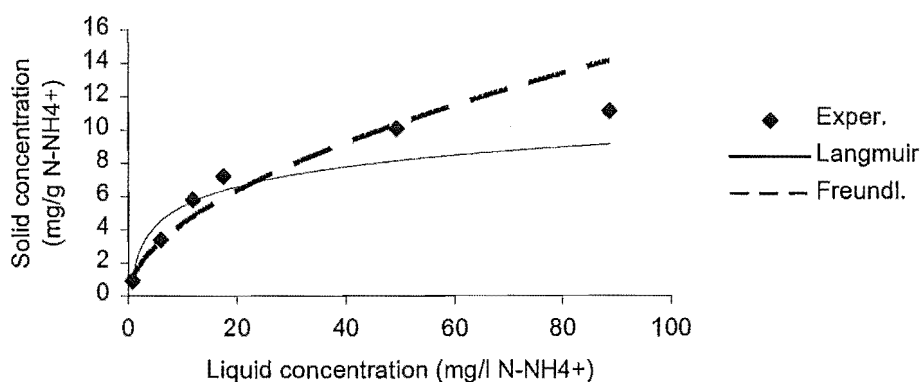


Figure 4.12 Equilibrium isotherm data for ammonium uptake onto mordenite fitted to the Langmuir and the Freundlich uptake models

Table 4.11 Values for the Langmuir and Freundlich coefficients for the mordenite $C_{N-NH_4^+} = 10-200\text{mg/l}$, particle size: 0.7-1mm

Langmuir parameter	NH_4^+ only	Mg	Ca	K
b	9.479	8.865	9.615	13.089
K	0.139	0.149	0.128	0.051
r^2	0.993	0.990	0.997	0.999
Freundlich parameter				
k	1.255	1.215	1.240	0.908
$1/n$	0.540	0.536	0.528	0.607
r^2	0.961	0.965	0.962	0.942

Values from Table 4.11 indicate that the Langmuir model provides a slightly more consistent fit to the mordenite data compared with the Freundlich model. Similar behavior to that observed for clinoptilolite can be noticed; at lower concentrations the fit is satisfactory in both models while at higher concentrations neither model provides an accurate fit except for potassium, where results obtained for mordenite fit the Langmuir model very well across the whole range of concentrations.

The Langmuir maximum NH_4^+ removal capacity (b) for mordenite (9.479 g/kg) is higher than the one for clinoptilolite (6.588g/kg) which is consistent with the higher uptake capacity for mordenite reported earlier. However, this is not always the case (Nguyen and Tanner, 1998), which is proved through the values for the same constants when interfering cations were present. The values for the maximum removal capacity should be smaller when interfering cations were present compared to the values obtained when only ammonia was present in the solution. This lack of correlation was probably due to the fact that for the higher concentrations, the model did not provide an accurate fit.

When compared with published results, values for both the Langmuir constants obtained here are higher than the values reported for New Zealand clinoptilolite and mordenite (Nguyen and Tanner, 1998) which again is in correlation with the higher ammonia uptake capacities for both the materials reported here.

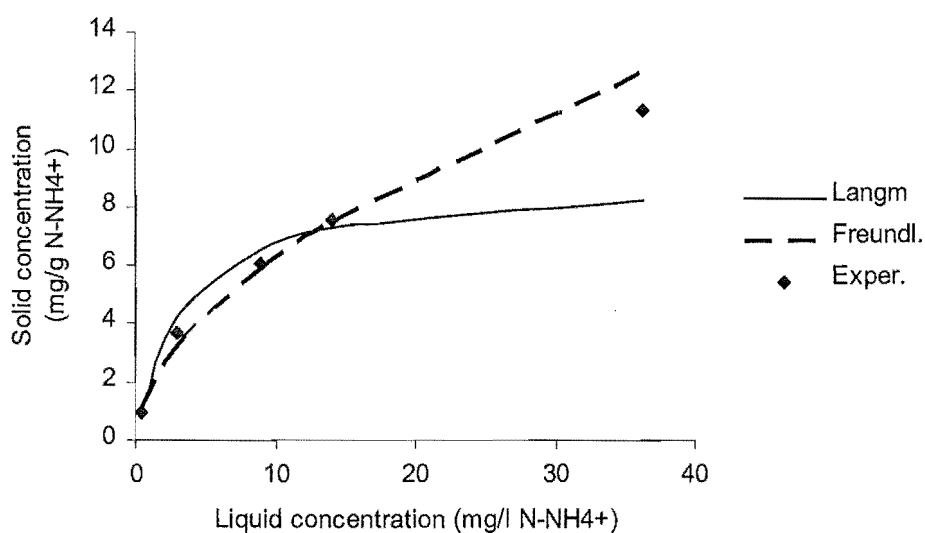


Figure 4.13 Equilibrium isotherm data for ammonium uptake onto MN 500 fitted to the Langmuir and the Freundlich uptake models

Table 4.12 Values for the Langmuir and Freundlich coefficients for the MN 500 $C_{N-NH_4^+} = 10-200\text{mg/l}$, particle size: 0.7-1mm

Langmuir parameter	NH_4^+ only	Mg	Ca	K
b	9.025	10.905	10.438	10.060
K	0.296	0.048	0.114	0.167
r^2	0.996	0.999	0.997	0.996
Freundlich parameter				
k	1.754	0.953	1.173	1.416
$1/n$	0.549	0.599	0.574	0.551
r^2	0.987	0.980	0.981	0.983

According to the results obtained for the uptake onto MN 500, it looks like the uptake onto this material lies between the values predicted by the two proposed mathematical models. Similar results were reported by Jorgensen (2002) for ammonia removal on to MN 500 in the presence of the organics and by Singh and Prasad (1997) for ammonia removal on to synthetic zeolite. It is concluded that the synthetic materials are more likely to follow the Freundlich adsorption model for ammonia removal, which means that either the adsorption surface is not homogeneous (all sites are not equally available for adsorption) or that the adsorbate on the synthetic materials does not form only one layer on the adsorbent surface. The other possible reason is swelling of the synthetic resins. Jorgensen

(2002) excluded the possibility that, on MN 500 adsorption of ammonia is occurring rather than ion exchange.

4.2.2 Saline water

In Section 1.3.1 the problem of ammonia accumulation in sea water was underlined and the necessity of finding reliable means of removing it. Experimental equilibrium studies in saline water were conducted based on the procedure described in Section 3.2.1.2.

The first goal of this section was to identify materials with the best characteristics for ammonia removal from saline water. Subsequently, the chosen materials would be biologically activated if possible, in order to improve ammonia uptake. Synthetic ion exchanger MN 500 as well as products of the zeolitic nature (ZZ, Mg.NZ and Zecer 56) were chosen for the preliminary uptake experiments.

The results of each batch experiment were calculated using aqueous phase analysis for ammonium ion concentrations. The uptake of the ammonium ion onto the exchanger was calculated from the initial and final solution concentration, the amount of exchanger added and the solution volume. The adsorption and ion exchange process were not quantified separately. The results obtained for each system were fitted to the Langmuir and Freundlich adsorption models (as explained in the previous section) and are presented in Figures 4.14-4.16 for MN 500, ZZ and Mg.NZ respectively. The particle size in all the experiments was in the range 0.7-1mm and the salinity of the artificial sea water was maintained at 40g/l.

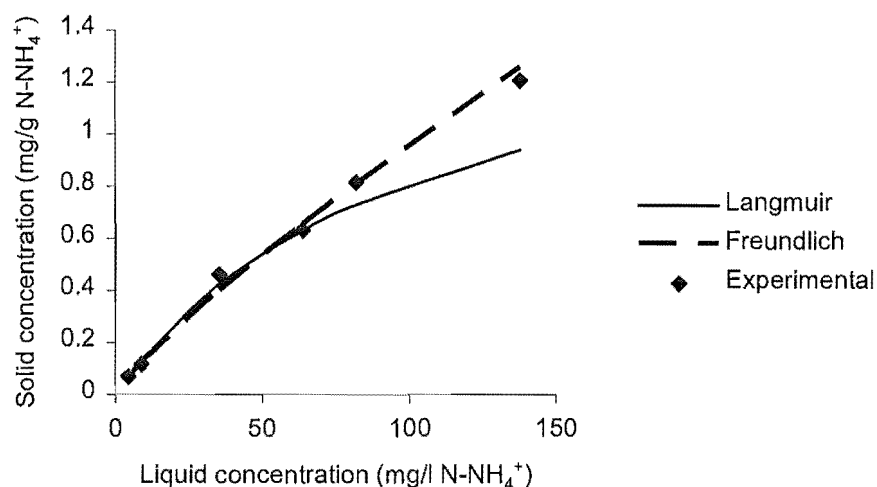


Figure 4.14 Equilibrium isotherm for ammonia uptake onto MN 500 from saline water

The percentage of ammonia ion removed varied from 13.93% to 8.05% and decreased as the initial ammonia concentration increased. At the lower initial ammonia concentrations (5, 10, 40 and 70mg/l calculated as N-NH₄⁺) both theoretical models can be used to describe the ammonia adsorption onto the MN 500 while at the higher concentrations (90 and 150mg/l) the Freundlich adsorption isotherm provided a better fit.

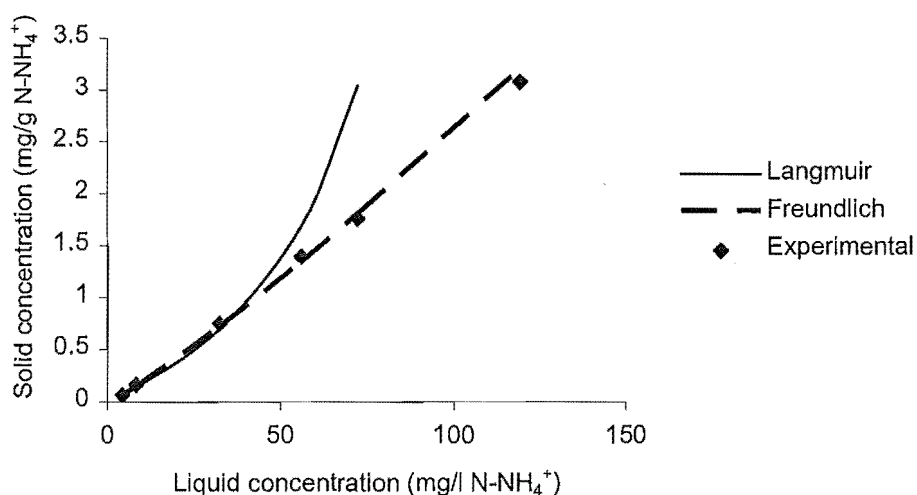


Figure 4.15 Equilibrium isotherm for ammonia uptake onto ZZ from saline water; model fitting

The percentage of ammonium ion removed was generally higher (varied from 13.30% to 20.50%) and increased as initial ammonia concentration increased. In the case of modified zeolite ZZ there was a difference in the equilibrium results, as seen in Figure 4.15. Across the whole range of concentrations, the ammonium ion uptake data was accurately fitted only to the Freundlich isotherm relationship.

Equilibrium results for Mg.NZ are similar to those obtained for MN 500. For smaller initial ammonium ion concentrations (5, 10 and 40mg/l) both theoretical models could be applied, while for the higher concentrations, (90 and 150mg/l) the Freundlich model would be more accurate, although not as precise as it was for MN 500 and ZZ. The percentage of ammonium ion removed varied from 12.87% to 15.93% and its decrease and increase did not seem to depend upon the initial ammonium ion concentration in any direction. This can be seen more clearly from Table 4.13 where equilibrium results for MN 500, ZZ and Mg.NZ are compared.

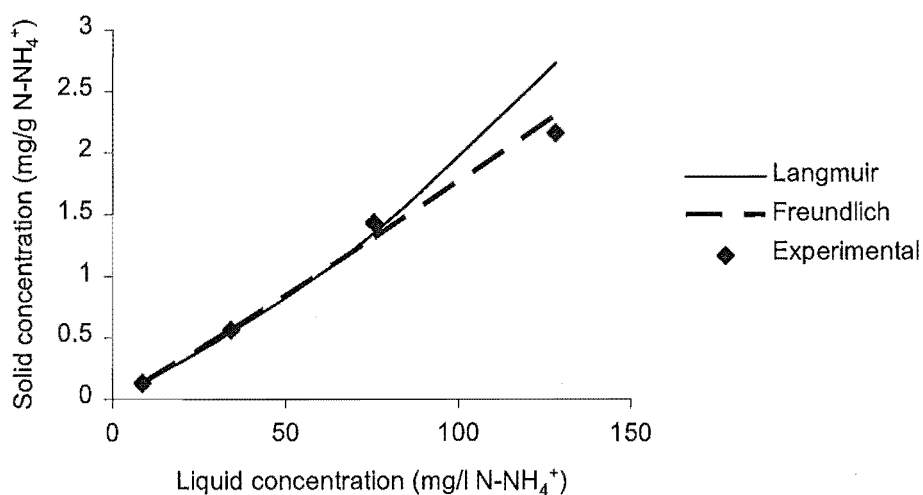


Figure 4.16 Equilibrium isotherm for ammonia uptake onto Mg.NZ from saline water

Table 4.13 Equilibrium data for ammonia uptake onto MN 500, ZZ and Mg.NZ from saline water; (Init. conc. and C_e = [mg/l], $Q_{e_{exp}}$ = [mg/g])

Init. Conc.	MN 500			ZZ			Mg.NZ		
	C_e	$Q_{e_{exp}}$	Per. rem.	C_e	$Q_{e_{exp}}$	Per. rem.	C_e	$Q_{e_{exp}}$	Per. rem.
5	4.30	0.07	13.93	4.34	0.07	13.30	4.33	0.07	13.93
10	8.84	0.12	11.64	8.33	0.17	16.69	8.71	0.13	12.87
40	35.37	0.46	11.57	32.50	0.75	18.74	34.35	0.56	14.12
70	63.66	0.63	9.06	56.06	1.39	19.91	-	-	-
90	81.83	0.82	9.08	72.40	1.76	19.56	75.66	1.43	15.93
150	137.92	1.21	8.05	119.25	3.08	20.50	128.34	2.17	14.44

Values for the coefficients calculated by using experimental data for ammonium uptake by each material are given in Table 4.14.

Table 4.14 Values for the Langmuir and Freundlich coefficients for ammonia uptake onto MN 500, ZZ and Mg.NZ from saline water

Langmuir parameter	MN 500	ZZ	MgNZ
b	1.611	-1.760	-5.828
K	0.010	-0.009	-0.003
r^2	0.991	0.987	0.999
Freundlich parameter			
k	0.202	0.014	0.013
$1/n$	0.839	1.143	1.069
r^2	0.996	0.998	0.997

Table 4.15 represents the adsorption data for Zecer 56. These results cannot be modelled with either of the two theoretical models used in this work. It seems that this ion-exchange material has a smaller number of sites available for the ammonium ion uptake compared to the other materials studied here. But it also appears that these sites are highly selective for ammonium uptake in the presence of other cations in the seawater (mainly Ca^{++} , Mg^{++} and K^+). It therefore appears that they become saturated even if ammonium ions are present in small concentrations since ammonium ion uptake is not significantly increased with increased concentration. This could be the reason that Zecer 56 showed the best results for the small initial concentrations (5mg/l) when 24.10% of ammonia was removed, while the other materials had only up to the 14% of removal for the same initial concentration.

Table 4.15 Equilibrium data for ammonia uptake onto Zecer 56 from saline water

Initial concentr.	Ce (mg/l)	Q _e _{exp} (mg/g)	Percentage removed
5	3.79	0.12	24.1
10	8.14	0.19	18.65
40	37.08	0.29	7.3
70	65.76	0.42	6.06
90	86.68	0.33	3.69
150	148.64	0.14	0.91

All the ion-exchangers not only removed ammonium ions but also other cations present in the solution. The uptake of Ca^{++} , Mg^{++} and K^+ was also measured in order to establish which, if any, contributed to inhibition of ammonium ion uptake. The results are shown in Table 4.16. Since the amounts of K^+ , Mg^{++} and Ca^{++} are much greater when compared to the concentration of other ions present in saline water (concentrations of K^+ , Mg^{++} and Ca^{++} were 321.8mg/l, 1129.0mg/l and 457.5mg/l respectively) only these cations were measured. Since some of the materials were initially in the sodium form, this metal concentration was not tracked, although it is present in saline water.

Since the valence of the measured cations and therefore the number of the occupied sites is different, the results in Table 4.16 are given in “milliequivalents removed per gram of dry material”. This gave a better comparison and it can be seen that each material exhibited different behaviour in terms of selectivity for potassium, magnesium and calcium.

Table 4.16 Inhibitory effect of other cations on ammonia removal from saline water

Reduction in ion-exchange capacity for NH_4^+ (meq/g)				
	<i>MN 500</i>	<i>ZZ</i>	<i>Mg.NZ</i>	<i>Zecer 56</i>
K^+	0.36	4.69	5.08	2.14
Mg^{++}	3.01	1.08	4.16	5.98
Ca^{++}	0.87	0	0	4.64

In terms of K^+ uptake, ZZ and Mg.NZ have similar behaviour to natural zeolites, which generally have slightly higher selectivity for K^+ than NH_4^+ cations (McVeigh, 1999). It is interesting that Ca^{++} does not inhibit uptake of NH_4^+ on these two materials at all. Mg^{++} significantly inhibited NH_4^+ uptake onto MN 500, while Ca^{++} and K^+ were removed in smaller amounts. The inhibitory effect on Zecer 56 was caused mainly by divalent cations. It can be seen that the overall inhibitory effect was the smallest on MN 500 and ZZ. The fact that MN 500 removed relatively small quantities of K^+ compared to ammonia (see Table 4.13) possibly indicates that not only ion exchange but also some adsorption took place on the surface of this material. This possibility was excluded for the fresh water in the previous section, but since the ionic composition of the saline water was significantly different, adsorption still might be possible.

4.3 Batch equilibrium studies with bacteria

4.3.1 Ammonia removal on biologically active materials in fresh water

Section 3.2.2 of this work outlined the details of the experiments done in this area. Results obtained for the ammonia removal by bacteria in the flasks containing zeolites as well as MN 500 are given in the Figure 4.17 and Table 4.16.

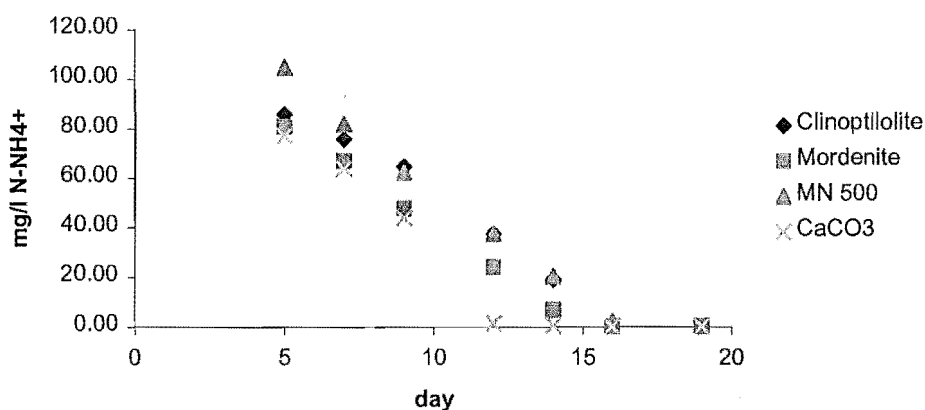


Figure 4.17 Reduction in ammonia concentration in the flask containing nitrifying bacteria and ion exchangers which were ammonia saturated prior to use (fresh water)

Table 4.17 Reduction in ammonia concentration (mg/l N-NH_4^+) in a flask containing nitrifying bacteria and different materials (initial $\text{CN-NH}_4^+=152.2\text{mg/l}$ in solution, without ammonia on the materials).

Day	Clinoptilolite	Mordenite	MN500	CaCO_3
5	85.83	81.10	105.02	77.45
7	75.83	66.99	81.97	63.75
9	64.66	47.69	62.41	43.96
12	37.49	24.00	37.49	1.51
14	19.06	6.85	20.46	0.72
16	0.30	0.13	2.36	0.30
19	0.19	0.37	0.13	0.15

The best ammonia concentration reduction is observed in the flask containing CaCO_3 as a bacteria carrier (ammonia concentration in solution dropped below 1mg/l after 14 days). This is expected as all other materials were ammonia saturated prior to the experiment and slow desorption occurred during the observed period, increasing the overall ammonia concentration in the solution. In the flasks containing zeolites, ammonia concentration reached values below 1mg/l after 16 days, while the flask with MN 500 had the slowest rate of ammonia reduction. This is in agreement with the highest reported uptake capacity for the synthetic ion exchanger (0.96meq/g compared to the values of 0.66 and 0.80meq/g for clinoptilolite and mordenite respectively). Even though mordenite has a higher uptake capacity, and therefore had more ammonia adsorbed at the beginning of the experiment, overall ammonia reduction was better in the flask containing this zeolite compared to the flask with clinoptilolite. This can be attributed to the better conditions for bacteria growth on the surface of the mordenite compared to the surface of clinoptilolite. One possible reason for this phenomenon might be so called “nutritional effect” reported by Vieira et al. (2001). They suggested that adding kaolin (a mineral which consists mainly of Al_2O_3 and SiO_2) improved nitrification due to the release of some ions which acted like oligoelements and contributed to the bacterial metabolism.

Mass balances were done only for the flask containing CaCO_3 since all other materials were ammonia saturated before the bacteria broth was added. Therefore, the ammonia concentration at the time of sampling could not be calculated since

the amount still retained by the material could not be determined. Data showing the changes in nitrate, nitrite, ammonium and total nitrogen are presented in Figure 4.18.

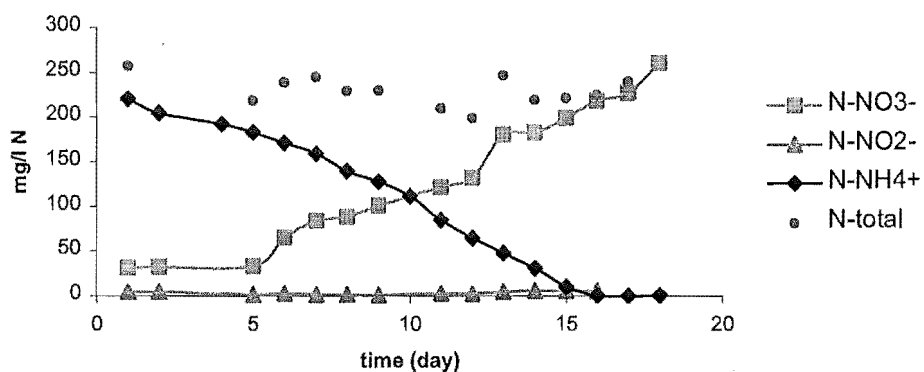


Figure 4.18 Nitrite, nitrate, ammonia and total nitrogen concentration for nitrification in DI water (CaCO_3)

Table 4.18 Nitrite, nitrate, ammonia and total nitrogen concentration for nitrification in DI water (CaCO_3)

Days	Ammonia (mg/l N-NH_4^+)	Nitrite (mg/l N-NO_2^-)	Nitrate (mg/l N-NO_3^-)	Total nitrogen (mg/l N) ($\sigma^*=15.44$)
1	220.50	5.04	31.5	257.04
2	204.75	4.52		
4	192.50			
5	183.22	1.74	33.6	218.56
6	171.55	2.98	65.1	238.95
7	159.30	1.79	84	245.08
8	139.64	1.62	88.2	229.46
9	128.08	1.22	100.8	230.02
10	111.82	27.05		
11	84.87	3.17	121.8	209.84
12	64.42	2.56	132.3	199.28
13	48.10	18.23	180.6	246.93
14	30.84	5.96	182.7	219.5
15	10.36	11.42	199.5	221.28
16	0.50	5.92	218.4	224.81
17	0.25	12.35	226.8	239.39
18	0.31		260.4	

* Standard deviation

The calculated total nitrogen concentration over the 19 - days period has a standard deviation of 15.44, which is 6.55% of the mean value of 229 mg/l. This variation could not be attributed to the nitrogen loss, since there is no constant decrease in total nitrogen concentration. It is likely that it is due to the errors made during the weight and ammonia measurements.

Results presented in Figure 4.17 indicated that neither of the ion exchangers had an inhibitory effect on the nitrification process and that zeolites might be a better option for the combined biological and ion exchange process than a synthetic exchanger.

Based on the ammonia depletion over time data and using the equation 4.3 (Horan, 1991) the specific growth rate (μ) of nitrifying bacteria in the flask containing CaCO_3 was calculated. Calculation in detail is given in Appendix IV.

$$\ln X = \ln X_0 + \mu t \quad (4.3)$$

where: - X – cell concentration;
 - X_0 – cell concentration at $t=0$;
 - t – time
 - μ – specific growth rate.

A value of specific growth rate of 0.01h^{-1} was obtained, which was lower than the value of 0.07h^{-1} reported by McVeigh for bacteria growth in a packed bed of clinoptilolite and the values of 0.03 and 0.05h^{-1} reported by Keen (1984) and Ydstebo (1991) respectively. A value of 0.05h^{-1} was obtained for the growth on a porous glass medium which probably had a higher surface area which allowed better bacteria colonisation. The maximum growth rate obtained by Orhon et al. (2000), which was 0.01h^{-1} and 0.004h^{-1} for 20°C and 10°C respectively for tannery wastewater, is lower than the value reported here. These results are for the growth in the presence of the heterotrophic organisms which compete strongly with nitrifying organisms. Rozich and Castens (1986) obtained a value of 0.05d^{-1}

for growth in a synthetic medium free of organic carbon to discourage the growth of competitive heterotrophic organisms. There were similar conditions in our experiment, since organic matter was not present in large concentrations. However, Rozich and Castens' start-up phase of the reactor, before the reported growth rate was measured, was a period of six weeks; whereas we started measurements one day after the inoculum was introduced into the broth. In addition, their initial ammonia concentrations were only 100mg/l N-NH_4^+ compared to our concentration of 220mg/l N-NH_4^+ . The lower concentration might provide better conditions for bacterial growth in terms of substrate inhibition. The specific growth was not calculated for the growth on ion exchangers since it was not possible to measure exact ammonia concentrations in the flasks with this material for the reasons described above.

In order to compare adsorption on biologically active and non-active materials, batch experiments were carried out following the procedure explained in Section 3.2.2 of this work. A brief outline of the procedure is given in Figure 4.19.

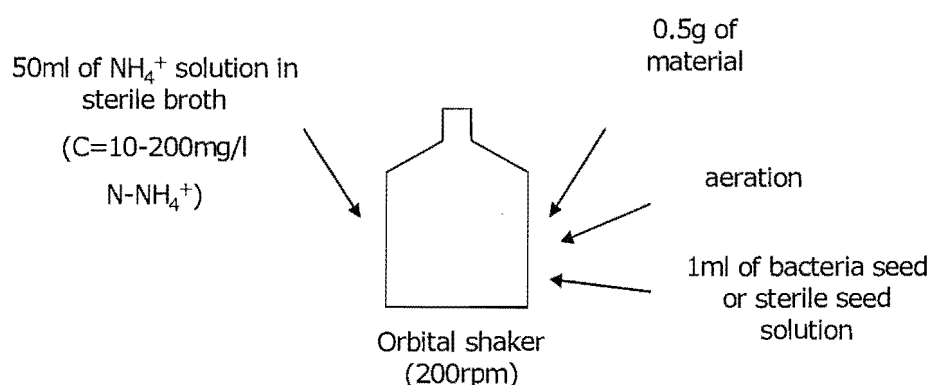


Figure 4.19 Ammonia removal onto biologically active materials

The results obtained for the non-saline medium are presented in Table 4.19. The results of each batch experiment were calculated using aqueous phase analysis for ammonium ion concentrations. The uptake of the ammonium ion onto the

exchanger without bacteria was calculated from the initial and final solution concentrations, the amount of exchanger added and the solution volume. For the bacteria-active materials, all ammonia still captured in the material was replaced by potassium chloride and measured. The solid phase concentration was then recalculated based on the mass of the ion exchanger added. The solid phase concentration (Q_e) is expressed in $mg\ N-NH_4^+/g\ of\ exchanger$.

Table 4.19 Ammonia removal on biologically free and active materials in non saline water.

a)

Init. amm. conc. (mg/l N-NH ₄)	Clinoptilolite			
	without bacteria		with bacteria	
	%	Qe(mg/g)	%	Qe(mg/g)
	removed		removed	
10.08	84.69	0.85	97.73	0.02
40.08	78.51	3.15	98.72	0.05
70.08	70.23	4.92	98.48	0.14
90.08	59.86	5.39	83.30	1.84
150.08	51.73	7.76	84.17	2.41
200.08	48.46	9.70	86.72	2.35

b)

Init. amm. conc. (mg/l N-NH ₄)	Mordenite			
	without bacteria		with bacteria	
	%	Qe(mg/g)	%	Qe(mg/g)
	removed		removed	
10.08	83.13	0.84	95.91	0.03
40.08	91.56	3.27	98.58	0.04
70.08	75.71	5.31	99.16	0.05
90.08	71.84	6.47	93.32	0.36
150.08	65.01	9.76	84.00	2.05
200.08	54.97	11.00	84.03	2.12

c)

Init. amm. conc. (mg/l N-NH ₄)	MN 500			
	without bacteria		with bacteria	
	%	Qe(mg/g)	%	Qe(mg/g)
	removed		removed	
10.08	58.04	0.59	74.08	0.21
40.08	55.13	2.21	71.28	1.00
70.08	48.92	3.43	71.43	1.79
90.08	43.94	3.96	79.44	1.65
150.08	43.39	6.51	68.98	4.31
200.08	38.42	7.69	67.97	6.02

The results show that removal of ammonia is generally better on natural materials (clinoptilolite and mordenite) when compared to the synthetic ion exchanger MN 500. This can be noticed on biologically free materials as well as on the materials that had bacteria attached. Therefore, natural zeolites not only have higher ammonia capacity when other ions are present in the solution, but also are better media for bacterial growth. Section 4.1.1.2 outlined the results for ammonia ion capacities without any interfering ions, as well as the effect of individual ions commonly present in water on ammonium ion uptake. In such conditions the synthetic ion exchanger had the greatest values for ammonium uptake, but also the reduction in capacity, when other cations were present, was also the biggest. Therefore, the results obtained in this section can be explained by the fact that zeolites have a lower ion-exchange capacity than many synthetic ion-exchange resins, but they generally exhibit a high selectivity for NH_4^+ ions. Since the bacteria broth contained not only ammonium but other cations (see Appendix III) the ammonium uptake onto MN 500 was significantly reduced.

If mordenite is compared to clinoptilolite, first we can notice that without bacteria, mordenite exhibited better ammonia removal at higher initial ammonia concentrations, which is in agreement with our previous results. In terms of biological regeneration both materials show similar results, which suggest that the nitrifiers perform more effectively on the clinoptilolite compared to the mordenite. According to the literature data (Siddiqi, 1967), high ammonia concentration (over 80mg/l) will cause very significant nitrification inhibition, which did not happen in our experiments, probably because the ion exchange materials served as a buffer to protect the bacterial population from fatal initial ammonia concentrations. Once that ammonia from the solution was oxidized by bacteria, more ions were released from the material and the process continued.

4.3.2 Ammonia removal on biologically active materials in saline water

The experiments in saline water were done following the same procedure as explained above, with the only difference being that instead of bacterial broth

made in non-saline water, the artificial sea water with salinity of 20g/l was used as a base for the growth medium for nitrifying organisms. The procedure in detail is given in Section 3.2.2 and Appendix III. Results obtained for the ammonia removal by bacteria in the flasks containing ammonia saturated ZZ and MN 500, as well as CaCO_3 are given in Figure 4.20 and Table 4.19.

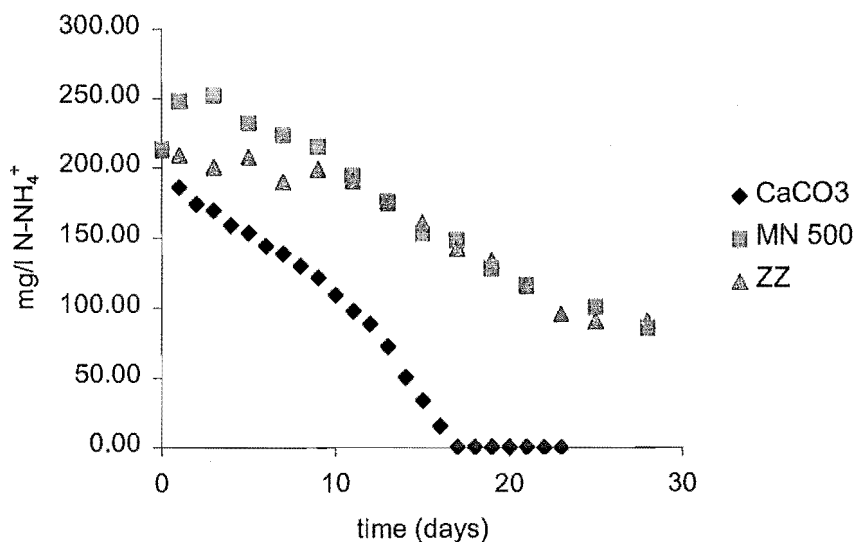


Figure 4.20 Reduction in ammonia concentration in the flask containing nitrifying bacteria and ion exchangers which were ammonia saturated prior to the use (saline water)

Table 4.20 Reduction in ammonia concentration in a flask containing nitrifying bacteria and different materials

Days	CaCO ₃	MN 500	ZZ
0	213.08	213.08	213.08
1	185.87	247.77	209.29
2	174.13		
3	169.24	252.26	200.46
4	159.19		
5	153.46	232.26	207.79
6	144.35		
7	139.15	223.26	189.94
8	130.37		
9	122.13	215.39	199.02
10	109.40		
11	98.00	194.78	190.63
12	88.86		
13	72.77	176.15	175.51
14	50.62		
15	33.81	153.12	161.02
16	15.84		
17	0.26	148.25	142.51
18	0.26		
19	0.25	128.41	133.59
20	0.25		
21	0.25	116.55	116.13
22	0.18		
23	0.15		95.66
25		100.95	90.64
28		85.89	90.32

In the flask containing CaCO₃, ammonia was completely removed after 17 days. In the flask with MN 500, nitrification was slower, but still was going on after 28 days with ammonia levels being reduced to the values of 86mg/l N-NH₄⁺, while in the flask containing ZZ, the biological process stopped after 25 days. The next graph represents nitrate levels in each flask, which will show that the order of nitrate concentration in the flasks was the same (CaCO₃>MN 500>ZZ).

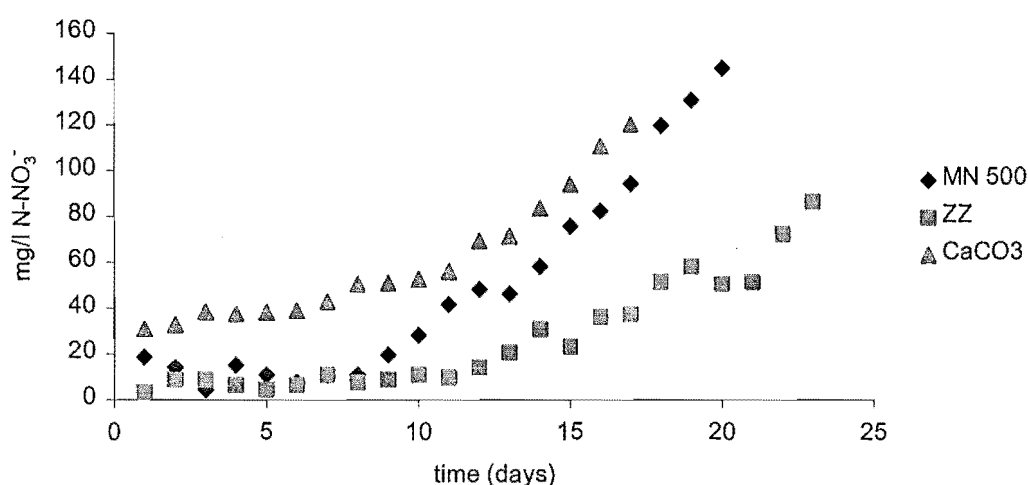


Figure 4.21 Nitrate concentration in the flasks with different ammonia saturated MN 500 and ZZ as well as with CaCO₃ (saline water)

Figure 4.22 and Table 4.21 give the nitrogen mass balance for the nitrification process in saline water. Constant nitrogen loss is obvious during the experiment. Since the pH was checked and regularly adjusted, the possibility was excluded that the high pH caused more unionised ammonia in the solution, which would be air stripped during the aeration of the flask.

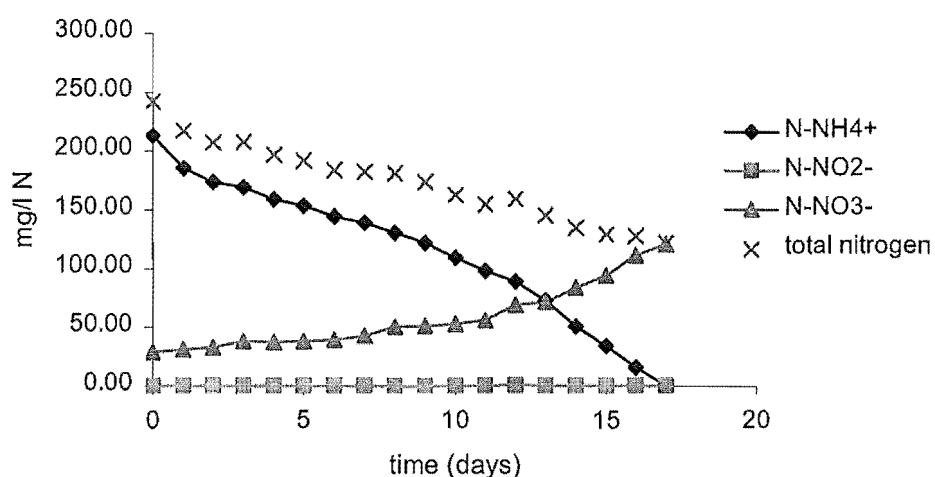


Figure 4.22 Nitrite, nitrate, ammonia and total nitrogen concentration for nitrification in saline water (CaCO₃)

Table 4.21 Nitrite, nitrate, ammonia and total nitrogen concentration for nitrification in saline water (CaCO_3)

Days	Ammonia (mg/l N- NH_4^+)	Nitrite (mg/l N- NO_2^-)	Nitrate (mg/l N- NO_3^-)	Total nitrogen
0	213.08	0.21	29	242.29
1	185.87	0.27	31	217.15
2	174.13	0.36	33	207.49
3	169.24	0.23	38.5	207.97
4	159.19	0.25	37.7	197.15
5	153.46	0.32	38.4	192.17
6	144.35	0.25	39.1	183.71
7	139.15	0.29	42.9	182.35
8	130.37	0.15	50.6	181.11
9	122.13	0.08	51.2	173.42
10	109.40	0.40	52.8	162.60
11	98.00	0.53	56.1	154.62
12	88.86	1.01	69.3	159.17
13	72.77	0.55	71.5	144.81
14	50.62	0.46	83.6	134.69
15	33.81	0.67	94.1	128.58
16	15.84	0.65	111	127.49

If nitrites and nitrates loss was the reason for the total nitrogen reduction, then the same method used for specific growth calculation, applied for growth in non-saline water, can be used here. A value of 0.004h^{-1} was obtained, which, as expected, was lower than the value for the growth in a non-saline medium. The calculation in detail is given in Appendix IV.

Results obtained for the MN 500 and ZZ in a saline medium when the materials were not ammonia saturated and the initial ammonia concentrations varied between 10 and 200mg/l N-NH_4^+ , are presented in Table 4.22.

Table 4.22 Ammonia removal on biologically free and active materials in saline water.

a)

Init. amm. conc. (mg/l N-NH ₄)	MN 500			
	<i>without bacteria</i>		<i>with bacteria</i>	
	%	Q _e (mg/g)	%	Q _e (mg/g)
	<i>removed</i>		<i>removed</i>	
10.02	47.94	0.48	67.65	0.06
40.02	46.84	1.87	88.07	0.10
70.02	47.46	3.32	93.86	0.08
90.02	49.72	4.48	92.94	0.11
150.02	52.51	7.88	85.25	0.37
200.02	52.05	10.41	78.74	0.61

b)

Init. amm. conc. (mg/l N-NH ₄)	ZZ			
	<i>without bacteria</i>		<i>with bacteria</i>	
	%	Q _e (mg/g)	%	Q _e (mg/g)
	<i>removed</i>		<i>removed</i>	
10.02	26.69	0.27	61.78	0.17
40.02	62.17	2.49	61.57	0.54
70.02	60.04	4.20	68.15	0.76
90.02	63.23	5.69	66.13	1.00
150.02	57.93	8.69	63.88	1.60
200.02	57.69	11.54	64.66	1.89

ZZ exhibited better removal than MN 500 when the medium was bacteria free, which is in agreement with the results from Section 4.2.2. While in non saline water MN 500 did not show good biological regeneration, it served as a good medium for bacteria growth in saline water. Since better nitrification was obtained with MN 500, we had less ammonia remaining on this material compared to the ZZ once the process was finished (Q_e values from the Table 4.22). A possible reason for better nitrification on MN 500 is that during the process of modification of the natural material, the structure has been changed so that the surface is not suitable for bacteria growth any more. Another reason for better

performance of synthetic material might be that during the process of material pre-treatment not all zinc ions were replaced with the sodium ions and that the remaining zinc accumulates and reaches a concentration, at which an inhibitory effect on nitrifying bacteria occurs. If this is the case, it should be eliminated in column experiments where all eventually-released zinc would be eventually washed out with the passing solution without accumulation. Although both materials used have significantly less capacity for ammonia removal in sea water due to the high concentrations of other salts, the buffering effect in solutions with high initial ammonia concentrations still exists to protect bacteria from ammonia inhibition at the beginning of the process. Column experiments in a saline medium with bacteria would have to be carried out in brackish water, which has less salinity (see section 1.6) to prevent saturation of the column too early, since many other cations, together with ammonium are present in the saline water.

4.4 Kinetic studies

4.4.1 MN 500

The kinetics of ammonia removal onto synthetic and natural ion exchangers were studied by applying the experimental procedure explained in Section 3.2.3 of this work. The results obtained were correlated using models already present in the literature. These are reviewed in Section 1.4.5.1 and the values for the particle characteristics are shown in Table 4.4. Values for the adsorption isotherms constants were calculated and are presented in Section 4.1.1.3. Calculation of the diffusion coefficients in detail is explained in Appendix V.

4.4.1.1 External Mass Transfer Model

Results for the reduction of ammonia concentration over time due to adsorption onto synthetic ion exchanger MN 500 are given in Figures 4.23-4.26.

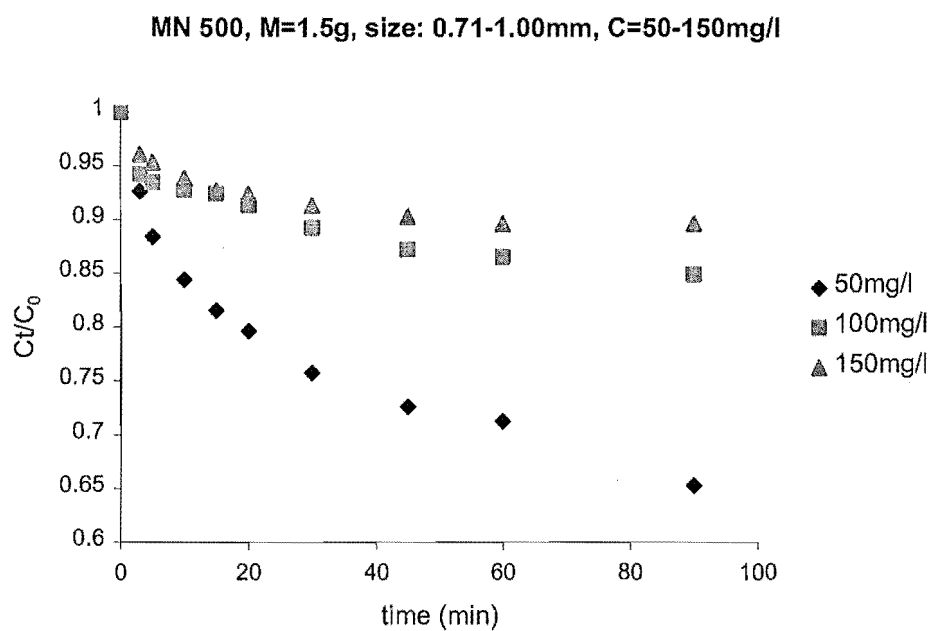


Figure 4.23 Ammonia uptake onto MN 500; different initial ammonia concentrations

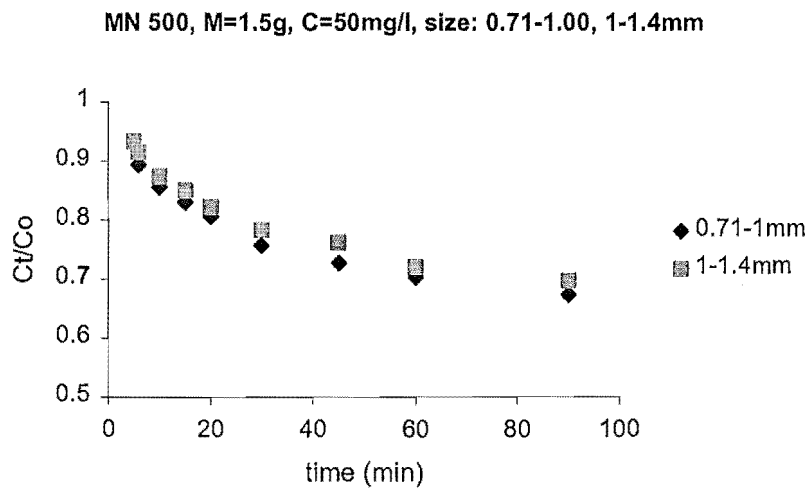


Figure 4.24 Ammonia uptake onto MN 500; different particle size

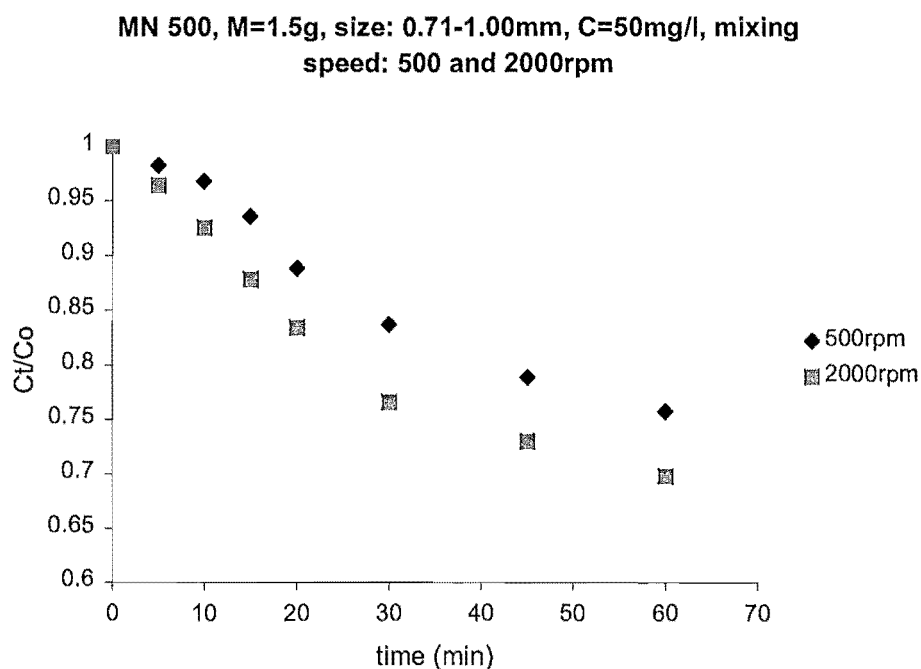


Figure 4.25 Ammonia uptake on to MN 500; different mixing speed

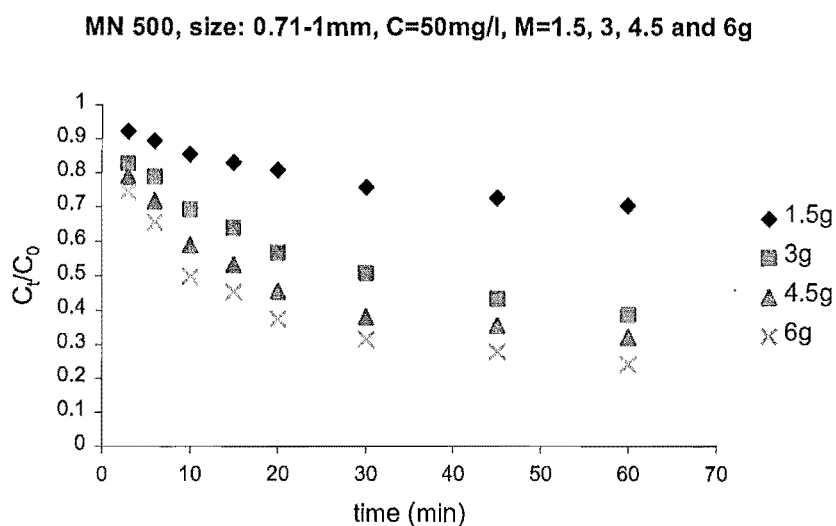


Figure 4.26 Ammonia uptake on to MN 500; different amount of material

According to the equilibrium data presented in Section 4.1.1.3, the Langmuir isotherm provided the slightly better fit and hence the Langmuir parameters were used for further calculations. The external diffusion coefficient was calculated

according to the single resistance mass transfer model (Appendix V) and the values obtained are given in the next table.

Table 4.23 External diffusion parameter for MN 500. If not changed in the table $C_{N-NH_4^+} = 50\text{mg/L}$, $d_p = 0.7\text{-}1.0\text{mm}$, $M = 1.5\text{g}$, mixing speed: 2000 rpm

Initial ammonia concentration (mg/L)	$k_f \times 10^3$ (cm/s)	r^2
50	24.5	0.997
100	12.3	0.931
150	8.2	0.948
Mass of material (M) (g)		
1.5	24.5	0.997
3	45.1	0.9981
4.5	54	0.9987
6	78.8	0.995
Mixing speed (rpm)		
500	3.6	0.926
1750	21	0.891
2000	24.5	0.997
Particle diam. (mm)		
0.7-1.0	24.5	0.997
1-1.4	20.2	0.972

The values of k_f were linearised to show the effects of mixing speed, initial ammonia concentration and mass of the ion exchanger as shown in Figure 4.27.

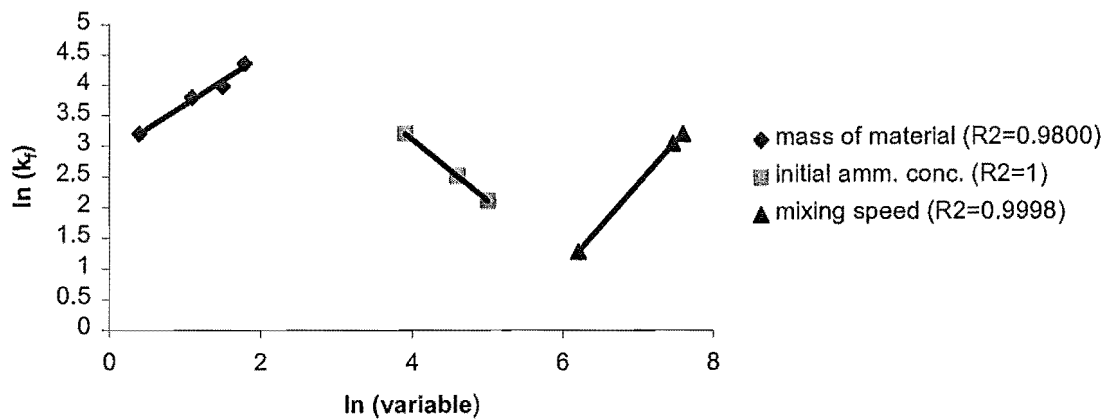


Figure 4.27 External mass transfer coefficient correlation for MN 500

An increase in the initial ammonia concentration is shown to decrease the value of k_f . On the other hand, an increase in the mass of the ion exchanger increased the values of k_f . In this case, at the same stirrer speed more intensive turbulence in the liquid phase might be expected since the power dissipation per unit volume of liquid would be likely to increase, thus explaining the increase in the values of k_f . Particle size also affected k_f . Larger particles have less specific area available for mass transfer, thus reducing the overall diffusion rate. The results in Figure 4.27 also show that an increase in mixing speed increases the value of k_f , as might be expected. As the mixing speed increases, the thickness of the boundary layer decreases, increasing the diffusion rate. The trend is similar to behaviour observed under similar conditions during adsorption onto activated carbon (Walker and Weatherley, 1999).

4.4.1.2 Internal Mass Transfer Model

The calculated values of the internal diffusion parameter k_d , (based on Equation 1.21 from Section 1.4.5.1) are shown in the next table. An example of the detailed calculation is given in Appendix V.

Table 4.24 Internal diffusion parameter for MN 500. If not changed in the table, $C_{N-NH_4^+} = 50\text{mg/L}$, $d_p = 0.7\text{-}1.0\text{mm}$, $M = 1.5\text{g}$, mixing speed: 2000 rpm

Initial ammonia concentration (mg/L)	k_d (mg N- $NH_4^+/\text{gmin}^{0.5}$)	r^2
50	4.4	0.999
100	5.2	0.931
150	5.93	0.948
Mass of material (M) (g)		
1.5	4.4	0.999
3	4.33	0.975
4.5	3.96	0.991
6	3.61	0.990
Mixing speed (rpm)		
500	2.22	0.751
1750	4.17	0.987
2000	4.4	0.999
Particle diam. (mm)		
0.7-1.0	4.4	0.999
1-1.4	3.91	0.995

The data in Table 4.24 show that the values of k_d change with experimental conditions. The changes are similar to those observed in the case of adsorption onto activated carbon (O'Connor, 1995; Walker, 1995, Allen et al, 1989). One obvious explanation for the variations in the values of k_d is that the rate of exchange was not exclusively controlled by particle side diffusion. The increase in k_d , observed with respect to the mixing speed, supports this and is consistent with reduced film resistance. The values of k_d also increase modestly with respect to the initial concentration. This is consistent with a reduction in the role of liquid film resistance at higher concentrations. Similar behaviour was reported for activated carbon adsorption systems (O'Connor, 1995; Walker, 1995). An increase of the particle diameter would tend to enhance the relative importance of particle side resistance and the results in Table 4.24 are consistent with this, though the effect is relatively minor. The effect is similar to the one observed in the case of film diffusion when smaller specific areas associated with larger particles lead to reductions in observed exchange. The effect is translated from the film around the particle to the particle itself. It is concluded that, at an initial

concentration of 50mg/L and at a stirrer speed of 2000rpm, particle diffusion control is dominant since the values of k_d are relatively constant.

The results obtained for the ion exchange process onto MN 500 have considerable similarity with those obtained for activated carbon, although there is no clear evidence of two stage internal diffusional behaviour which has been observed for example in activated carbon adsorption under particle diffusion conditions (Allen et al., 1989). It is therefore possible that in the case of MN 500, all regions and sites are equally available.

It is also clear that under the conditions of the kinetic experiments, both liquid film mass transfer resistance and particle side resistance were present at stirrer speeds of below 2000rpm.

4.4.2 Natural zeolites

4.4.2.1 External Mass Transfer Model

The ammonia uptake curves for clinoptilolite are given in Figures 4.28-4.31: the corresponding experimental conditions are shown in each figure.

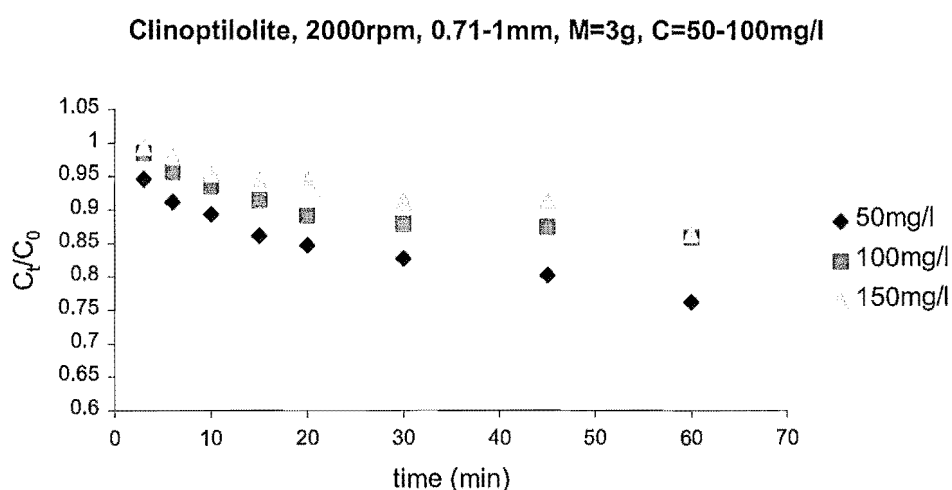


Figure 4.28 Ammonia uptake onto clinoptilolite; different initial ammonia concentration

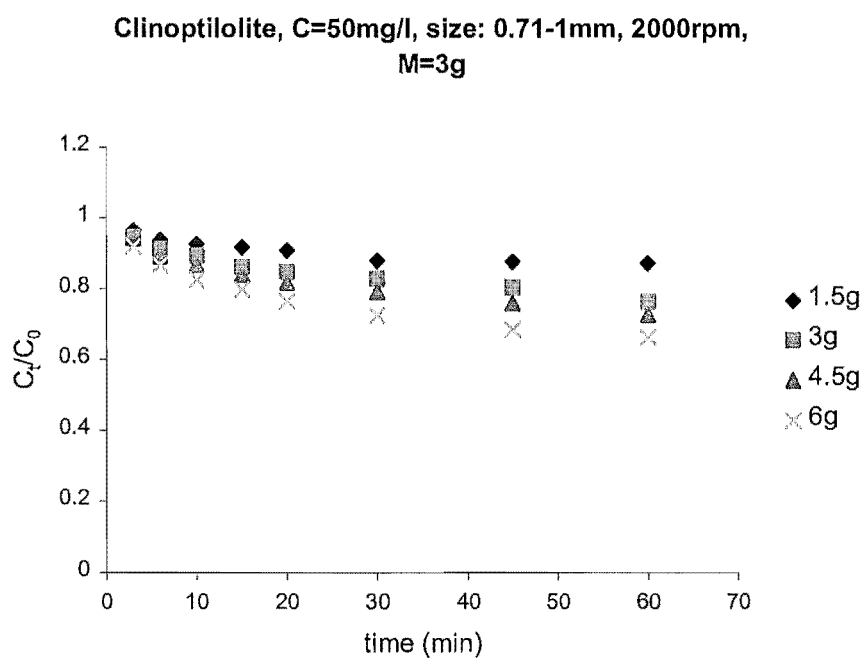


Figure 4.29 Ammonia uptake onto clinoptilolite; different mass of material

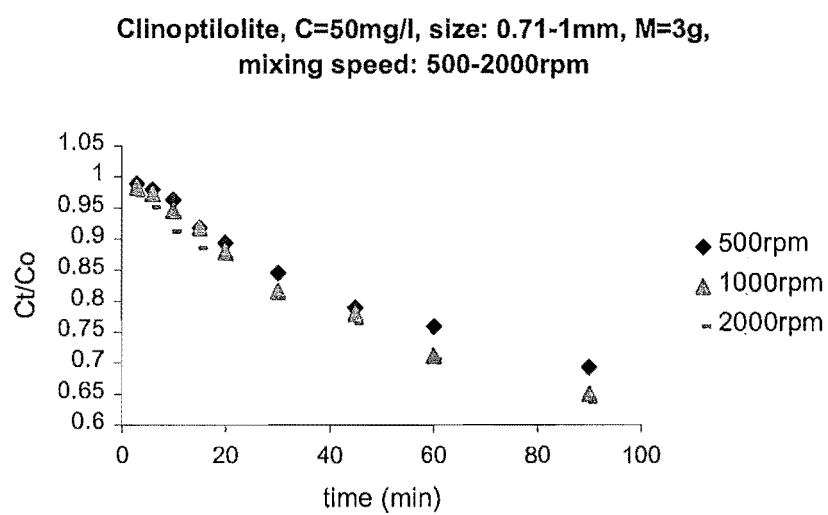


Figure 4.30 Ammonia uptake onto clinoptilolite; different mixing speed

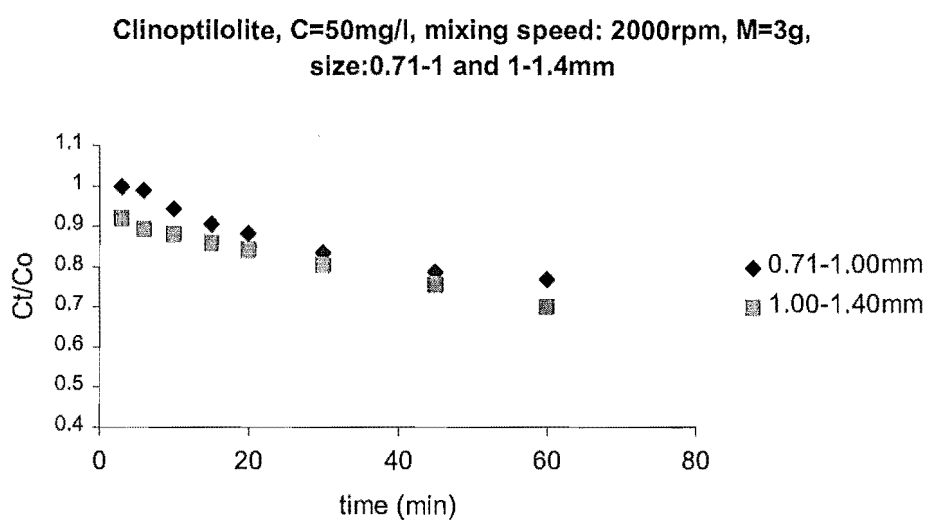


Figure 4.31 Ammonia uptake onto clinoptilolite; different particle size

The values for the external diffusion coefficient, calculated by using equations 1.18 and 1.19, are given in Table 4.25 while the correlation of the calculated diffusion coefficients with the varied parameters is given in Figure 4.32.

Table 4.25 External diffusion parameter for clinoptilolite. If not changed in the table, $C_{N-NH_4^+} = 50\text{mg/L}$, $d_p = 0.7\text{-}1.0\text{mm}$, $M = 3\text{g}$, mixing speed: 2000 rpm

Initial ammonia concentration (mg/L)	$k_f \times 10^3 \text{ (cm/s)}$	r^2
50	18.1	0.978
100	15.4	0.970
150	9.1	0.957
Mass of material (M) (g)		
1.5	35.3	0.876
3	18.1	0.978
4.5	7.2	0.934
6	6.8	0.954
Mixing speed (rpm)		
500	9.1	0.996
1000	16.3	0.988
2000	18.1	0.978
Particle diam. (mm)		
0.7-1.0	18.1	0.978
1-1.4	12.7	0.989

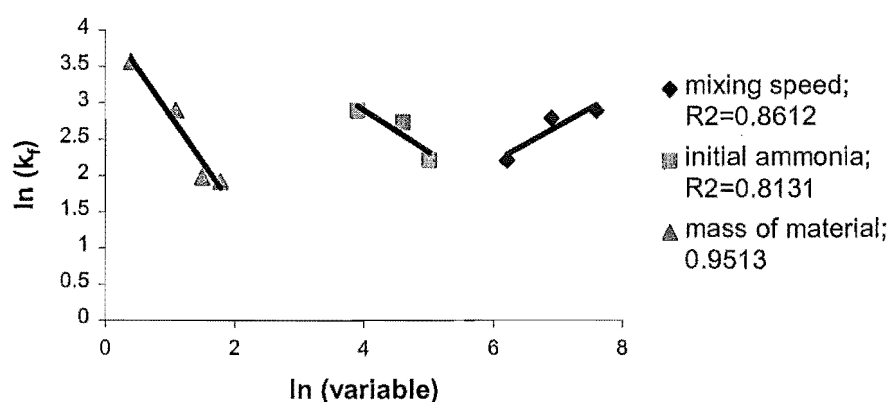


Figure 4.32 External mass transfer coefficient correlation for clinoptilolite

The same procedure was followed for analysis of the kinetic properties of another natural zeolite, mordenite. Figures 4.33-4.36 present kinetic data, showing decrease in the ammonia concentration over a total period of 60 minutes.

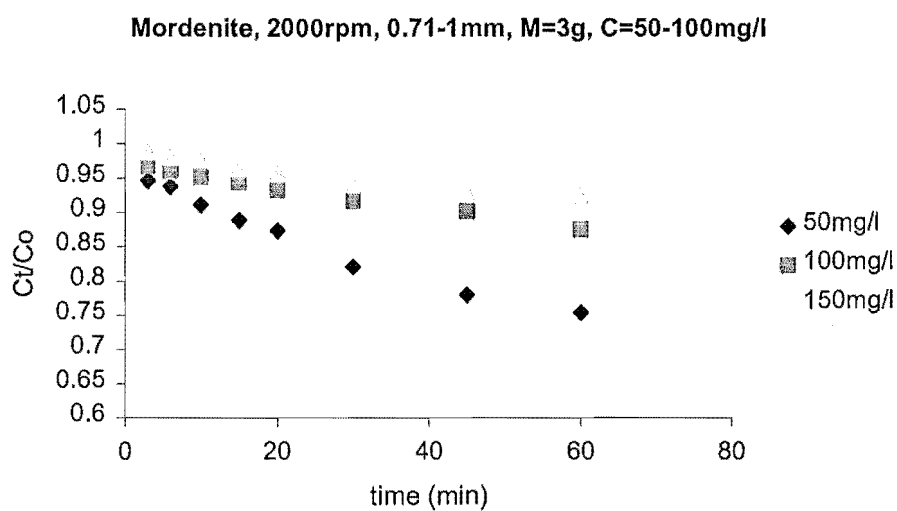


Figure 4.33 Ammonia uptake onto mordenite; different initial ammonia concentration

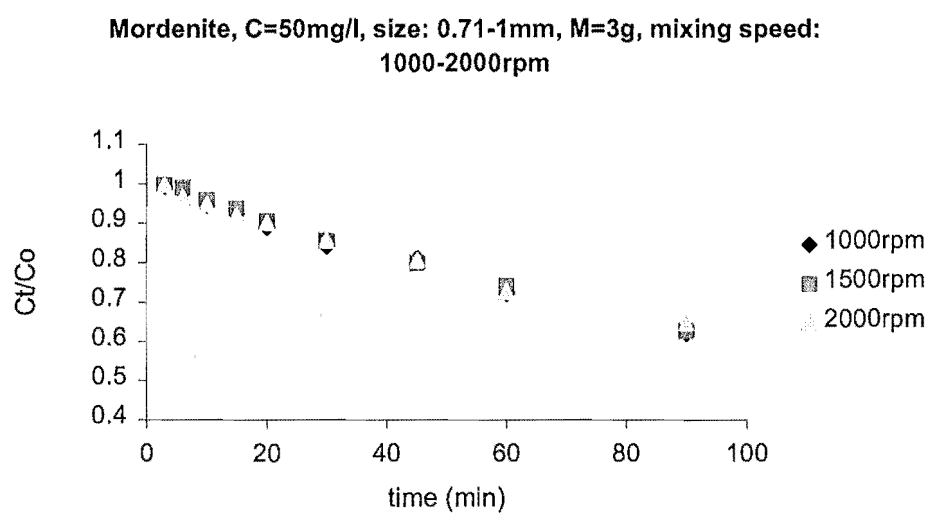


Figure 4.34 Ammonia uptake onto mordenite; different mixing speed

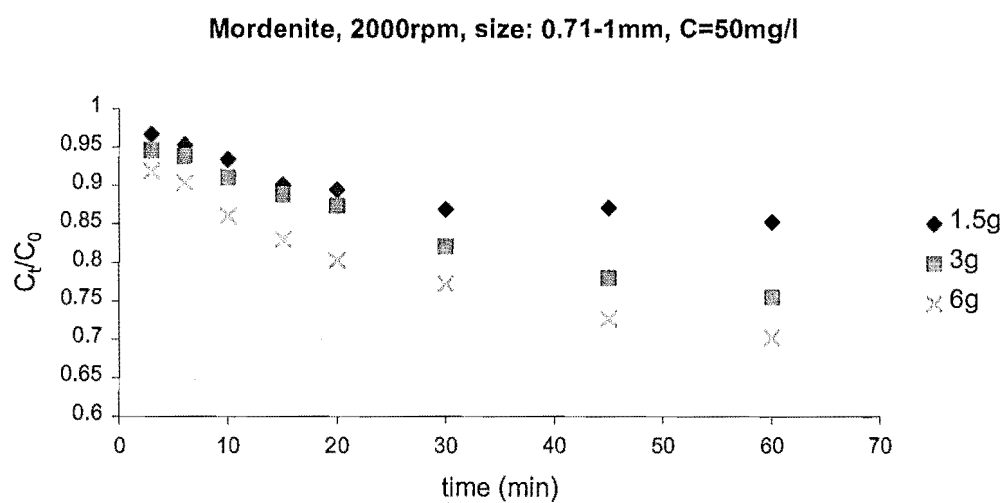


Figure 4.35 Ammonia uptake onto mordenite; different mass of the material

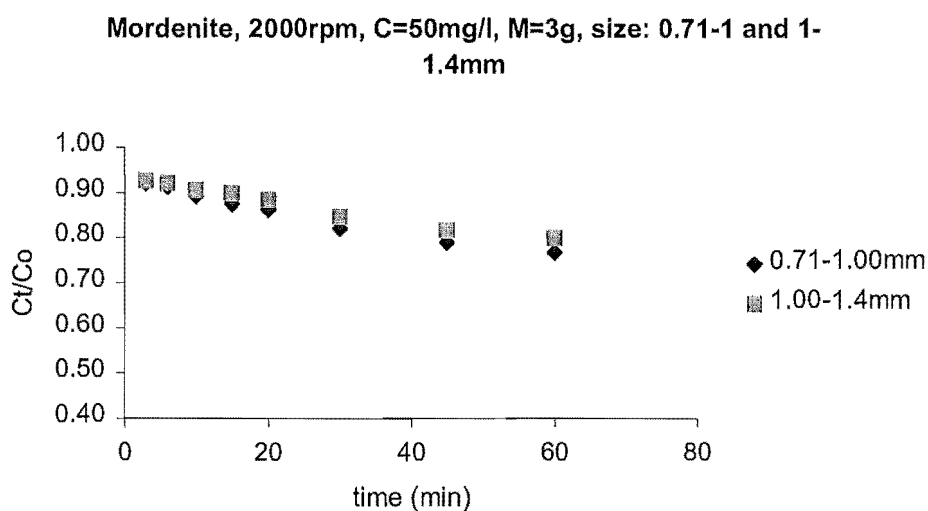


Figure 4.36 Ammonia uptake onto mordenite; different size of the particles

The Furasawa-Smith model (Section 1.4.5.1) was applied and the external diffusion coefficients were calculated. The values obtained are shown in Table 4.26. Figure 4.37 shows the correlation of the diffusion coefficients with the change in experimental conditions.

Table 4.26 External diffusion parameter for mordenite. If not changed in the table, $C_{N-NH_4^+} = 50\text{mg/L}$, $d_p = 0.7\text{-}1.0\text{mm}$, $M = 3\text{g}$, mixing speed: 2000 rpm

Initial ammonia concentration (mg/L)	$k_f \times 10^3$ (cm/s)	r^2
50	9.1	0.923
100	2.5	0.997
150	1.5	0.973
Mass of material (M) (g)		
1.5	16.9	0.996
3	9.1	0.923
6	8.5	0.946
Mixing speed (rpm)		
1000	6.6	0.985
1500	8.1	0.906
2000	9.1	0.923
Particle diam. (mm)		
0.7-1.0	9.1	0.923
1-1.4	8.5	0.971

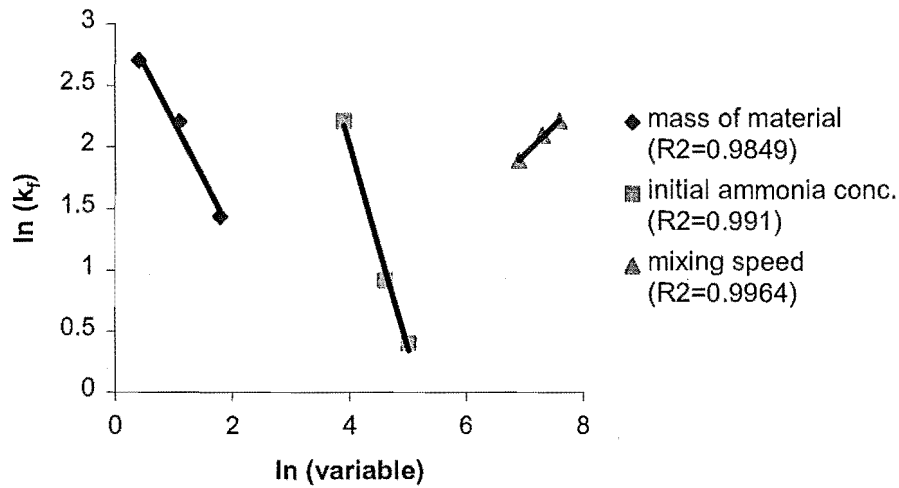


Figure 4.37 External mass transfer coefficient correlation for mordenite

Results for the ammonia uptake were successfully fitted into the proposed model for the film diffusion. The clinoptilolite and mordenite both exhibited an increase in the mass transfer resistance when the initial ammonia concentration increased. This was also observed in the case of the MN 500. A higher concentration of ammonium cations in the solution probably caused more interaction and competition for the available sites, decreasing the value of the diffusion coefficient. The effect is more obvious for mordenite. These results are similar to the findings for clinoptilolite reported by McVeigh (1999) and are in agreement with theoretical predictions for ion exchange kinetics (Helfferich, 1962).

An increase in the mixing speed improved the external mass transfer by reducing the thickness of the adherent liquid (boundary) layer around the particle. The effect is less obvious in the case of mordenite where differences among the values for different mixing speeds are within the limits of experimental and calculation error, leading to the conclusion that a mixing speed of over 1000rpm does not have a significant influence on external mass transfer resistance. However, coefficients were calculated, since data for higher mixing speeds constantly show slightly improved removal kinetic.

On the other hand, an increased mass of the ion exchanger in the solution decreased the value for the external diffusion coefficient. This finding is interesting when compared with the results obtained for the synthetic ion exchanger MN 500 (Section 4.4.1) where the opposite effect was reported, even though larger mass directly increases the specific surface area according to the model used (Equation 1.19). A possible reason for this might be reduced effectiveness of mixing as the mass of the solids in the system was increased, however, different behaviour of natural zeolites compared to the MN 500 cannot be explained.

As expected, the film diffusion was improved by reducing the particle size, since larger particles have less specific area available for mass transfer (see calculation in Appendix V). Again, the effect was quite modest for mordenite, but the trend of better removal on smaller mordenite particles was consistent during the experiment.

McVeigh (1999) calculated an external coefficient for clinoptilolite and obtained values in the range of $5.9\text{--}26.8 \times 10^{-4} \text{ cm/s}$ for the mixing speed of 400rpm and different particle size and initial ammonia concentrations. Our results for clinoptilolite's external diffusion coefficients are higher, being in the range of $6.8\text{--}35.3 \times 10^{-3} \text{ cm/s}$. However, the mixing speed used by McVeigh was only 400rpm compared to 2000rpm in our experiment: the lower speed can significantly slow down film diffusion. In addition, the initial ammonia concentration was $77.78 \text{ mg/g N-NH}_4^+$ compared to 50 mg/l in our experiments, which is again a parameter that increases the resistance for the mass transfer through the boundary layer. However, even with the same experimental conditions, it is not likely that different samples, even of the same kind of zeolite, will show the same kinetic characteristics owing to the variations in the structure and the surface topology.

According to the values presented and the variations in the external diffusion coefficient of the zeolites, it can be concluded that a smaller particle size, a lower

initial ammonia concentration and a reduced contact time will improve ammonia removal.

4.4.2.2 Internal Mass Transfer Model

Internal diffusion parameters for clinoptilolite and mordenite were calculated using equation 1.21 and the values obtained are given in Tables 4.27 and 4.28 together with the model correlation values.

Table 4.27 Internal diffusion parameter for clinoptilolite. If not changed in the table, $C_{N-NH_4^+} = 50\text{mg/L}$, $d_p = 0.7\text{-}1.0\text{mm}$, $M = 3\text{g}$, mixing speed: 2000 rpm

Initial ammonia concentration (mg/L)	k_d (mg $NH_4^+/g\ min^{0.5}$)	r^2
50	1.67	0.988
100	2.15	0.938
150	2.67	0.901
Mass of material (M) (g)		
1.5	2.18	0.985
3	1.67	0.988
4.5	1.33	0.986
6	1.29	0.994
Mixing speed (rpm)		
500	1.35	0.868
1500	1.52	0.923
2000	1.67	0.988
Particle diam. (mm)		
0.7-1.0	1.67	0.988
1-1.4	1.66	0.985

Table 4.28 Internal diffusion parameter for mordenite. If not changed in the table, $C_{N-NH_4^+} = 50\text{mg/L}$, $d_p = 0.7\text{-}1.0\text{mm}$, $M = 3\text{g}$, mixing speed: 2000 rpm

Initial ammonia concentration (mg/L)	k_d (mg NH_4^+ /g $\text{min}^{0.5}$)	r^2
50	1.49	0.976
100	1.53	0.988
150	1.74	0.985
Mass of material (M) (g)		
1.5	2.32	0.976
3	1.49	0.976
4.5	1.12	0.952
6	1.08	0.994
Mixing speed (rpm)		
1000	1.15	0.745
1500	1.32	0.795
2000	1.49	0.976
Particle diam. (mm)		
0.7-1.0	1.49	0.976
1-1.4	1.41	0.931

Results from Tables 4.27 and 4.28 show that the values of internal diffusion parameter k_d change with the change in the experimental conditions, in the same way as the one observed for the synthetic ion exchanger MN 500. The values obtained for the clinoptilolite are slightly higher when compared to the values obtained for the mordenite for the same experimental conditions. It can again be concluded that the mass transfer rate is not completely controlled by particle diffusion. The modest increase of k_d with increased mixing speed is observed with both natural zeolites and happens because of the reduced resistance in the liquid with better agitation. Variations in the values of k_d for natural zeolites are much less obvious, compared to the synthetic ion exchanger. Furthermore, the change in the particle size has almost no effect on the k_d value for both of the zeolites, which could exclude the particle diffusion control.

Based on these results, it can be concluded that both particle and film transfer resistance controlled the ammonia uptake on clinoptilolite and mordenite.

Probably the role of film resistance was greater here, since for most of experiments the values of k_f were much more dependent on the experimental parameters. McVeigh (1999) also concluded that film diffusion mostly controlled the uptake of ammonia on clinoptilolite from the United Kingdom. However, he noticed two stages for the diffusion through the particle which could not be distinguished in our experiments. One reason for his observation might be that the low mixing speed of only 400rpm (used in his experiments), allowed diffusion through the macro channels to be separated from the diffusion through the smaller pores. Another possible explanation is that the structure of the clinoptilolite used in his experiment was different, either owing to the different origin or to the purification process, to which commercial zeolites are exposed.

4.5 Kinetic studies on biologically active materials

Experiments in this area were designed to investigate whether bacteria colonies on the surface of the material disturb mass transfer during the ion exchange process. The procedure is explained in Section 3.2.3. Figures 4.38-4.40 show the reduction in ammonia concentration over time on biologically free and active clinoptilolite, mordenite and MN 500.

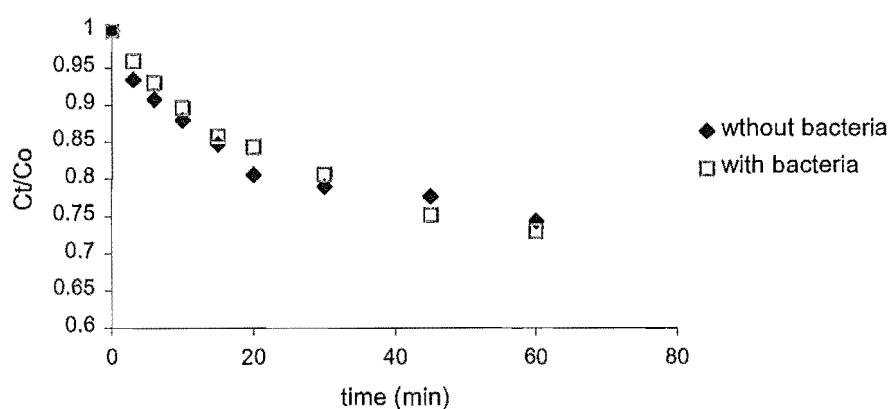


Figure 4.38 Ammonia concentration for biologically free and active clinoptilolite ($M=4.5\text{g}$, $C_{\text{init}}\cdot\text{N}\cdot\text{NH}_4^+=40\text{mg/l}$, mixing speed: 2000rpm, $d_p=0.7\text{-}1\text{mm}$)

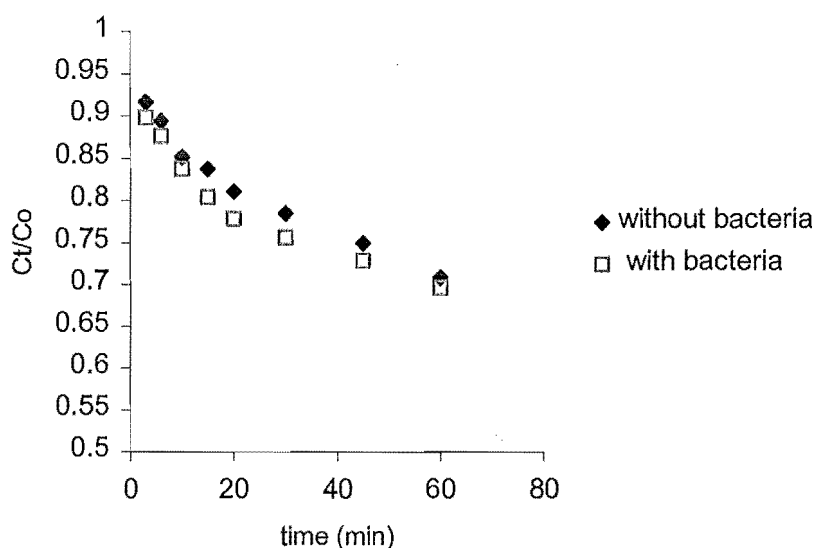


Figure 4.39 Ammonia concentration for biologically free and active mordenite (M=4.5g, $C_{init-N-NH_4^+}=40\text{mg/l}$, mixing speed: 2000rpm, $d_p=0.7\text{-}1\text{mm}$)

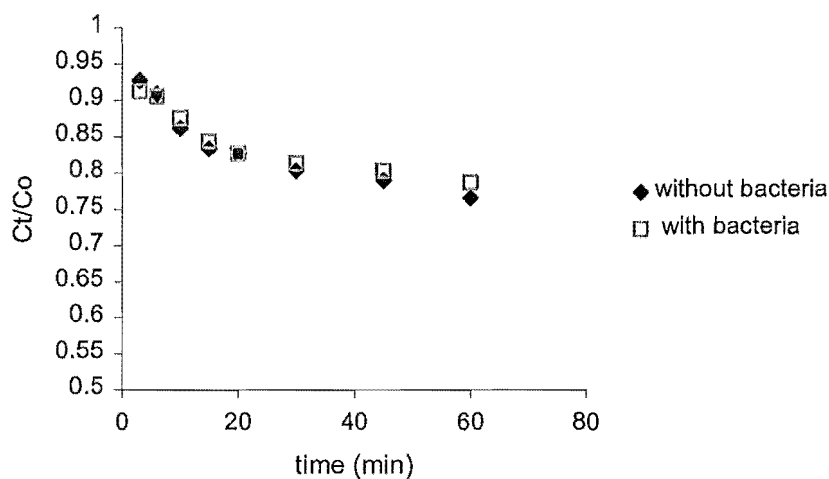


Figure 4.40 Ammonia concentration for biologically free and active MN 500 (M=4.5g, $C_{init-N-NH_4^+}=40\text{mg/l}$, mixing speed: 2000rpm, $d_p=0.7\text{-}1\text{mm}$)

The graphs presented show that mordenite with bacteria biofilm showed better removal for the whole period of the experiment, while free clinoptilolite performed better in the first 30 minute after which time biologically activated clinoptilolite had better ammonia removal. It can be concluded that even if some

resistance to mass transfer is present owing to bacteria film growing on the surface, that effect is overcome by bacteria activity which in the case of mordenite is noticeable from the very beginning of the experiment and in the case of clinoptilolite after 30 minutes.

In the case of MN 500 it appears that bacteria neither have any influence on mass transfer resistance nor have enough time to start to consume and degrade ammonia. The latter possibility is in agreement with results presented in Section 4.3.1 which show that the synthetic ion exchanger MN 500 was not as good a support for bacteria growth in non saline water as natural materials.

4.6 Column studies - fresh water

Based on the results for bacteria growth on different materials we chose to use the natural zeolites, clinoptilolite and mordenite, for column studies in fresh water. Even though the kinetic studies indicated that smaller particle size, as well as the higher velocity through the column, would improve the column performance, we had to consider the biological part of the process as well. Particles which are too small could cause column fouling and the retention time within the column must be sufficient to allow effective reaction and conversion. The biological reaction kinetics are therefore an important factor in determining appropriate residence time. It could be argued that bacteria could consume cations already captured by the ion exchanger but it is more likely that microbes only live attached to the surface while consuming free ammonia from the solution. Particle size in all column experiments ranged from 0.7-1.4mm. Material was packed to a height of 200mm and the feed flowrate for each column was chosen to ensure that the flow velocities for column with different diameters were the same. The flow rate never exceeded the value of 4BV/h. The pH was regularly checked and if needed, sodium bicarbonate was introduced with the feeding solution to increase the pH value within the column to the value of 7.5.

4.6.1 Column studies without bacteria

The next figure (4.41) shows a comparison between the ammonia uptake onto the packed bed of clinoptilolite and mordenite. The columns' performances were

quantified in terms of breakthrough curves as shown and the ratio of effluent/initial ammonia concentration is plotted against the number of the bed volumes of the feeding solution which was passed through the column. In this case, the feed was a solution of ammonia in deionised water. The results are tabulated according to concentration in Appendix VI (the number of the table is indicated in the figure).

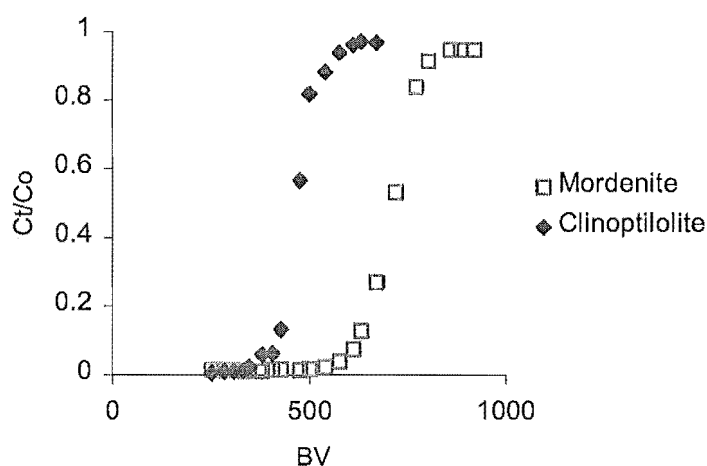


Figure 4.41 The uptake values for the packed bed of clinoptilolite and mordenite. Particle size: 0.7-1.4mm, initial ammonia concentration: 20mg/l N-NH_4^+ , flow rate: 4BV/h, column diameter: 30mm, 2nd running, (Table 7.1)

From the curves presented in Figure 4.41 it may be noted that mordenite performed significantly better than clinoptilolite. The breakthrough within the column packed with mordenite started after 600BV passed, compared to only 380BV of feeding solution which was enough to saturate the column with the clinoptilolite. These findings agree with the higher batch equilibrium uptake capacity for the mordenite reported in Section 4.2.1.1. We calculated the uptake capacity for each of the materials at the point when the breakthrough started. The calculation is given in detail in Appendix VII. We opted for this point since this would be the point where the columns should be replaced even though material still had the potential to remove some of the ammonium ions. The results are given in

Table 4.29, together with the maximum values obtained for the batch studies, already given in Sections 4.2.1.1 and 4.2.1.2.

The next figure (4.42) gives a similar comparison, with real wastewater used as a feeding solution. Since the initial ammonia concentration in the creek water was insignificant (0.02mg/l N-NH_4^+) we did not take this value into the calculation.

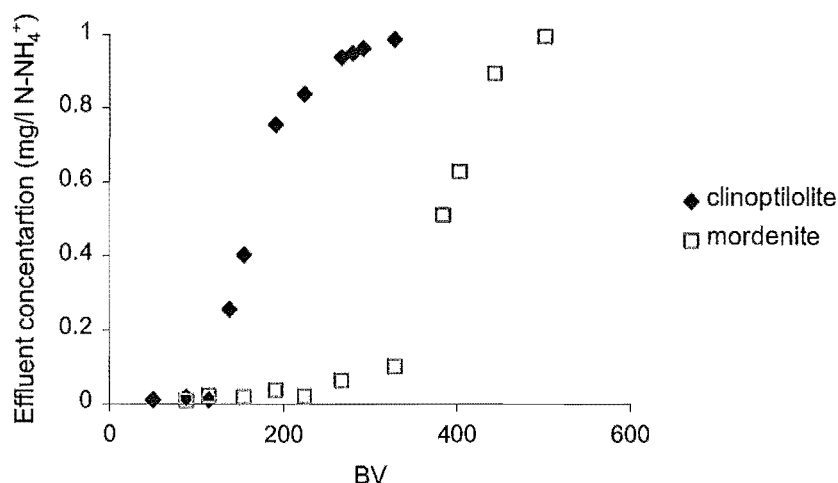


Figure 4.42 The uptake values for the packed bed of clinoptilolite and mordenite. Particle size: 0.7-1.4mm, initial ammonia concentration: 40mg/l N-NH_4^+ , creek water, flow rate: 2BV/h , column diameter: 30mm, (Table 7.2)

Table 4.29 Uptake capacities for clinoptilolite and mordenite

Clinoptilolite			Mordenite		
uptake capacity, meq/g			uptake capacity, meq/g		
batch	column, DI water	column, creek water	batch	column, DI water	column, creek water
0.66	0.76	0.48	0.80	0.84	0.64

Even though the flow rate and the initial ammonia concentrations were not the same for the DI water and creek water experiments, some conclusions can be drawn. For both the materials, column uptake capacity was higher compared to the one obtained in the batch experiments even though we were dealing with the concentrations of 20 and 40mg/l in the columns compared to the value of 200mg/l

for the batch studies. Again, it should be emphasised that the column capacity was calculated at the point where material was still capable of ammonia adsorption but not in an acceptable quantity. In the case of the creek water mordenite again performed better than the clinoptilolite, with less reduction in the uptake capacity due to the presence of other cations (a 23% reduction for mordenite compared to the 36.84% reduction for clinoptilolite). This can be explained by the fact that other cations have less influence on ammonia uptake on mordenite than the clinoptilolite, as explained in the Section 4.2.1.2.

The following results will show the change in packed bed performance in connection with the regeneration of the column. Figures 4.43 and 4.44 compare the performance of the columns packed with clinoptilolite and mordenite after regeneration has been performed according to the procedure given in Section 3.2.6.

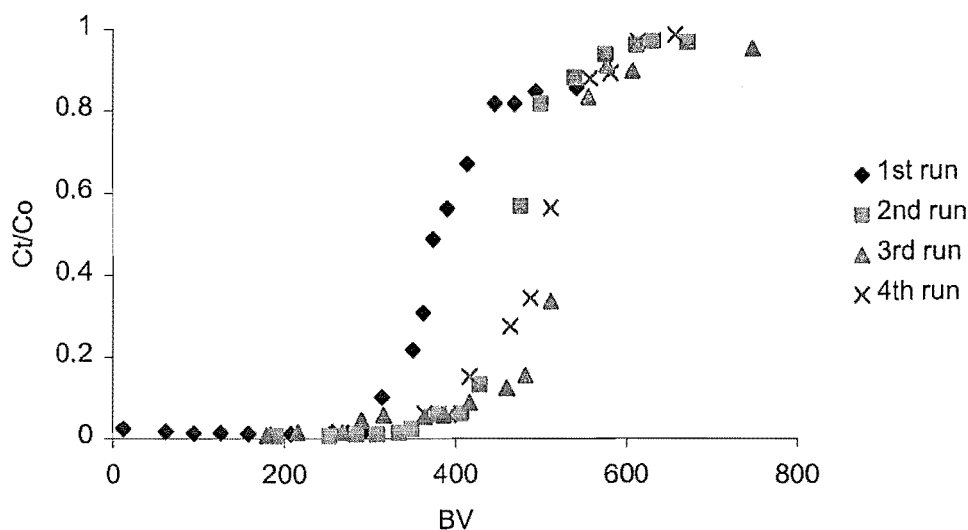


Figure 4.43 The uptake values for the packed bed of clinoptilolite. Particle size: 0.7-1.4mm, initial ammonia concentration: 20mg/l N-NH_4^+ , flow rate: 4BV/h, column diameter: 30mm, (Table 7.3)

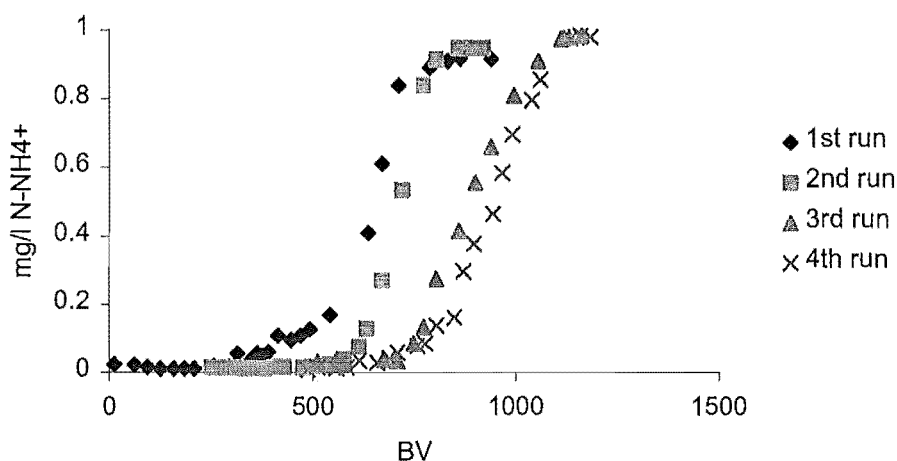


Figure 4.44 The uptake values for the packed bed of mordenite. Particle size: 0.7-1.4mm, initial ammonia concentration: 20mg/l N-NH₄⁺, flow rate: 4BV/h, column diameter: 30mm, (Table 7.4)

The first observation from the graphs is that after each of the regenerations, the start of the breakthrough was shifted towards the higher number of BV of the feeding solution passed through the column. The effect of the higher uptake capacity is noticeable on both of the materials. However, in the column packed with clinoptilolite, the effect is significant only after the first regeneration (the breakthrough was shifted from 300BV to 380BV); while for the mordenite, it took three regenerations to reduce the effect. The possible explanation is a change in the structure of the material. In that way, some of the sites became more available with improved kinetics for ammonia removal. As a result, capacity was increased before the breakthrough which caused some changes in the uptake after the breakthrough. This will be explained below. The results could also be explained by an incomplete pretreatment procedure whereby the exchanger is not fully conditioned into homoionic form. (In that case, some of the sites on the zeolite were not exchanged for the Na⁺ ions, but remained occupied by the other cations). It is most likely that the cations involved were: Ca⁺⁺, Mg⁺⁺ or K⁺. After this two things might happen:

1) Ammonium cations might manage to displace some of the above mentioned cations from the exchange sites. Then the sodium ions from the regenerant solution would displace ammonium ions and make sites more available in the next cycle. With these sites now easily available, ammonium ions would manage to displace more of the interfering cations, allowing sodium ions again to make them more likely to be exchanged in the next cycle. Less of the mordenite was probably in homoionic form prior to the experiment since the effect is more obvious in the column packed with this material. Jorgensen (2002) observed similar behaviour when regenerating clinoptilolite from the United Kingdom. He tried to specify exactly which cations were responsible for such behaviour, but it is likely that it involved a group of cations rather than only one.

2) The kinetics of the $\text{Na}^+ / (\text{Ca}^{++}, \text{Mg}^{++} \text{ or } \text{K}^+)$ exchange might improve in the case of column contact, since the exchanger material would always be in contact with the fresh solution and these cations were removed after regeneration, making sites available for the ammonium ions. However, if this was the case, the effect would probably be obvious only after the first regeneration and hence could be used only to describe the phenomenon on the column packed with clinoptilolite where the effect disappeared after the first regeneration.

In the experiments discussed above, the feeding solution was free of Ca^{++} , Mg^{++} and K^+ ions which will not be the case when treating real wastewater. We expect that the capacity will drop after each running cycle, when these cations are present in the solution. This will happen since sodium ions, even with the improved kinetics as a result of column regeneration, will not be able to displace all these cations from the sites. In that way, the sites will stay unavailable to the ammonium ions.

Another fact indicated by these breakthrough data is the increase in effluent ammonia concentration after the first regeneration which indicates that the increase in the uptake capacity caused by the regeneration disappears after the breakthrough. The ratio C_t/C_o after the breakthrough increased from 0.86-0.97

and from 0.92-0.95 for clinoptilolite and mordenite respectively, after the first regeneration. Again, mordenite exhibited the effect after the second regeneration as well (the ratio increased to the value of 0.98), while clinoptilolite did not show any increase in the Ct/Co ratio after the second regeneration. One possible explanation for the increase in the effluent concentration after the breakthrough was that, for some reason, the regeneration was not complete. This could happen due to the slower $\text{NH}_4^+/\text{Na}^+$ exchange kinetics for some exchange sites, so that the reduction of the flow rate, even to half the value of the flow rate used to run the columns, was not enough to allow complete regeneration. Another reason might be the change in the structure of the zeolite, which was reported to happen after alkaline regeneration (Section 2.2.5.1) and was mentioned as a possible reason for the increase in the uptake capacity mentioned above. The sites which became more available for the exchange became saturated in the first part of the experiment before the breakthrough occurred. Therefore, the capacity was just shifted; it reduced after the breakthrough but increased before it.

4.6.2 Column studies with bacteria

4.6.2.1 The impact of aeration on mass transfer within the column

For the experiments which involved bacteria, columns with the new design described in Section 3.2.4.1 were used. The first experiments were designed to check whether aeration within the column would have any impact on the ammonia removal. The next figure presents the comparison between the ammonia uptakes in the columns packed with clinoptilolite, with and without aeration. It can be concluded that the introduced air did not have any impact on the overall performance of the columns when bacteria were not present. This was expected, since the major advantage of aeration through the air permeable tubing is that large air bubbles, which will have an impact on the mass transfer within the column, are not formed.

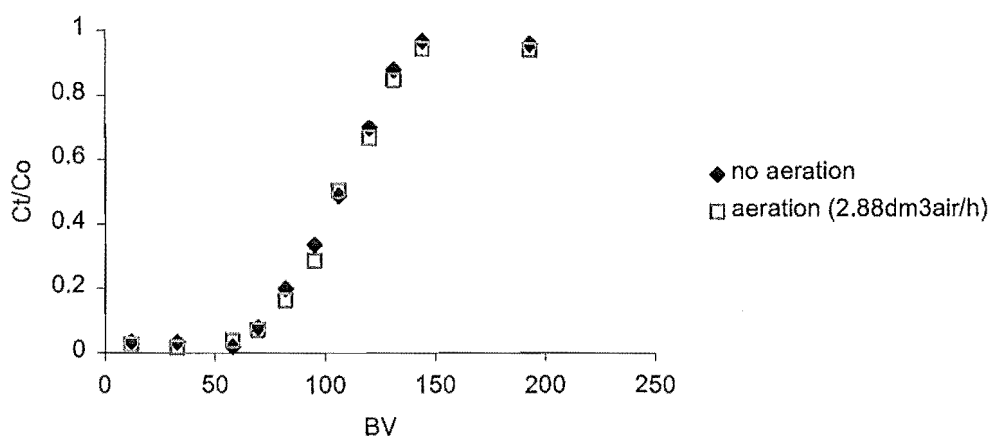


Figure 4.45 The uptake values for the packed bed of clinoptilolite. Particle size: 0.7-1.4mm, initial ammonia concentration: 40mg/l N-NH_4^+ , flow rate: 2BV/h, salmon fish farm water

4.6.2.2 Biologically active clinoptilolite

To compare the ammonia uptake on biologically active and non active clinoptilolite, one of the columns packed with clinoptilolite was biologically activated in the way described in Section 3.2.5.

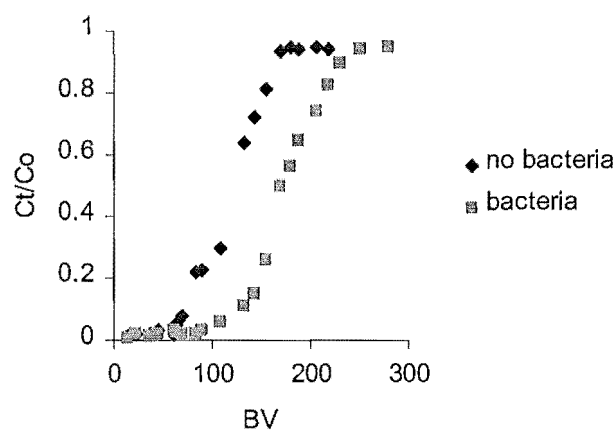


Figure 4.46 The uptake onto biologically active and non active clinoptilolite. Particle size: 0.7-1.4mm, initial ammonia concentration: 40mg/l N-NH_4^+ , flow rate: 1BV/h, creek water

Figure 4.46 shows that clinoptilolite which was not biologically activated performed well up to the 60BV of treated solution passed through the bed. Clinoptilolite with nitrifying bacteria introduced prior to the experiment had service time 30BV longer than the bacteria free bed. By introducing bacteria, the breakthrough uptake capacity was increased from 0.15 to the value of 0.22meq/g. One can notice that the slope of the breakthrough curves remained the same for both of the columns, which means that bacteria only postponed the breakthrough, but once it started, the kinetics of the physiochemical process was much faster, and the biological process did not contribute significantly to the overall performance of the column. McVeigh (1999) also obtained breakthrough curves with almost the same slope when comparing sterile and biologically active beds, for the removal of wastewater with insignificant biological activity. The same author obtained a different slope of the curves only when wastewater with already established bacteria activity was passed through the biologically active bed. This means that the performance of the bed after the breakthrough can be biologically improved only if nitrification is already established in the treated wastewater. When we calculated the residence time of the solution within the column taking into account flow rate and the voidage of the column (Appendix VIII), the value of 30 minutes was obtained. Haug and McCarty (1972) obtained 95% nitrification with 1 hour retention time at temperature of 22°C, while Copper and Williams (1990) reduced ammonia concentrations from 27mg/l to 3mg/l N-NH₃ with retention time of only 38 minutes. However, their growth time prior to the experiment was 10 weeks while we used bacteria after 3 weeks from inoculation into the growth media and 96 hours after inoculation on the ion exchanger. As discussed earlier, too long a period of bacteria growth on the packed bed would cause significant capacity loss due to the adsorption of ions present in the bacteria broth. This capacity loss should have been taken into consideration when comparing the performance of the biologically active and non-active materials, since the non-active bed did not suffer any capacity reduction due to the bacteria inoculation.

4.6.2.3 Biologically active mordenite

The next figure gives the comparison between biologically active and non-active packed bed of mordenite.

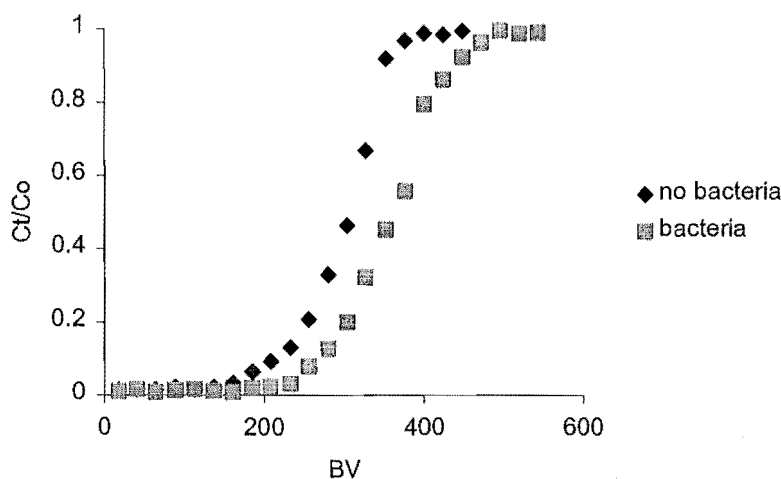


Figure 4.47 The uptake onto biologically active and non active mordenite. Particle size: 0.7-1.4mm, initial ammonia concentration: 40mg/l N-NH₄⁺, flow rate: 1BV/h, creek water

Figure 4.47 shows that bacteria introduced into the column packed with mordenite prolonged the bed service time from 161-233BV; increasing the breakthrough capacity from the value of 0.30meq/g without bacteria activity, to the value of 0.41meq/g when bacteria were active. Nitrifying bacteria again only improved the process before the breakthrough was reached since the both of the curves have similar slopes. However, slowing down the process after the breakthrough would not have much contribution to the overall process, since ammonia concentration in the effluent had already reached the values which indicate that the bed should be regenerated.

While doing the experiments which involved the packed bed of mordenite we discovered quite unusual behaviour of the nitrifying bacteria. After a set of experiments involving bacteria activity within the packed bed we performed alkaline regeneration as described in Section 3.2.6, which was performed at pH of

12 for 40 hours. The same columns were used for the new set of experiments with bacteria being introduced only in one, presuming that the other column would not exhibit bacteria activity any more. However, biological activity was present in both of the columns, leading to the conclusion that some of the bacteria can survive a regeneration procedure. Retaining some of the biological activity after the alkaline regeneration would improve overall performance of the column in the next running, since already established colony of nitrifying bacteria was proved to perform better compared to the organisms that were just introduced.

4.6.2.4 Comparison of the ammonia uptake onto biologically active clinoptilolite and mordenite

Since all the experiments involving bacteria and real wastewater do not allow for obtaining identical experimental conditions for two sets of the same experiment, the only way to compare the performance of biologically active clinoptilolite and mordenite was to use columns packed with each of the materials at the same time.

Bacteria were inoculated as described in Section 3.2.5. Since the inlet ammonia concentration of 40mg/l proved to be too high for a longer period of running the process, we only started with this concentration to allow bacteria to settle well onto the material, and then reduced the inlet ammonia first to 20 and then to 5 mg/l. To see how the system performs under the sudden increase in ammonia concentrations, shock loading of 40 and 80mg/l was introduced. Oxygen concentration also varied during the experiment from 0-2.88dm³/h air. The next figure gives the outlet ammonia concentrations for each of the columns over the bed volumes of the water passed through. Since the inlet ammonia concentration varied during the experiment we did not plot the C_t/C_o ratio since it was not possible to obtain it accurately. In addition, Figure 4.49 gives the nitrate concentrations in both columns during the experiment which will give a better picture of bacteria activity within the bed.

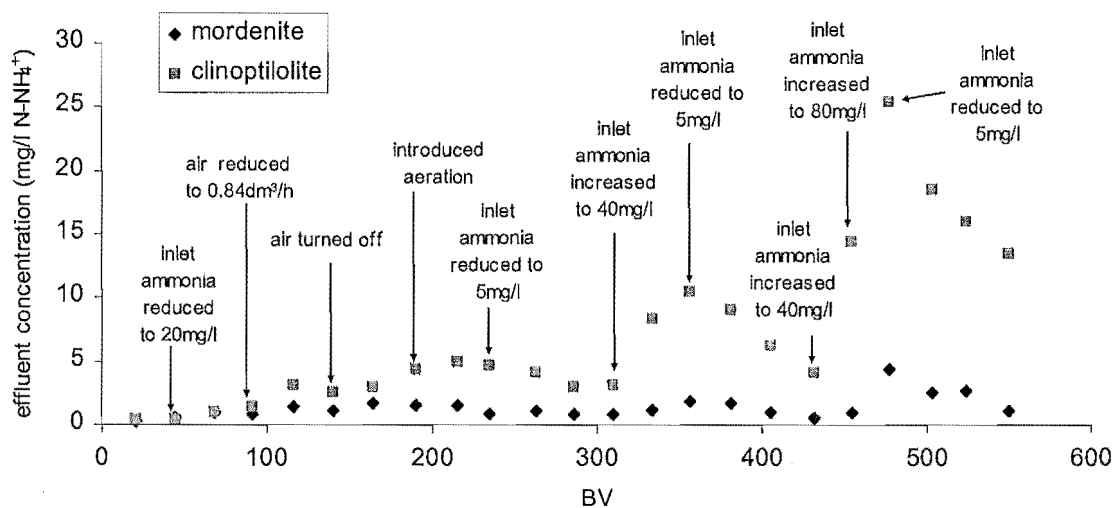


Figure 4.48 Ammonia uptake onto the biologically activated columns. If not indicated differently, particle size: 0.7-1.4mm, number of regenerations: 2, initial ammonia concentration: 40mg/l N-NH_4^+ , flow rate: 1BV/h, aeration: 2.88dm³/h, creek water (Table 7.5)

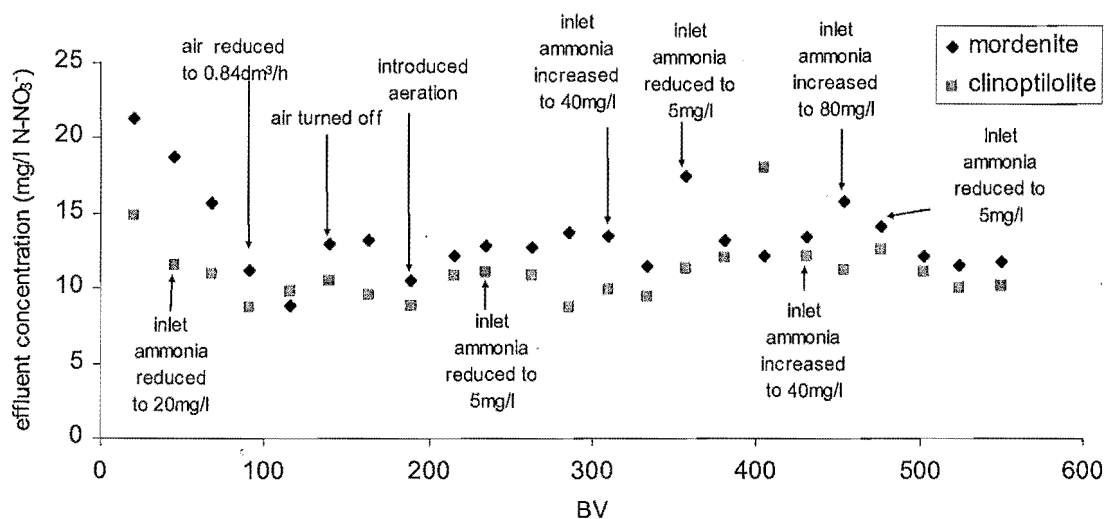


Figure 4.49 Nitrate concentration within the biologically activated columns. If not indicated differently, particle size: 0.7-1.4mm, number of regenerations: 2, initial ammonia concentration: 40mg/l N-NH_4^+ , flow rate: 1BV/h, aeration: 2.88dm³/h, creek water (Table 7.5)

The first observation from Figure 4.48 is that mordenite performed significantly better during the reactor running time. This is in agreement with the higher capacity data for batch and column experiments reported above, and less capacity reduction due to the presence of other cations but ammonium in the solution, attributed to mordenite. Generally, the trend for increase or decrease in the outlet ammonia concentration is same for both columns. However, fluctuations in the outlet ammonia concentration are more obvious for clinoptilolite.

4.6.2.5 The impact of initial ammonia concentration on the column performance

The change in the inlet ammonia concentration had an effect on the nitrification process (Figure 4.49). The initial decrease in nitrate concentration was probably due to a wash out of nitrates introduced in the columns during the process of bacteria immobilisation. The reduction of inlet ammonia concentration to 20mg/l appeared to initiate reduction in bacteria activity. Once the nitrifiers adapted to the new substrate concentration the nitrate levels started to rise again (after approximately 110BV of treated water passed through the columns, Figure 4.49). The next decrease in nitrate concentration was when inlet ammonia concentration was reduced to 5mg/l. This change had a bigger impact on the nitrification within the column packed with clinoptilolite since it took bacteria 48 hours to adjust to the new conditions. Increase of inlet ammonia concentration to 40mg/l was again a small drawback for biological activity, but the biological part of the reactor suffered less than in the case when inlet ammonia was reduced. Better bacterial activity as well as higher capacity are the most likely reasons that mordenite performed much better than clinoptilolite in the case of a radical increase of inlet ammonia. Better ammonia uptake by ion exchange onto mordenite was the most likely reason that nitrifying organisms on this material had a better buffering effect yielding a much better performance of the column when packed with mordenite. After 454BV had passed through the column, the inlet ammonia concentration was increased to a value of 80mg/l. In the case of mordenite the outlet ammonia concentration was raised up to the value of 5mg/l; it was reduced to the value of 1.16mg/l 72 hours after inlet concentration was reduced. The

second shock loading had a bigger effect on the nitrification process within both columns. After the inlet ammonia concentration was normalised, it took the bacteria 48 hours to speed up the nitrification process again (increase in nitrate levels after 524BV). The reason for this larger effect was probably capacity loss within the ion exchanger due to the water having already passed through the columns. Water contained other cations together with ammonia, which may have occupied sites leaving them unavailable for ammonium cations. As expected, biological activity within the bed appeared to regenerate only sites occupied by ammonium cations. Loss of capacity reduced the buffering effect of ion exchangers, leaving nitrifying organisms more exposed to a change in the inlet ammonia concentration, which proved to always reduce the biological activity within the bed.

However, the results obtained for equalization of the inlet ammonia peaks on biologically active mordenite are very good when compared to the results available from the literature. Beler-Baykal et al. (1994), increased the inlet ammonia concentration from 5 to 15mg/l for the time period of 4 hours and the outlet ammonia concentration increased to the value of more than 2mg/l. They used a bed packed with clinoptilolite and secondary wastewater with already established biological activity. In our experiments, in the case of the mordenite, with the inlet ammonia concentration of 40mg/l during the period of 24 hours, the effluent ammonia concentration was maintained below the value of 2mg/l. Theoretical residence time within the columns was almost the same. We can presume that the difference in the values for the bed voidage cannot be significant which means that real residence time was also similar for both experiments.

4.6.2.6 The impact of aeration onto the biological process within the column

If we look at Figure 4.50, the points where the amount of introduced air varied can be noted, as well as the changes in the effluent ammonia concentration caused by these variations.

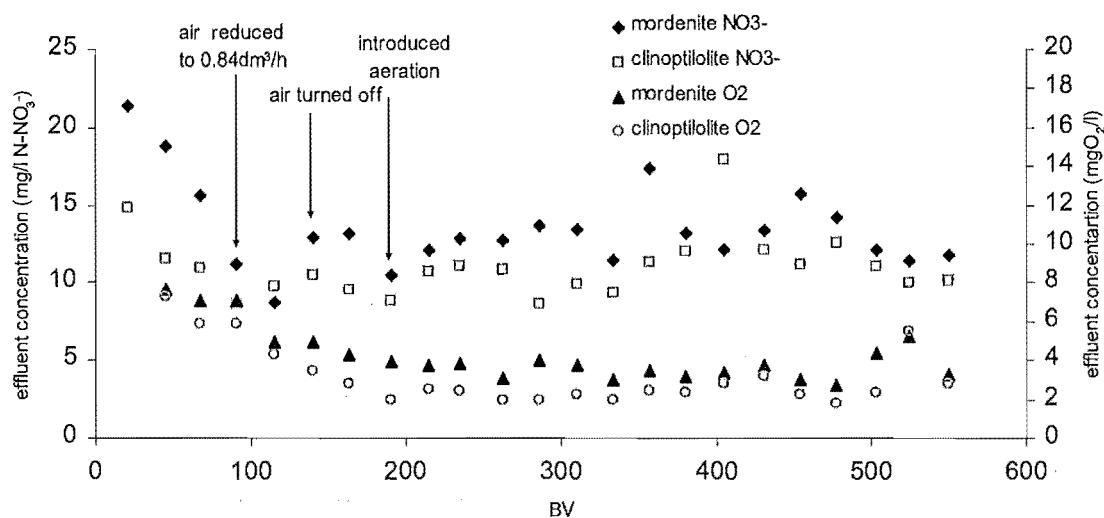


Figure 4.50 Nitrate and oxygen concentration within the biologically activated columns. If not indicated differently, particle size: 0.7-1.4mm, number of regenerations: 2, initial ammonia concentration: 40mg/l N-NH₄⁺, flow rate: 1BV/h, aeration: 2.88dm³/h, creek water

The results in Figure 4.50 show that the oxygen levels within the clinoptilolite column were constantly lower compared to the values within the mordenite bed. Nitrate levels were also lower for the clinoptilolite, which means that the oxygen level drop in oxygen level was not caused by better nitrification. Since clinoptilolite is a more brittle material than mordenite, it was probably crushed within the column while wastewater was passed. In that way, free space within the column was reduced and air distribution within the column was not even. If we look at the calculated and measured residence time for both columns given in Appendix VIII, it is noticeable that for the same flow rate, residence time within the column packed with clinoptilolite was lower compared to the values obtained for bed of mordenite. This means that the column packed with clinoptilolite had less available space between material particles. Poor aeration was probably the reason that clinoptilolite performed worse than mordenite when the combined process was applied within the column even though batch experiments with bacteria revealed better nitrification process on clinoptilolite. During batch

experiments flasks were shaken and aerated all the time, so that the oxygen diffusion was not a limiting parameter for the process.

Reduction of the air feedrate from the values of 2.88 to 0.84dm³/h initiated slower nitrification in the mordenite bed, since a reduction in the nitrate level was observed. However, this change in inlet air rate did not have the same effect on the nitrification process within the clinoptilolite. The complete shut down of aeration caused a drop in nitrate level in both columns. This increased again when the level of aeration was increased to 2.88dm³/h. As mentioned above, these variations in bacteria activity due to the oxygen variations did not cause significant change in the effluent ammonia concentration within the column packed with mordenite. If we look at the clinoptilolite bed, the decrease of inlet oxygen as well as the complete shut down of aeration increased effluent ammonia concentration.

The next figure gives the ammonia uptake within columns packed with mordenite which were inoculated and used at the same time. Both columns were a new design; however, one of the columns was not aerated using air permeable tubing. Air was introduced into the feeding solution in the first tank (see Figures 3.6 and 3.7) and feeding solution was introduced into the column after the second tank.

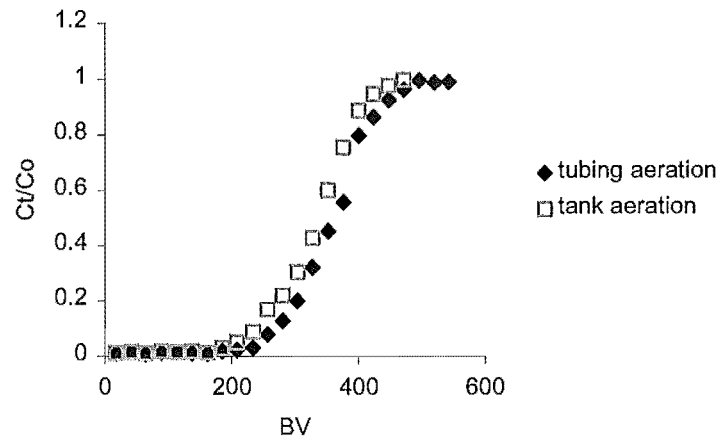


Figure 4.51 Ammonia uptake onto the biologically activated columns of mordenite. Particle size: 0.7-1.4mm, initial ammonia concentration: 40mg/l N-NH_4^+ , flow rate: 1BV/h, aeration: 2.88dm³/h (tubing) and 180dm³/h, creek water

Figure 4.52 represents the nitrate and oxygen concentrations within the columns during the experiment.

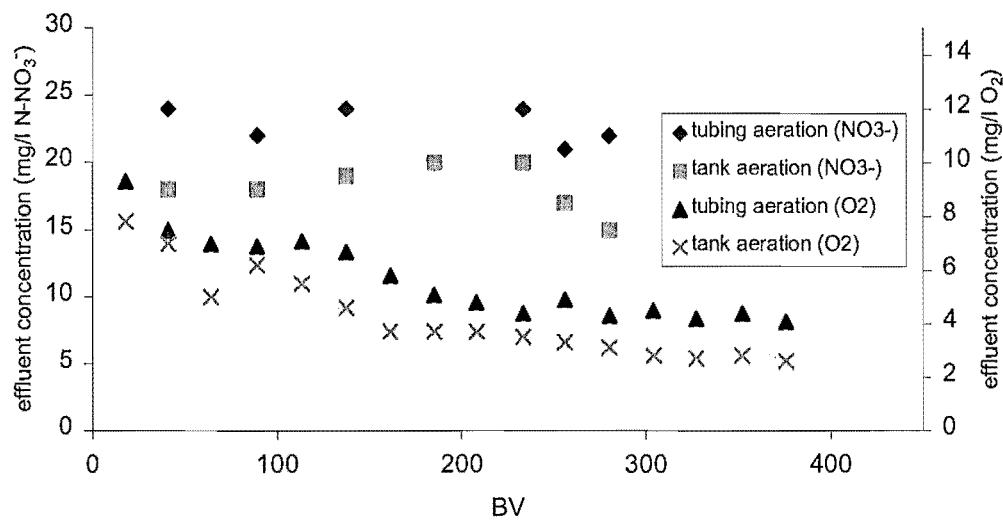


Figure 4.52 Nitrate and oxygen levels within the biologically activated columns of mordenite. If not indicated differently, particle size: 0.7-1.4mm, initial ammonia concentration: 40mg/l N-NH_4^+ , flow rate: 1BV/h, aeration: 2.88dm³/h (tubing) and 180dm³/h, creek water

It can be concluded that new aeration within the column did not significantly improve nitrification within the bed for the level of nitrification that was achieved in our experiments. However, the level of aeration achieved by the air pump was $180\text{dm}^3/\text{h}$ compared with only $2.88\text{ dm}^3/\text{h}$ achieved by permeable tubing. Even this was enough to maintain a constantly higher oxygen level within the new design column and to improve the nitrification process slightly, as can be seen from Figure 4.52. After 230BV passed through the columns the breakthrough had already started and the reactor was most probably working only as a biological reactor. This is the point from which the new aeration system managed to supply more air for the nitrification process compared to the pre-aeration within the feeding tank, since the nitrogen levels as well as the oxygen concentrations within the pre-aerated reactor started to decrease. In the cases of the treated influent having established colonies of nitrifiers, improved enhancement would be expected using the new in-situ aeration system.

4.7 Column studies – saline water

4.7.1 Column studies without bacteria

The experiments explained in section 4.3.2 show that synthetic material MN 500 exhibited better total ammonia removal in batch experiments in saline water when ion exchange was combined with the nitrification process. However, due to the higher capacity of ZZ for ammonia removal when bacteria were not present, this material was used in column experiments which involved saline water. Due to the very fast column saturation with cations present in the saline water, brackish water was used in the column experiments (salt content was 1g/l). The next figure gives a comparison of ammonia uptake on fresh and regenerated ZZ.

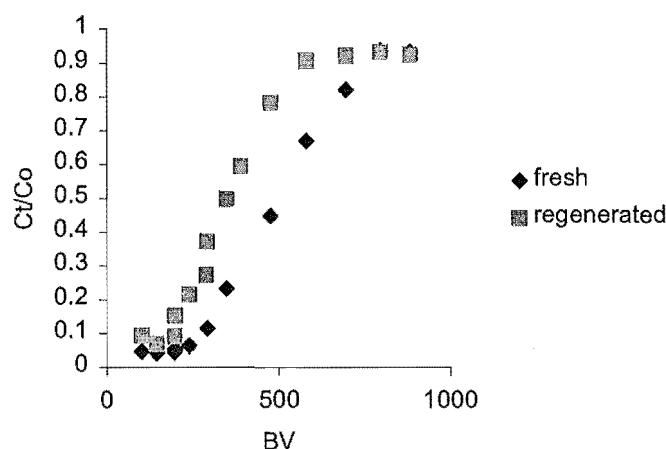


Figure 4.53 Ammonia uptake onto ZZ. Particle size: 0.7-1.4mm, initial ammonia concentration: 10mg/l N-NH₄⁺, flow rate: 4BV/h, salinity of water: 1g/l.

The first conclusion is that the effect of improved capacity after the first regeneration, which was noticed on natural zeolites during the experiments in a non-saline medium, is not noticeable. On the contrary, the uptake capacity was reduced after regeneration. This could be explained by the fact that ZZ was exposed to the pretreatment process which included heating at 450°C. This probably already caused the change in the structure so that alkaline regeneration could not cause any more changes as it did when natural zeolites were regenerated. The breakthrough capacity in the points where the effluent ammonia concentration started to rise above the acceptable value (200BV and 140BV for fresh and regenerated material respectively) was calculated by applying the procedure given in Appendix VII. The obtained values are given in Table 4.30 (second row) together with the values obtained for batch experiments (Section 4.2.2)

Table 4.30 Uptake capacities for ZZ

<i>Init. conc.</i>	Capacity (meq/g)		
	<i>batch results</i>	<i>column results</i>	
		<i>fresh</i>	<i>regenerated</i>
5	0.00		
10	0.01	0.14	0.10
40	0.05		
70	0.10		
90	0.13		
150	0.22		

Table 4.30 shows that the uptake capacity for the column experiments with a feed concentration of 10mg/l, was lower than the result obtained for the batch experiment when the initial ammonia concentration was 150mg/l (value of 0.22meq/g, Table 4.30), at the same pH and temperature. Even though material was always exposed to the fresh ammonia solution, the high concentration of other cations caused high competition with ammonium ions for available sites. This is the most likely reason why column conditions did not improve the uptake capacity above the highest value obtained for batch experiments, as it was the case for experiments using non-saline water.

4.7.2 Column studies with bacteria

The next figure (4.54) shows the performance of the two columns packed with ZZ when synthetic saline waste water was treated. Bacteria were introduced onto one of the columns by using the procedure explained in Section 3.2.5.

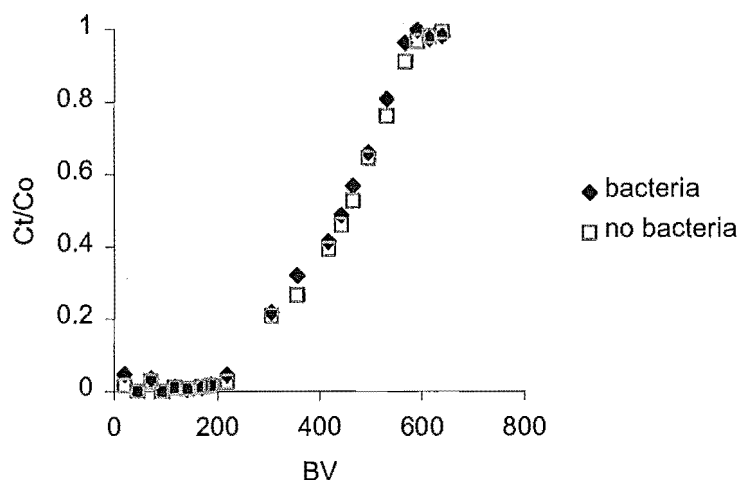


Figure 4.54 Ammonia uptake onto ZZ. Particle size: 0.7-1.4mm, initial ammonia concentration: 10mg/l N-NH_4^+ , flow rate: 1BV/h, salinity of water: 1g/l.

Even though the flow rate during the inoculation varied from the values of 0.5-3BV/h we did not manage to establish a biofilm onto the packed bed of ZZ which would have a significant contribution to the ammonia removal from the saline medium. The difference in the protein concentration in the passing solution, measured before and after the column, as well as the nitrate concentration indicated bacteria activity within the column. However, high salt concentration caused the physiochemical part of the reactor to be more dominant. The column with inoculated bacteria performed even worse compared to the bacteria free bed most likely due to the capacity loss during the inoculation process. This happened since the bacteria rich solution for the experiments in saline water, which was passed through the column, had a high salt concentration also (see Section 4.3.2).

5 Conclusions

5.1 *Material analysing*

The electron scanning microscope as well as the XRF analysis of the New Zealand mordenite and clinoptilolite revealed that these materials were similar to the same minerals from other parts of the world. The Si/Al ratio was higher for mordenite than for clinoptilolite. The surface photographs of the MN 500 proved the presence of micropores and macropores which are the reason for the higher surface area of this material compared to natural zeolites and the product of zeolitic nature, ZZ. New Zealand mordenite had the lowest surface area among the zeolitic materials.

5.2 *Batch equilibrium studies without bacteria*

5.2.1 *Fresh water*

Batch equilibrium studies in fresh water without interfering cations revealed that the ammonia uptake capacities for the material used were in the following order from the highest to the lowest: MN 500, mordenite and clinoptilolite. As expected, the synthetic material exhibited the highest uptake capacity. However, the presence of Ca^{++} , Mg^{++} , or K^{+} ions in the solution showed the high preference of natural zeolites for the ammonium ion. The influence of these cations on the ammonia removal was the highest for the synthetic material and the smallest for the mordenite. The presence of calcium ions had the most significant effect upon ammonium ion uptake onto clinoptilolite, followed by potassium ions. Magnesium ion had the least effect upon ammonium uptake onto clinoptilolite. The order of preference for mordenite could not be obtained, while for the MN 500 it was as follows: $\text{Mg}^{++} > \text{Ca}^{++} > \text{K}^{+}$.

The Langmuir adsorption model provided a better fit for the equilibrium data obtained for the ammonia uptake on natural zeolites from the fresh water, when compared to the fit obtained using the Freundlich model. However, the characteristic for the uptake onto MN 500 lies between the two proposed models.

5.2.2 Saline water

Ion exchange materials can remove ammonia from saline water. There was evidence of different categories of fixed sites in the modified zeolites, some of which had a very high affinity for ammonium ions and which rapidly become saturated. A product of zeolitic nature, ZZ, exhibited the highest uptake capacity for ammonia removal from saline water among the studied materials.

There was a significant variation in the extent to which divalent ions, Ca^{++} and Mg^{++} , inhibit ammonium ion uptake. The presence of potassium ions also inhibited ammonium ion uptake and in the case of some modified zeolites (ZZ and Mg.NZ) similar behaviour to that exhibited by natural zeolites was observed. It can be concluded that the overall inhibitory effect was the smallest on MN 500 and ZZ.

The Freundlich adsorption isotherm provided a better fit for batch equilibrium data obtained for experiments in saline water for all materials used, except for the modified zeolite Zecer 56. Equilibrium data obtained for this material did not fit into any of the proposed models.

5.3 Batch equilibrium studies with bacteria

5.3.1 Fresh water

The results show that the removal of ammonia was generally better on natural materials (clinoptilolite and mordenite) when compared to the synthetic ion exchanger MN 500. This was observed on biologically free materials as well as on the materials that had bacteria attached. Therefore, natural zeolites not only exhibited higher ammonia capacity but also were shown to be better media for bacteria growth. The nitrifiers performed more effectively on the clinoptilolite compared to the mordenite. The combined process demonstrated a potential buffering function for the ion exchange materials, protecting bacteria from the high ammonia concentrations (higher than 80mg/l N-NH_4^+), which are reported to cause inhibition of the nitrification process.

5.3.2 Saline water

A combined process could also be considered for ammonia removal from the saline medium. While MN 500 did not show good biological regeneration in non-saline water, it served as a good medium for bacteria growth in saline water; MN 500 showed better ammonia removal performance for the combined process in sea water compared with modified zeolite ZZ.

5.4 Kinetic experiments

Proposed analytical models, originally used for the modelling of the uptake data onto activated carbon, could successfully be used to describe the particle and film diffusion of the ammonium cation during the ion exchange process. These were based on predominantly liquid-film diffusion or predominantly particle side diffusion. Both models effectively described the rate behaviour for natural zeolites, as well as for the synthetic ion exchanger, MN 500. According to the values obtained it was concluded that choice of a smaller particle size, a lower initial ammonia concentration and a reduced contact time will improve ammonia removal onto all the ion exchange materials considered here.

Some resistance to mass transfer was present owing to bacteria film growing on the surface of the material, but the effect was overcome by bacterial activity.

5.5 Column studies

5.5.1 Fresh water

The natural zeolites, clinoptilolite and mordenite, were used for the column experiments in a non-saline medium. When bacteria were not present, both clinoptilolite and mordenite exhibited higher uptake capacity in column experiments than in batch experiments, with mordenite showing the higher capacity than clinoptilolite. Alkaline regeneration caused a shift in the uptake capacity; capacity was increased before the breakthrough and reduced after it, which improved the process since once the outlet concentration reached a certain level a column had to be replaced even though it still had potential to remove some of ammonia from the solution.

The combined process was successfully applied within packed beds of materials mentioned above. The new aeration system within the columns provided more efficient aeration compared to the pre-aeration of the feeding solution. The packed bed of mordenite performed better when it was biologically activated. Since clinoptilolite is a highly abrasive material, it produced dust that blocked small pores in the silicon tubing disabling good aeration. Bacteria activity postponed the breakthrough of the column with no influence on the process when the breakthrough started. The biological process within the bed can not replace completely the chemical regeneration since it is limited only to displacement of ammonia ions. However, it can prolong column life and reduce overall operational costs. The established biofilter was able to survive the alkaline regeneration carried out.

Mordenite performed better than clinoptilolite when a sudden increase in inlet ammonia concentration occurred. The combined reactor was able to tolerate the inlet ammonia concentration of 80mg/l over a period of 24 hours.

5.5.2 Saline water

To avoid fast column saturation, only brackish water was treated using the product of zeolitic nature, ZZ. Synthetic material MN 500 reached breakthrough too soon even when the water with salinity of 1g/l was used. Column experiments did not significantly improve the ammonia uptake capacity of ZZ owing to the high concentration of competing cations. The capacity drop occurred after alkaline regeneration.

Even though the batch experiment proved that the combined process was possible in the saline medium as well, biological activity within the column packed with ZZ was not established up to a satisfactory value.

6 Future work

The following work would usefully extend this research:

- Develop and look for more materials for a combined process since mordenite performed much better than the more exploited clinoptilolite. Manufacture synthetic particles, involving physical mixtures of adsorbents and ion exchangers, which might give a physical structure that is altered to optimise bacterial immobilisation.
- Find some other air permeable materials for better column aeration.
- Repeat the experiments involving the proposed combined system with the improved aeration for the waters with already established nitrifying activity, so that the role of the more efficient aeration is investigated more thoroughly.
- Develop other ways of combining ion exchange and biological processes for the saline medium since a packed bed was not convenient for bacteria inoculation without losing too much of the uptake capacity. The experiments involving wastewater with already established nitrifying activity might reveal some possibilities for more efficient application of the combined system for the high salt concentration waters.
- Look at the possibilities of applying the combined process to other systems with reaction products which could be removed in-situ by ion exchange.
- Develop more the theoretical aspect of the combined process by modelling the kinetics of the simultaneous bioreaction/ion exchange.

7 References

1. Adams Jr. C. E., Eckenfelder Jr. W. W., (1977), "*Nitrification Design Approach For High Strenght Ammonia Wastewaters*", Journal of Water Pollution Control Federation, Vol. 49, No. 3, pp. 413-421.
2. Aguilar-Armenta G., Hernandez-Ramirez G., Flores-Loyola E., Ugarte-Castaneda A., Silva-Gonzales R., Tabares-Munoz C., Jimenez-Lopez A., Castellon-Rodriguez E., (2001), "*Adsorption Kinetics of CO₂, O₂ and CH₄ in Cation-Exchanged Clinoptilolite*", Journal of Physical Chemistry B, Vol. 105, No. 7, pp. 1313-1319.
3. Allen S. J., McKay G., Khader K. Y. H., (1989), "*Intraparticle Diffusion During Adsorption onto Sphagnum Peat*", Environmental Pollution, Vol. 56, pp. 39-50.
4. Ames L. L., (1963) "*Mass Action Relationships of Some Zeolites in the Region of High Competing Cation Concentrations*", The American Mineralogist, Vol. 48, pp. 868-882.
5. Anastas P. T., Warner J. C., "*Green chemistry : theory and practice*", Oxford University Press, 1998.
6. Anthoniesen A. C., Loehr R. C., Prakasam T. B. S., Srinath E. G., (1976), "*Inhibition of Nitrification by Ammonia and Nitrous Acid*", Journal of Water Pollution Control Federation, Vol. 48, No. 5, pp. 835-852.
7. Barber W. P., Stuckey D. C., (2000), "*Nitrogen Removal in a Modified Anaerobic Baffled Reactor (ABR): 2, Nitrification*", Water Research, Vol. 34, No. 9, pp. 2423-2432.

8. Barrer R., Papadopoulos R., Rees L., (1967), "*Exchange of Sodium in Clinoptilolite by Organic Cations*", Journal of Inorganic Nuclear Chemistry, Vol. 29, pp.2047-2063.
9. Beler-Baykal B., Oldenburg M., Sekoulov I., (1994), "*Post Equalization of Ammonia Peaks*", Water Research, Vol. 28, No. 9, pp. 2039-2042.
10. Bish D. L., Ming D. W. (editors), "*Natural Zeolites, Occurrence, Properties, Application*", Reviews in Mineralogy & Geochemistry, Vol. 45 (2001).
11. Booker N. A., Cooney E., L., Priestley A. J., (1996), "*Ammonia Removal from Sewage Using Natural Australian Zeolite*", Water Science and Technology, Vol. 34, No. 9, pp. 17-24.
12. Bower C. E., Turner D. T., (1983), "*Nitrification in Closed Seawater Culture Systems: Effects of Nutrient Deprivation*", Aquaculture, Vol. 34, pp. 85-92.
13. Breck D. W., "*Zeolite Molecular Sieves*", Wiley, New York, 1974.
14. Briggs M. R., Funge-Smith S. J., (1996), "*Effects of Zeolites on Water Quality*", Aquaculture Research, Vol. 27, pp. 301-311.
15. Bryant C., Barkley W., Garret R., Gardner D., (1996), "*Biological Nitrification of Kraft Wastewater*", Water Science and Technology, Vol. 35, No. 1-2, pp. 147-153.
16. Burrell P. C., Keller J., Blackall L. L., (1998), "*Microbiology of a Nitrite-Oxidizing Bioreactor*", Applied and Environmental Microbiology, May, pp. 1878-1883.
17. Campbell G. Wildberger S., "*The Monitor's Handbook*", LaMotte Chemical Company, 1992.

18. Catalan-Sakairi M. A. B., Wang P.C., Matsumura M., (1997), "*Nitrification Performance of Marine Nitrifiers Immobilized in Polyester and Macro-Porous Cellulose Carriers*", Journal of Fermentation and Bioengineering, Vol. 84, No. 6, pp. 563-571.
19. Chen K. C, Lee S. C., Chin SC, (1998), "*Simultaneous Carbon-Nitrogen Removal in Wastewater Using Phosphorylated PVA-immobilized Microorganisms*", Enzyme and Microbial Technology, Vol. 23, No 5, pp. 311-320.
20. Christie T., Brathwaite B. and Thompson B., (2002) "*Mineral commodity report 23 – Zeolites*",. New Zealand Mining, Vol. 31, pp. 16-24.
21. Chudoba J., Cech J. and Chudoba P., (1976), "*The Effect of Aeration Tank Configuration on Nitrification Kinetics*", Journal of Water Pollution Control Federation, Vol. 57, No. 11, pp. 1078-1083.
22. Chung Y. C., Son D. H., You M. J., (2003), "*Treatment of Ammonium Reach Wastewater Using Natural Zeolite as a Medium in Biofilter*",
23. Cole-Palmer Catalogue 2005/2006, USA (2005)
24. Cooney E. L., Booker N. A., Shallcross D. C., Stevens G. W., (1999), "*Ammonia Removal From Wastewater Using Natural Australian Zeolite*", Separation Science and Technology, Vol. 34, No.12, pp. 2307-2327.
25. Cooper P. F., Willialms S. C., (1990), "*High-Rate Nitrification in a Biological Fluidized Bed*", Water Science and Technology, Vol. 22, No. 1/2, pp. 431-442.
26. Dale J. A., Nikitin N. V., Moore R., Opperman D., Crooks O., Naden D., Belsten E., Jenkins P., "*Macronet, the Birth and Development of a Technology*",

In: Gregg J. A., editor, Ion exchange at the millennium. London: Imperial College Press, 2000.

27. Davis M. L, Cornwell D. A, "*Introduction to Environmental Engineering*", Mc Graw Hill, 1996.
28. Dimova G, Mihailov G, Tzankov T., (1999), "*Combined Filter for Ammonia Removal-Part I: Minimal Zeolite Contact Time and Requirements for Desorption*", Water Science and Technology, Vol. 39, No. 8, pp. 123-129.
29. Dincer A. R., Kargi F., (1999), "*Salt Inhibition of Nitrification and Denitrification in Saline Wastewater*", Environmental Technology, Vol. 20, pp. 1147-1153.
30. Dryden H. T., "*Ammonium Ion Removal From Dilute Solutions and Fish Culture Water by Ion Exchange*", PhD research dissertation, Department of Chemical Engineering, Heriot-Watt University, Edinburgh, 1984.
31. Dreyden H. T., Weatherley L. R., (1987), "*Aquaculture Water Treatment by Ion Exchange: I. Capacity of Hector Clinoptilolite at 0.01-0.05N*", Aquacultural Engineering, Vol. 6, pp. 39-50.
32. Dreyden H. T., Weatherley L. R., (1987a), "*Aquaculture Water Treatment by Ion Exchange: II. Selectivity Studies with Clinoptilolite at 0.01N*", Aquacultural Engineering, Vol. 6, pp. 51-68.
33. Dreyden H. T., Weatherley L. R., (1989), "*Aquaculture Water Treatment by Ion Exchange: Continuous Ammonium Ion Removal with Clinoptilolite*", Aquacultural Engineering, Vol. 8, pp. 109-126.

34. Eaton AD, Cleceri LS and Greenberg AE, "*Standard Methods for the Examination of Water and Wastewater*", 19th edition American Public Health Association, Washington DC, USA (1995).
35. Emerson K., Russo R. C., Lund R. E., Thurston R. V., (1975), "*Aqueous Ammonia Equilibrium Calculations: Effect of pH and Temperature*", Journal of the Fisheries Research Board Canada, Vol. 32, pp. 2379-2383.
36. Erikson R. J., (1985), "*An Evaluation of Mathematical Models for the Effects of pH and Temperature on Ammonia Toxicity to Aquatic Organisms*", Water Research, Vol. 19, pp. 1047-1058.
37. Fdz-Polanco, Mendez E., Uruena M. A., Villaverde S., Garcia P. A., (2000), "*Spatial Distribution of Heterotrophs and Nitrifiers in a Submerged Biofilter for Nitrification*", Water Research, Vol. 34, No. 16, pp. 4081-4089.
38. Ford D. L., Churchwell R. L., (1980), "*Comprehensive Analysis of Nitrification of Chemical Processing Wastewaters*", Journal of Water Pollution Control Federation, Vol. 52, No. 11, pp. 2726-2746.
39. Freundlich H., (1907), "*Adsorption in Solution.*", Phys. Chemie, Vol. 57, pp. 384-410.
40. Fry B. A., *The Nitrogen Metabolism of Micro-organisms*, Methuen&Co. Ltd, London, 1955.
41. Furukawa K., Ryu S., Fujita M., Fukunaga I., (1993), "*Nitrogen Pollution of Leachate at a Sea Based Solid Waste Disposal Site and Its Nitrification Treatment by Immobilized Acclimated Nitrifying Sludge*", Journal of Fermentation and Bioengineering, Vol. 77, pp. 413-418.

42. Furusawa T. and Smith J. M., (1973) Ind. Eng. Chem. Fundam., Vol. 12, No. 2, pp. 197-202.
43. Gisvold B., Odegaard H., Follesdal M., (2000), "*Enhanced Removal of Ammonium by Combined Nitrification/Adsorption in Expanded Clay Aggregate Filters*", Water Science and Technology, Vol. 41, No. 4-5, pp. 409-416.
44. Gross A., Nemirovsky A., Zilberg D., Khaimov A., Brenner A., Snir E., Ronen Z., Nejdat A., (2003), "*Soil Nitrifying Enrichments as Biofilter Starters in Intensive Recirculating Saline Water Aquaculture*", Aquaculture, Vol. 223, No. 1-4, pp. 51-62.
45. Groeneweg J., Sellner B., Tappe W., (1994), "*Ammonia Oxidation in Nitrosomonas at NH_3 Concentrations Near K_m : Effects of pH and Temperature*", Water Research, Vol. 28, No. 12, pp. 2561-2566.
46. Gurdeep S., Prasad B., (1997), "*Removal of Ammonia From Coke-Plant Wastewater by Using Synthetic Zeolite*", Water Environment Research, Vol. 69, No. 2, pp. 157-161.
47. Haug R. T., McCarty P. L., (1972), "*Nitrification with submerged filters*", Journal of Water Pollution Control Federation, Vol. 44, pp. 2086-2102.
48. Helfferich F., "*Ion Exchange*", Mc Graw Hill, 1962.
49. The Purolite Company, "*Hypersol-Macronets Sorbent Resins; Purolite Technical Bulletin*", 1999.
50. Hockenbury M. R., Leslie Grady C. P., (1977), "*Inhibition of Nitrification-Effects of Selected Organic Compounds*", Journal of Water Pollution Control Federation, Vol. 49, No. 3, pp. 768-777.

51. Horan N. J., *"Biological Wastewater Treatment Systems"*, John Wiley & Sons, 1991.
52. Hovanec T. A., DeLong E. F., (1996), *"Comparative Analysis of Nitrifying Bacteria Associated with Freshwater and Marine Aquaria"*, Applied and Environmental Microbiology, Vol. 62, No.8, pp. 2888-2896.
53. Huguenin J. E., Colt J., *"Design and Operating Guide for Aquaculture Seawater Systems"*, Elsevier, 1989.
54. Jones R. D., Hood M. A., (1980), *"Effects of Temperature, pH, Salinity and Inorganic Nitrogen on the Rate of Ammonium Oxidation by Nitrifiers Isolated From Wetland Environments"*, Microbial Ecology, Vol. 6, pp. 339-347.
55. Jorgensen T. C., *"Removal of Ammonia From Wastewater by Ion Exchange in the Presence of Organic Compounds"*, MSc research dissertation, Department of Chemical Engineering, University of Canterbury, 2002.
56. Jorgensen T. C., Weatherley L. R., *"Ion Exchange Removal of Ammonium Ion from Wastewater onto Clinoptilolite in the Presence of Organics"*, 6th World Congress of Chemical Engineering, Melbourne, 2001.
57. Jorgensen T. C., Weatherley L. R., (2003), *"Ammonia Removal from Wastewater by Ion Exchange in the Presence of Organic Contaminants"*, Water Research, Vol. 37, pp. 1723-1728.
58. Kanokwaree k., Doran P. M., (1998), *"Application of Membrane Tubing Aeration and Perfluorocarbon To Improve Oxygen Delivery To Hairy Root Cultures"*, Biotechnology Programme, Vol. 14, No. 3, pp. 479-486.
59. Keen G. A., *"Nitrification in Continuous Culture"*, PhD research dissertation, University of Aberdeen, 1984.

60. Kiely G., *"Environmental engineering"*, Maidenhead, England: McGraw-Hill, 1997.
61. Kithome M., Paul J. W., Lavkulich L. M., Bomke A. A., (1998), *"Kinetics of Ammonium Adsorption and Desorption by the Natural Zeolite Clinoptilolite"*, Soil Science Society of America Journal, Vol. 62, pp. 622-629.
62. Klieve J. R., Semmens M. J., (1980), *"An Evaluation of Pretreated Natural Zeolites for Ammonium Removal"*, Water Research, Vol. 14, pp. 161-168.
63. Knowlton G. D., White T. R., (1981), *"Thermal Study of Types of Water Associated With Clinoptilolite"*, Clays and Clay Minerals, Vol. 29, No. 5, pp.403-411.
64. Kochany J., Lugowski A., (1998), *"Application of Fenton's Reagent and Activated Carbon for Removal of Nitrification Inhibitors"*, Environmental Technology, Vol. 19, pp. 425-429.
65. Koon J., Kaufman W., (1975), *"Ammonia Removal From Municipal Wastewater by Ion Exchange"*, Journal of Water Pollution Control Federation, Vol. 47, No. 3, pp. 448-465.
66. Krumer G., Rosenthal H., (1983), *"Efficiency of Nitrification in Trickling Filters Using Different Substrates"*, Aquacultural Engineering, Vol. 2, pp. 49-67.
67. Kuhlman W., (1987), *"Optimization of a Membrane Oxygenation System for Cell Culture in Stirred Tank Reactors"*, Development of Biological Standards, Vol. 66, pp. 263-268.
68. Kunin R., Myers R. J., *"Ion Exchange Resins"*, Chapman&Hall, 1951.
69. Lahav O., Green M., (1998), *"Ammonium Removal Using Ion Exchange and Biological Regeneration"*, Water Research, Vol. 32, No. 7, pp. 2019-2028.

70. Langmuir, I., (1918), "*Adsorption of Gases on Plane Surfaces of Glass, Mica and Platinum*", J. Amer. Chem. Soc., Vol. 40, pp. 1361-1403.
71. Lankford P. W, Eckenfelder W. W., Torrens K. D., (1988), "*Reducing Wastewater Toxicity*", Chemical Engineering, Vol. 7, pp. 72-81.
72. Lekang O. I., Kleppe H., (2000), "*Efficiency of Nitrification in Trickling Filters Using Different Filter Media*", Aquacultural Engineering, Vol. 21, No. 3, pp. 181-199.
73. Liberti L., Helferrich F. G., "*Mass Transfer and Kinetics of Ion Exchange*", Martinus Nijhoff Publishers, The Hague, Boston, Lancaster, (1983).
74. Lin S. H., Wu C. L., (1996), "*Removal of Nitrogenous Compounds From Aqueous Solution by Ozonation and Ion Exchange*", Water Research, Vol. 30, No. 8, pp. 1851-1857.
75. Lovel R. T., "*Nutrition and Feeding Fish*", Van Nostrand Reinhold, USA, 1989.
76. Lopez-Alcala J. M., Rodriguez Fuentes G., Lopez-Ruiz J. L., "*Modification of a Zeolite for Improved Ammonium Retention*", IV Convegno Nazionale Scienza e Tecnologia delle Zeoliti, Universit  A. Volta, Milano/Como, Italy, 1998.
77. Lopez-Alcala J. M., Lopez-Ruiz J. M., "*Elimination of Ammonium in Seawater by Zeolitic Products*", Proceedings of the 13th International Zeolite Conference, Montpellier, France, 2001.
78. Mauret M., Paul E., Puech-Costes E., Maurette M. T., Baptiste P., (1996), "*Application of Experimental Research Methodology to the Study of Nitrification in Mixed Culture*", Water Science and Technology, Vol. 34, No. 1-2, pp. 245-252.

79. McKay G., Blair H.S., Gardner J., (1983), "*The Adsorption of Dyes in Chitin. III. Intraparticle Diffusion Processes*", J. Appl. Polymer Sci., Vol. 28, pp. 1767-1778.
80. McKenzie L. D., Cornwell D. A., "*Introduction to Environmental Engineering*", Mc Graw Hill, 1996.
81. McVeigh R. J., "*The Enhancement of Ammonium Ion Removal Onto Columns of Clinoptilolite In the Presence of Nitrifying Bacteria*", PhD research dissertation, Department of Chemical Engineering, The Queens University of Belfast, 1999.
82. Meade T. L., "*Closed System Salmonid Culture in the United States*", Rhode Island University, Kingston, Marine Advisory Service, 1976.
83. Metcalf & Eddy, Tchobanoglous G., "*Wastewater Engineering : Treatment Disposal Reuse*", New York : McGraw-Hill, (1979).
84. Metropoulos K, Maliou E., Loizidou M., Spyrellis N, (1993), "*Comparative Studies between Synthetic and Natural Zeolites for Ammonium Uptake*" *Journal of Environmental Science and Health*, Vol. 28, No. 7, pp. 1507-1518.
85. Ming D. W., Allen E. R., (2001), "*Use of Natural Zeolites in Agronomy, Horticulture and Environmental Soil Remediation*", *Reviews in Mineralogy and Geochemistry*, Vol. 45, pp. 619-654.
86. Mumpton F. A. and Fishman P. H., (1977) "*The application of natural zeolites in animal science and aquaculture*" *Journal of Animal Science* Vol. 45. No. 5, pp. 1188-1203.

87. Mumpton F. A., (1976), "*Natural Zeolites: a New Industrial Mineral Commodity*", Zeolite 76, International Conference on the Occurrence, properties and Utilization of Natural Zeolites, Pergamon Press, Oxford, pp. 3-31.
88. Muraviev D. N., Khamizov R. K., "*Sustainable Development and Ion Exchange: Green Ion Exchange Technologies*", In: Ion exchange at the millennium. London: Imperial College Press, 2004.
89. Ng W. J., Kho K., Ong S. L., Sim T. S., Ho J. M., (1996), "*Ammonia Removal From Aquaculture Water by Means of Fluidised Technology*", Aquaculture, Vol. 139, pp. 55-62.
90. Nguyen, M. L., Tanner, C. C. (1998) "*Ammonia Removal From Wastewaters Using Natural New Zealand Zeolites*", New Zealand Journal of Agricultural Research, Vol 41, pp. 427-446.
91. Njoroge B. N. K., Mwamachi S. G., (2004), "*Ammonia Removal From an Aqueous Solution by the Use of a Natural Zeolite*", Journal of Environmental Engineering Science, Vol. 3, pp. 147-154.
92. O'Connor JM, "*Removal of Naturally Occurring Colour and Associated Metals from Upland Waters by Adsorption*", PhD research dissertation, The Queen's University of Belfast, 1995.
93. Odell L. H., Kirmeyer G. J., Wilczak A., Jacangelo J. G., Marcinko J. P., Wolfe R. W., (1996), "*Controlling Nitrification in Chloraminated Systems*", Journal of AWWA, Vol. 88, No. 7, pp. 86-98.
94. Orhon D, Genceli E. A., Sozen S., (2000), "*Experimental Evaluation of the Nitrification Kinetics for Tannery Wastewaters*", Water of South Africa, Vol. 26, No. 1., pp. 46-50.

95. Papadopoulos A., Kapetanios E. G., Loizidou M., (1996), "*Studies in the Use of Clinoptilolite for Ammonia Removal From Leachates*", Journal of Environmental Science and Health, Vol. 31, No. 1, pp. 211-220.
96. Picioreanu C., Loosdrecht M. C. M., Heijnen J. J., (2000), "*Two-Dimensional Model of Biofilm Detachment Caused by the Internal Stress from Liquid Flow*", Biotechnology and Bioengineering, Vol. 72, No. 2, pp 205-218.
97. Preston K. T., Alleman J. E., (1994), "*Co-immobilization of Nitroifying Bacteria and Clinoptilolite for Enhanced Control of Nitrification*", Proceedings of the 48th Industrial Waste Conference, pp. 407-412.
98. Richardson R. L., Mills A. L., Herman J. S., Hornberger G. M., (2000), "*Effect of Humic Material on Interactions Between Bacterial Cells and Mineral Surfaces*", LMECOL Contribution, 2000-01.
99. Rijnaarts H. H. M., Norde W., Bouwer E. J., Lyklema J., Zehnder A. J. B., (1995), "*Reversibility and Mechanism of Bacterial Adhesion*", *Colloids and Surfaces B: Biointerfaces*, Vol. 4, No. 1, pp. 5-22.
100. Rodriguez Fernandez P. M., Lopez Alcala J. M., Lopez Ruiz J. L., "*Treatment by Zeolitic Products for the Elimination of Ammonium Contained in Water of Different Salinities*", Water Pollution VII: Modelling, Measuring and Prediction, Cadiz, Spain, Book of Proceedings, pp. 343-348, 2003.
101. Roger T. H., Perry L., (1972), "*Nitrification with Submerged Filters*", Water Science and Technology, Vol. 44, pp. 2086-2012.
102. Rozich A. F., Castens D. J., (1986), "*Inhibition Kinetics of Nitrification in Continuous-Flow Reactor*", Journal of Water Pollution Control Federation, Vol. 58, No. 3, pp. 220-226.

103. Schoeman J. J., (1986), "*Evaluation of a South African Clinoptilolite for Ammonia-Nitrogen Removal From an Underground Mine Water*", Water SA, Vol. 12, No. 2, pp. 73-82.
104. Semmens M. J., Porter P. S., (1979) "*Ammonium Removal by Ion Exchange Using Biologically Restored Regenerant*", Journal of Water Pollution Control Federation, Vol. 51, No. 12, pp. 2928-2940.
105. Semmens M. J., Wang J. T., Booth A. C., (1977a), "*Nitrogen Removal bu Ion Exchange Biological Regeneration of Clinoptilolite*", Journal of Water Pollution Control Federation, Vol. 49, No. 12, pp. 2431-2444.
106. Semmens M. J., Wang J. T., Booth A. C., (1977b), "*Biological Regeneration of Ammonium Saturated Clinoptilolite. Mechanism of Regeneration and Influence of Salt Concentration*", Environmental Science and Technology, Vol. 11, pp. 260-265.
107. Shan H., Obbard J.P, (2003), "*Ammonia Removal From Freshwater Using Nitrifying Bacteria Enriched From a Seawater Aquaculture Pond*", Biotechnology Letters, Vol. 25, No. 17, pp. 1469-1471.
108. Sheng H. L., Chang L. W., (1996), "*Removal of Nitrogenous Compounds from Aqueous Solution by Ozonation and Ion Exchange*", Water Research, Vol. 30, No. 8, pp. 1851-1857.
109. Sherman J. D., (1978), "*Ion Exchange Separations with Molecular Sieve Zeolites*", A.I.Ch.E. Symposium series, Vol. 74, No.179, pp. 98-116.
110. Sherrad J. H., (1976), "*Destruction of Alkalinity in Aerobic Biological Wastewater Treatment*", Journal of Water Pollution Control Federation, Vol. 48, pp. 1834-1839.

111. Siddiqi R. H., Specce R. E., Engelbrecht R. S., Schmidt J. W., (1967), *"Elimination of Nitrification in the BOD Determination With 0.10M Ammonia Nitrogen"*, Journal of Water Pollution Control Federation, Vol. 39, No. 4, pp. 579-589.
112. Sims R. C., Little L. W., (1973), *"Enhanced Nitrification by Addition of Clinoptilolite to Tertiary Activated Sludge"*, Environmental Letters, Vol. 4, No. 1, pp. 27-34.
113. Singh G., Prasad B., (1997), *"Removal of Ammonium From Coke-Plant Wastewater by Using Synthetic Zeolite"*, Water Environmental Research, Vol. 69, No. 2, pp. 157-161.
114. Skudder A. J., *"Ammonium Ion Exchange on Zeolites"*. PhD research dissertation, University of Cambridge, 1976.
115. Soderberg R. W., Meade J. W., (1991), *"The Effects of Ionic Strength on Un-ionized Ammonia Concentration"*, Progressive Fish-Culturist, Vol. 53, pp. 118-120.
116. Streat M., Sweetland L. A., (1997), *"Physical and Adsorptive Properties of Hypersol-Macronet Polymers"*, Reactive and Functional Polymers, Vol. 35, pp. 99-109.
117. Surmacz-Gorska J., Cichon A., Miksch K., (1997), *"Nitrogen Removal From Wastewater With High Ammonia Nitrogen Concentration Via Shorter Nitrification and Denitrification"*, Water Science and Technology, Vol. 36, No. 10, pp. 73-78.
118. Tanaka H., Dunn I. J., (1982), *"Kinetics of Biofilm Nitrification"*, biotechnology and Bioengineering, Vol. 24, No. 3, pp. 669-689.

119. Tanaka J, Matsumara M., (2003), "*Application of Ozone Treatment for Ammonia Removal in Spent Brine*", Advances in Environmental Research, Vol. 7, No. 4, pp. 835-845.
120. Tchobanoglous G., Schroeder E., "*Water quality : characteristics, modeling, modification*", Addison-Wesley, 1985.
121. Tsitsishvili G. V., Andronikashvili T. G., Kirov G. N., Filizova L. D., "*Natural Zeolites*", Ellis Horwood, London, 1992.
122. Thermo Orion, "*Ammonia Electrode Instruction Manual, Model 95-12*", Orion Research, 1997.
123. Turner J. C. R., Church M. R., Johnson A. S. W., Snowdon C. B., (1965), "*An Experimental Verification of the Nernst-Planck Model for Diffusion in an Ion Exchange Resin*", Chemical Engineering Science, Vol. 21, pp. 317-325.
124. Uhl W., Gimbel R., (2000), "*Dynamic Modelling of Ammonia Removal at Low temperatures in Drinking Water Rapid Filters*", Water Science and Technology, Vol. 41, No. 4-5, pp. 199-206.
125. United States Environmental Protection Agency, "*Manual, Nitrogen Control*", EPA-625-R-93-010, Office of Research and Development, Risk Reduction Engineering Laboratory, Cincinnati, 1993.
126. United States Environmental Protection Agency, "*Update of Ambient Water Criteria for Ammonia*", EPA-822-R-99-014, Office of Water, Washington, 1999.
127. United States Environmental Protection Agency, "*Wastewater Technology Fact Sheet-Trickling Filters Nitrification*", EPA-832-F-00-015, Office of Water, Washington, D. C., 2000.

128. Van Loosdrecht M. C. M., Lyklema J., Norde W., Chraa G., Zehnder J. B., (1987), "*Electrophoretic Mobility and Hydrophobicity as a Measure To predict the Initial Steps of Bacterial Adhesion*", Applied and Environmental Microbiology, Vol. 53, No. 8, pp. 1898-1901.
129. Van Loosdrecht M. C. M., Lyklema J., Norde W., Schraa G., Zehnder J. B., (1987a), "*The Role of the Bacterial Cell Wall Hydrophobicity in Adhesion*", Applied and Environmental Microbiology, Vol. 53, No. 8, pp. 1893-1897.
130. Vandevivere P., Ficara E., Terras C., Julies E., Verstraete W., (1998), "*Copper-Mediated Selective Removal of Nitrification Inhibitors from Industrial Wastewaters*", Environmental Science and Technology, Vol. 32, pp. 1000-1006.
131. Verstraete W., Alexander M., (1973), "*Heterotrophic Nitrification in Samples of Natural Ecosystems*", Environmental Science and Technology, Vol. 7, No. 1, pp. 39-42.
132. Vieira M. J., Pacheco A. P., Pinho I. A., Melo L. F., (2001), "*The Effect of Clay Particles on the Activity of Suspended Autotrophic Nitrifying Bacteria And on the Performance of an Air-Lift Reactor*", Environmental Technology, Vol. 22, pp. 123-135.
133. Walker G. M., "*Industrial Wastewater Treatment Using Biological Activated Carbon*", PhD research dissertation, The Queen's University of Belfast, 1995
134. Walker G. M. and Weatherley L. R. (1999), "*Kinetics of Acid Dye Adsorption on GAC*", Water Research, Vol. 33, No 8, pp. 1895-1899.
135. Watanabe Y., Yamada H., Kokusen H., Tanaka J., Moriyoshi Y., Komatsu Y., (2003), "*Ion Exchange Behavior of Natural Zeolites in Distilled Water*,

- Hydrochloric Acid and Ammonium Chloride Solution*", Separation Science and Technology, Vol. 38, No 7, pp. 1519-1532.
136. Water Environmental Research Foundation (WERF), (2002), "*Membranes Breathe Fresh Air Into Wastewater Treatment*", http://www.werf.org/press/spring02/02sp_membraneresearch.cfm, taken from the internet April, 2005.
 137. Weatherley L. R., MCVeigh R. J., (2000), "*The Enhancement of Ammonium Ion Removal Onto Columns of Clinoptilolite in the Presence of Nitrifying Bacteria*", Ion Exchange at the Millennium, edited by Greig J. A., SCI Cambridge UK, pp. 133-141.
 138. Webster C. E., Cottone A., Drago R. S., (1999), "*Multiple Equilibrium Analysis Description of Adsorption on Na-Mordenite and H-Mordenite*", Journal of American Chemical Society, Vol. 121, No. 51, pp. 12127-12139.
 139. Weber M. A., Barbarick K. A. and Westfall D. G., (1983), "*Ammonium Adsorption by Zeolite in a Static and a Dynamic System*", J. Environ. Qual., Vol. 12, No. 4, pp. 549-552.
 140. Wiesmann U., (1994), "*Biological Nitrogen Removal From Wastewater*" Advances in biochemical engineering/biotechnology, Vol. 51, pp. 114-153.
 141. Wikipedia; The Free Encyclopaedia, <http://en.wikipedia.org/wiki/Salinity>. taken from the internet November, 2004.
 142. Wood C. M., "*Ammonia and Urea Metabolism and Excretion*", Physiology of Fishes, CRC Press, 1993.

143. Woods N., *"The Removal of Ammonia from Industrial Wastewater"*, MSc research dissertation, Department of Chemical Engineering, The Queen's University of Belfast, 1997.
144. Wolfe R. L., Lieu N. I., *"Nitrifying Bacteria in Drinking Water. In Encyclopedia of Environmental Microbiology"*, edited by G. Bitton, John Wiley and Sons, New York, 2001.
145. WPCF, *"Standard Methods for the Examination of Water and Wastewater"*, 14th Ed.', 1975.
146. Yang P. P., Nitisoravut S., Wu JY S., (1994), *"Nitrate Removal Using a Mixed Culture Entrapped Microbial Cell Immobilization Process Under High Salt Condition"*, Water Research, Vol. 29, No. 6, pp. 1525-1532.
147. Ydstebo L., *"Kinetics of Biofilm Nitrification on Porous Glass Media"*, MSc research dissertation, Department of Chemical Engineering, The Queen's University of Belfast, 1997.
148. Zhaohui L., (1999), *"Sorption Kinetics of Hexadecyltrimethylammonium on Natural Clinoptilolite"*, Langmuir, Vol. 15, pp. 6438-6445.

8 Appendices

Appendix I: Dependence of the milliequivalent and mass concentration of ions

If we have the mass concentration of 60mg/l of Ca^{++} ion and want to calculate the milliequivalent (meq) concentration the procedure would be as follows:

Since the atomic weight of Ca^{++} ion is 40g/mol = 40mg/mmol, and the calcium is a divalent cation, the mass concentration of 60mg/l of Ca^{++} ions will be equivalent to:

$$\frac{60\text{mg/l}}{\frac{40\text{mg/mmol}}{2\text{meq/mmol}}} = \frac{60\text{mg/l}}{20\text{mg/meq}} = 3\text{meq/l}$$

Appendix II: The mass balance calculations and modelling of the isotherm data

The modelling of the batch experimental results will be explained by using data obtained for the clinoptilolite without interfering cations (Figure 4.11).

Langmuir adsorption isotherm

The ammonia concentration in the solution, after the equilibrium was achieved (C_e) was measured. The solid concentration was then calculated by using the following equation:

$$Q_{\text{exp}} = \frac{(C_{\text{init}} - C_e) \cdot V_{\text{sol}}}{m_{\text{mat}}}$$

where: - Q_{exp} – calculated solid concentration (mg N-NH₄⁺/g material);
- C_{init} – initial ammonia concentration in the flask (mg/l);
- V_{sol} – volume of the solution in the flask (l);
- m_{mat} – mass of the ion exchanger (g).

For the initial concentration of 10mg/l the calculation would be as follows:

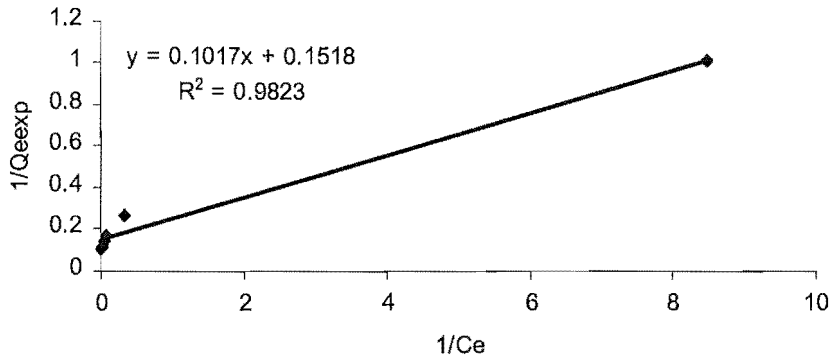
$$Q_{e_{\text{exp}}} = \frac{(10 - 0.118) \text{ mg/l} \cdot 50 \cdot 10^{-3} \text{ l}}{0.5 \text{ g}} = 0.988 \text{ mg/g}$$

When the linear shape of the Langmuir adsorption isotherm was taken;

$$\frac{1}{Q_e} = \frac{1}{kbC_e} + \frac{1}{b}$$

and $1/Q_{e_{\text{exp}}}$ versus $1/C_e$ was plotted, the following was obtained:

Langmuir isotherm for Clinoptilolite; (only ammonia)



The following values were obtained from the graph:

$$1/b=0.1518 \rightarrow b=6.588$$

$$1/(kb)=0.1017 \rightarrow k=1.493$$

$$R^2=0.982$$

By using the constants obtained and the measured concentration C_e , the values for the $Q_{e(Lang)}$ were obtained by using the equations:

$$\frac{1}{Q_e} = \frac{1}{kbC_e} + \frac{1}{b} \rightarrow Q_{e(Lang)} = \frac{1}{\frac{1}{kbC_e} + \frac{1}{b}}$$

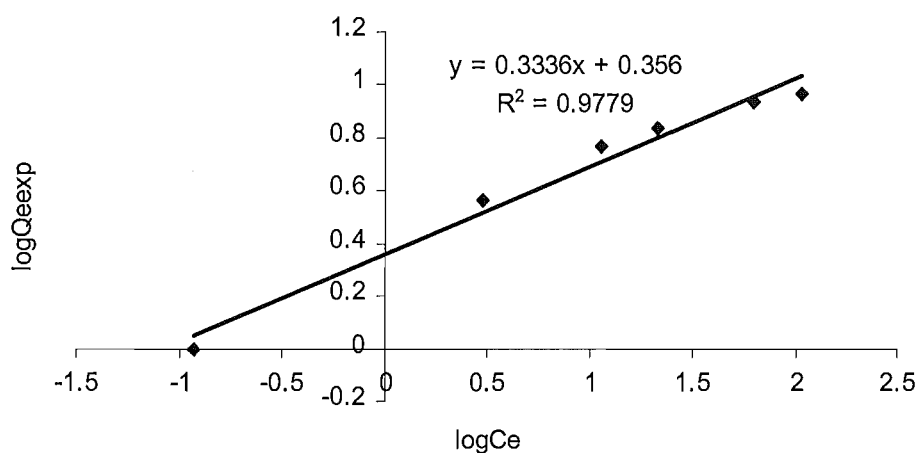
Freundlich adsorption isotherm

To model the results by using the Freundlich adsorption model the values for C_e and Q_{eexp} obtained above were used. The linear shape of the Freundlich isotherm is:

$$\log Q_e = \frac{1}{n} \log C_e + \log k$$

By plotting the $\log Q_{eexp}$ versus $\log C_e$ the following graph was obtained:

Freundlich isotherm for Clinoptilolite; only NH_4^+



The values for the coefficients obtained from the graph were:

$$\log k = 0.356 \rightarrow k = 2.270$$

$$1/n = 0.3336$$

$$R^2 = 0.978.$$

By using the following equation and the obtained values for the coefficients, the values for $Q_{e(\text{Fr})}$ were obtained:

$$\log Q_e = \frac{1}{n} \log C_e + \log k$$

The calculated values for the whole range of concentrations were as follows:

Cinit. (mg/l N-NH_4^+)	Ce (mg/l N-NH_4^+)	Qe(exp.) (mgN-NH4+/g)	1/Ce	1/Qe	Qe(Lang)	logCe	logQe	Qe(Fr)
10	0.118	0.988	8.489	1.012	0.985	-0.929	-0.005	1.105
40	3.052	3.695	0.328	0.271	5.402	0.485	0.568	3.304
70	11.473	5.853	0.087	0.171	6.224	1.060	0.767	5.161
90	21.628	6.837	0.046	0.146	6.390	1.335	0.835	6.388
150	63.822	8.618	0.016	0.116	6.519	1.805	0.935	9.195
200	107.445	9.256	0.009	0.108	6.547	2.031	0.966	10.957

Appendix III: Broth for the bacteria growth (Woods, 1997)

Following chemicals were dissolved in 2000ml of deionised or saline water:

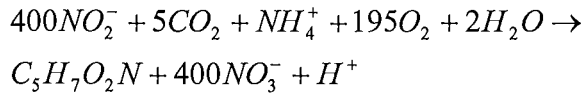
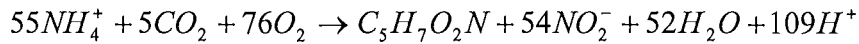
(NH ₄)Cl	1.905g
NaHPO ₄	1.0g
NaCl	4.0g
MgSO ₄ x7H ₂ O	0.4g
FeSO ₄ x7H ₂ O	0.1g
CaCO ₃	12.0g

2ml trace of element solution:

Fe(III)-citrate	1000mg/l
MnCl ₂ x4H ₂ O	10mg/l
ZnCl ₂	5mg/l
LiCl	5mg/l
KBr	2.5mg/l
KI	2.5mg/l
CuSO ₄	0.005mg/l
CaCl	1000mg/l
Na ₂ MoO ₄ x2H ₂ O	1mg/l
CoCl	5mg/l
SnCl ₂ xH ₂ O	0.5mg/l
BaCl ₂	0.5mg/l
AlCl ₃	1mg/l
H ₃ BO ₃	10mg/l
EDTA	20mg/l

Appendix IV: Calculation of the bacteria specific growth

The biomass in the reactor was calculated on the basis of the consumed ammonia during the growth period. The process will be explained for the data obtained for the growth in non-saline water. According to the following equations:



55.1mol of NH_4^+ will produce 1.1mol of biomass, or

1g of NH_4^+ will produce 0.13g of bacteria.

When we calculated the total ammonia consumed for each sample taken (Table 4.18) and multiplied it by 0.13 to obtain the bacteria cell mass, the following results were obtained:

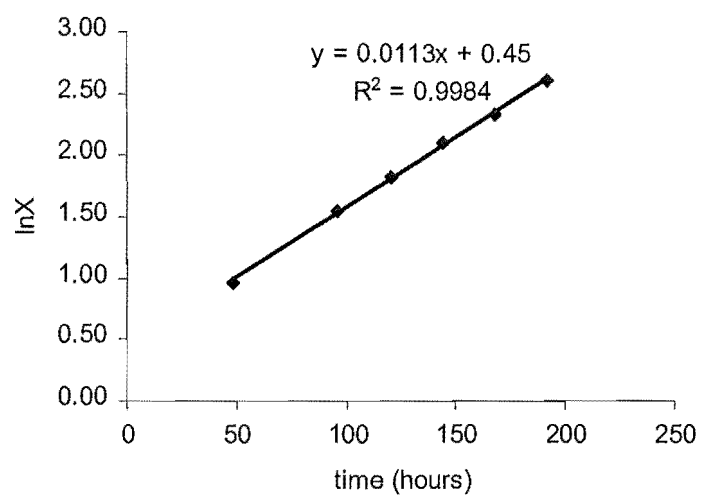
hours	N-NH_4^+ concentration	N-NH_4^+ consumed	NH_4^+ consumed	total NH_4^+ consumed	bacteria cell mass	$\ln(x)$
24.00	220.50					
48.00	204.75	15.75	20.25	20.25	2.63	0.9679
96.00	192.50	12.25	15.75	36.00	4.68	1.5433
120.00	183.22	9.28	11.93	47.93	6.23	1.8294
144.00	171.55	11.67	15.00	62.93	8.18	2.1017
168.00	159.30	12.25	15.75	78.68	10.22	2.3243
192.00	139.64	19.56	25.15	103.83	13.50	2.6027
216.00	128.08	11.56	14.86	118.69	15.43	2.7363
240.00	111.82	16.26	20.91	139.60	18.15	2.8987
264.00	84.87	47.45	61.01	200.61	26.02	3.2589
288.00	64.42	20.45	26.30	226.91	29.54	3.3857
312.00	48.10	16.32	20.98	247.89	32.26	3.4738
336.00	30.84	17.26	22.19	270.08	35.15	3.5596
360.00	10.36	20.48	26.33	296.41	38.48	3.6501
384.00	0.50	9.86	12.68	309.09	40.22	3.6944
408.00	0.25	0.24	0.30	309.39	40.26	3.6954

According to the following equation:

$$\ln X = \ln X_0 + \mu t$$

- where: - X – cell concentration;
 - X_0 – cell concentration at $t=0$;
 - t – time
 - μ – specific growth rate (h^{-1}).

The plot of $\ln X$ versus time will give the straight line



where $\mu = 0.01\text{h}^{-1}$

Appendix V: Modelling of the results obtained for the kinetic experiments

The calculations for the kinetic experiments will be explained by using the data obtained for the ammonia uptake onto MN 500, initial ammonia concentration 50mg/l, particle size 0.7-1mm, mass of the material 1.5g (Figure 4.26).

External mass transfer coefficient

The results were correlated using the following equation:

$$\ln \left[\frac{C_t}{C_0} - \frac{1}{1 + m_s K} \right] = \ln \left[\frac{m_s K}{1 + m_s K} \right] + \left[\frac{-1 + m_s K}{m_s K} k_f S_s t \right]$$

$$m_s = \frac{M}{V} \quad \text{and} \quad S_s = \frac{6m_s}{d_p \rho_p}$$

where: - d_p - particle diameter (cm)

- K - Langmuir constant (l/g)

- k_f - mass transfer coefficient between liquid and outer surface of particles

(m/s)

- M - mass of ion exchanger (g)

- m_s - concentration of particle in the free liquid (g/l)

- S_s - specific surface area available for mass transfer (cm^{-1})

- t - time (s)

- V - volume of the particle free liquid (cm^3)

- ρ - particle true density (g/cm^3)

- C_0 - initial solute concentration (mg/l)

- C_t - liquid phase concentration at time t (mg/l)

Specific surface area available for mass transfer was calculated according to the following example:

$$S_s = \frac{6 \frac{M}{V}}{d_p \rho_p} = \frac{6 \cdot \frac{1.5 \text{ g}}{3000 \text{ cm}^3}}{0.0855 \text{ cm} \cdot 1.04 \text{ g} / \text{cm}^3} = 0.0337 \text{ cm}^{-1}$$

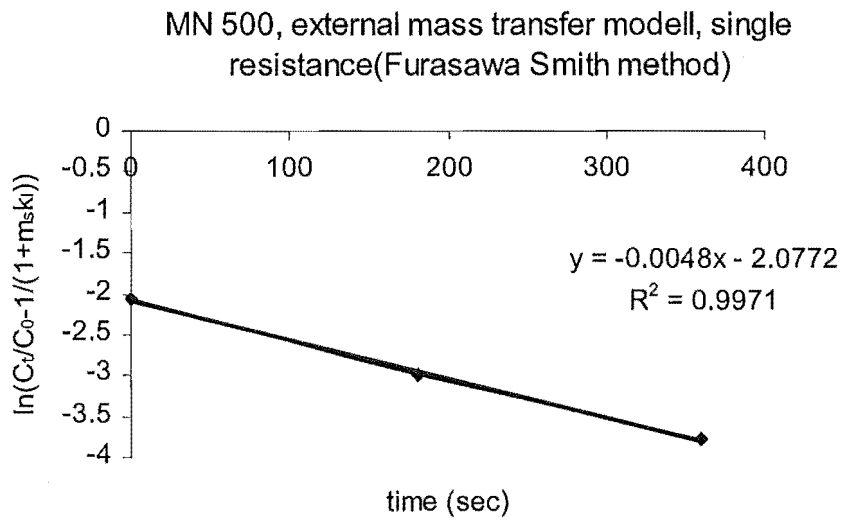
The left side of the equation was calculated for the each sample taken according to the following example, which is for the sample taken 180 seconds after the experiment started:

$$\ln \left[\frac{C_t}{C_0} - \frac{1}{1 + m_s K} \right] = \ln \left[0.92123 - \frac{1}{1 + 0.5 \cdot 0.296} \right] = -2.995$$

The calculated values for each time point were as follows:

time (sec)	C_t/C_0	$\ln(C_t/C_0 - 1/(1+m_s k))$
0	1	-2.0500
180	0.9213	-2.9961
360	0.8941	-3.7794

When we plotted the $\ln \left[\frac{C_t}{C_0} - \frac{1}{1+m_s K} \right]$ versus time the following graph was obtained



The values obtained from the graph were:

$$\frac{-1+m_s K}{m_s K} k_f S_s = -0.0048 \rightarrow k_f = 0.0245 \text{ cm/s}$$

$$R^2 = 0.9971$$

Internal mass transfer coefficient

To test the experimental rate data against the time we used the following equation:

$$k_d = \frac{1}{t^{0.5}} \cdot Q_t \rightarrow Q_t = k_d \cdot t^{0.5}$$

where: - k_d - mass transfer coefficient within the particle (mg/gmin^{0.5})
- Q_t - solid phase concentration at the particle (mg/g)
- t - time (min)

Q_t was calculated in the following way:

$$Q_t = \frac{(C_0 - C_t) \cdot V}{M}$$

where: - M - mass of ion exchanger (g)
- V - volume of the particle free liquid (cm³)
- C_0 - initial solute concentration (mg/l)
- C_t - liquid phase concentration at time t (mg/l)

For the sample taken 3minute after the experiment started, the Q_t was

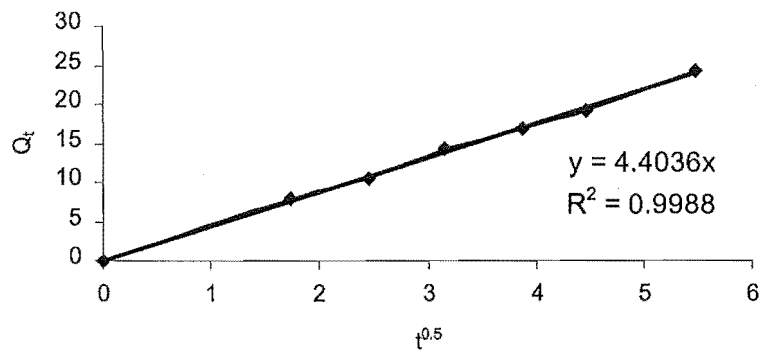
$$Q_t = \frac{(50 - 46.06) \text{ mg/l} \cdot 3 \text{ l}}{1.5 \text{ g}} = 7.88 \text{ mg/g}$$

The calculated values for each time point were as follows:

<i>time (min)</i>	<i>C_t</i>	<i>SQRT(t)</i>	<i>Q_t</i>
3	46.06	1.7321	7.8750
6	44.71	2.4495	10.5893
10	42.82	3.1623	14.3694
15	41.55	3.8730	16.8924
20	40.33	4.4721	19.3411
30	37.86	5.4772	24.2761

When the Q_t was plotted versus the square root of the time the following graph was obtained:

Internal mass transfer model for MN 500 in DI water,
C=50mg/l, M=1.5g, t=3-30min



The following values were obtained from the graph:

- $k_d = 4.4 \text{ mg/gmin}^{0.5}$

- $R^2 = 0.9988$

Appendix VI

Table 7.1 The uptake values for clinoptilolite and mordenite; particle size: 0.7-1.4mm, initial ammonia concentration: 20mg/l $N-NH_4^+$, flow rate: 4BV/h, column diameter: 30mm (Figure 4.41)

Mordenite		Clinoptilolite	
<i>BV</i>	<i>effluent conc. $N-NH_4^+$</i>	<i>BV</i>	<i>effluent conc. $N-NH_4^+$</i>
252	0.28	190	0.13
284	0.28	252	0.14
308	0.28	284	0.21
334	0.22	308	0.21
348	0.24	334	0.28
380	0.22	348	0.48
406	0.32	380	1.19
428	0.32	406	1.25
476	0.29	428	2.66
500	0.33	476	11.37
540	0.47	500	16.39
576	0.77	540	17.66
612	1.49	576	18.78
632	2.57	612	19.24
672	5.39	632	19.44
720	10.67	672	19.37
772	16.79		
804	18.27		
860	18.94		
886	18.94		
920	18.94		

Table 7.2 The uptake values for the packed bed of clinoptilolite and mordenite; particle size: 0.7-1.4mm, initial ammonia concentration: 40mg/l $N-NH_4^+$, creek water, flow rate: 2BV/h, column diameter: 30mm, (Figure 4.42)

Clinoptilolite		Mordenite	
<i>BV</i>	<i>effluent conc. $N-NH_4^+$</i>	<i>BV</i>	<i>effluent conc. $N-NH_4^+$</i>
50	0.49	88.4	0.37
88.4	0.74	114	0.93
114	0.49	154.8	0.74
138	10.23	190.8	1.50
154.8	16.19	224.4	0.84
190.8	30.22	266.8	2.54
224.4	33.56	328.3	4.10
266.8	37.57	384	20.45
280	38.06	403.3	25.13
292.3	38.55	444.2	35.84
328.3	39.54	472.3	40.07
		502.3	39.87

Table 7.3 The uptake values for clinoptilolite; particle size: 0.7-1.4mm, initial ammonia concentration: 20mg/l $N-NH_4^+$, flow rate: 4BV/h, column diameter: 30mm (Figure 4.43)

1st run		2nd run		3rd run		4th run	
<i>BV</i>	<i>effluent conc. $N-NH_4^+$</i>	<i>BV</i>	<i>effluent conc. $N-NH_4^+$</i>	<i>BV</i>	<i>effluent conc. $N-NH_4^+$</i>	<i>BV</i>	<i>effluent conc. $N-NH_4^+$</i>
12	0.49	190	0.13	180	1.46	364	1.23
62	0.35	252	0.14	216	1.56	392	1.16
94	0.27	284	0.21	268	1.15	416	3.06
126	0.29	308	0.21	290	1.02	464	5.50
158	0.24	334	0.28	316	1.14	488	6.89
184	0.18	348	0.48	364	1.07	512	11.30
208	0.24	380	1.19	386	1.16	558	17.59
256	0.30	406	1.25	416	1.77	582	17.87
274	0.27	428	2.66	460	2.48	614	19.43
294	0.37	476	11.37	482	3.10	658	19.74
314	2.03	500	16.39	512	6.73		
350	4.36	540	17.66	556	16.68		
362	6.17	576	18.78	578	18.23		
374	9.74	612	19.24	608	17.96		
390	11.25	632	19.44	748	19.06		
414	13.43	672	19.37				
446	16.39						
470	16.39						
494	16.94						
542	17.13						

Table 7.4 The uptake values for the packed bed of mordenite; particle size: 0.7-1.4mm, initial ammonia concentration: 20mg/l $N-NH_4^+$, flow rate: 4BV/h, column diameter: 30mm, (Table 4.44)

1st run		2nd run		3rd run		4th run	
BV	effluent conc. $N-NH_4^+$	BV	effluent conc. $N-NH_4^+$	BV	effluent conc. $N-NH_4^+$	BV	effluent conc. $N-NH_4^+$
12	0.47	252	0.28	512	0.62	488	0.16
62	0.44	284	0.28	556	0.66	512	0.30
94	0.33	308	0.28	578	0.54	558	0.25
126	0.22	334	0.22	674	0.75	582	0.31
158	0.20	348	0.24	708	0.67	614	0.69
184	0.23	380	0.22	748	1.69	658	0.57
208	0.23	406	0.32	772	2.64	688	0.84
256	0.37	428	0.32	804	5.49	708	1.17
274	0.30	476	0.29	860	8.30	756	1.55
294	0.31	500	0.33	900	11.10	776	1.70
314	1.10	540	0.47	940	13.20	804	2.74
350	0.79	576	0.77	996	16.20	848	3.22
362	1.11	612	1.49	1056	18.20	870	5.93
374	1.00	632	2.57	1112	19.48	896	7.56
390	1.20	672	5.39	1132	19.57	944	9.29
414	2.15	720	10.67	1164	19.65	966	11.66
446	1.89	772	16.79			992	13.92
470	2.15	804	18.27			1040	15.92
494	2.54	860	18.94			1062	17.09
542	3.38	886	18.94			1136	19.49
636	8.21	920	18.94			1160	19.62
672	12.19					1184	19.55
712	16.78						
788	17.83						
832	18.18						
864	18.35						
940	18.30						

Table 7.5 The uptake values for clinoptilolite and mordenite; particle size: 0.7-1.4mm, initial ammonia concentration: 20mg/l N-NH₄⁺, flow rate: 4BV/h, column diameter: 30mm (Figures 4.48 and 4.49)

BV	Mordenite		Clinoptilolite	
	Ct (mg/l N-NH ₄ ⁺)	mg/l N-NO ₃ ⁻	Ct (mg/l N-NH ₄ ⁺)	mg/l N-NO ₃ ⁻
21	0.29	21.4	0.48	14.8
45	0.57	18.8	0.45	11.6
68	0.95	15.7	1.05	11
91	0.91	11.2	1.39	8.7
116	1.42	8.8	3.09	9.8
140	1.17	13	2.61	10.5
164	1.64	13.2	2.97	9.6
190	1.58	10.5	4.33	8.9
215	1.52	12.2	4.98	10.8
235	0.91	12.9	4.64	11.1
263	1.19	12.7	4.15	10.9
286	0.87	13.7	2.90	8.7
310	0.84	13.4	3.15	9.9
334	1.10	11.4	8.40	9.4
357	1.88	17.4	10.47	11.3
381	1.64	13.2	9.12	12
405	1.06	12.1	6.18	18
431	0.60	13.4	4.16	12.1
454	0.92	15.8	14.50	11.2
477	4.32	14.2	25.49	12.6
503	2.48	12.2	18.55	11.1
524	2.66	11.5	16.04	10
550	1.17	11.8	13.45	10.2

Appendix VII: The breakthrough uptake capacity calculation (Table 4.29)

Clinoptilolite (DI water)

$$BV = r^2\pi h = (1.5\text{cm})^2\pi 20\text{cm} = 141.3\text{cm}^3$$

For clinoptilolite, the breakthrough started after 380BV passed through the column.

$$380BV \times 141.3\text{cm}^3 = 53.69\text{l}$$

Since the initial ammonia concentration was 20mg/l N-NH₄⁺ the overall ammonia kept by the material was:

$$53.69\text{l} \times 20\text{mg/l} = 1073.88\text{mg N-NH}_4^+$$

The mass of material packed within the column was 99.80g which means that the uptake capacity was:

$$1073.88\text{mg} / 99.80\text{g} = 10.76\text{mg N-NH}_4^+/\text{g material} = 0.76\text{meq/g}$$

Mordenite (DI water)

For mordenite, the breakthrough started after 600BV passed through the column.

$$600BV \times 141.3\text{cm}^3 = 84.78\text{l}$$

Since the initial ammonia concentration was 20mg/l N-NH₄⁺ the overall ammonia kept by the material was:

$$84.78\text{l} \times 20\text{mg/l} = 1695.60\text{mg N-NH}_4^+$$

The mass of material packed within the column was 144.8g which means that the uptake capacity was:

$$1695.60\text{mg} / 144.8\text{g} = 11.71\text{mg N-NH}_4^+/\text{g material} = 0.84\text{meq/g}$$

Appendix VIII: Residence time calculations

The calculation of the residence time will be explained on the example of the data obtained for the column packed with clinoptilolite.

The specific surface area of the column with the new design was:

$$A = 20.5\text{cm}^2$$

and the bed volume was

$$BV = 410\text{cm}^3$$

For the flow of 1BV/h the velocity would be

$$Vel = \frac{BV}{A} = \frac{410\text{cm}^3 / h}{20.5\text{cm}^2} = 0.33\text{cm} / \text{min}$$

Based on the calculated velocity, theoretical residence time was

$$Rtime = \frac{\text{columnheight}}{Vel} = \frac{20\text{cm}}{0.33\text{cm} / \text{min}} = 60.61\text{min}$$

The residence time obtained by measuring the concentration of the dye injected in the column was:

$$Rtime_{\text{exp}} = 25.46\text{min}$$

Therefore, the voidage of the column was:

$$\varepsilon = \frac{Rtime_{\text{exp}}}{Rtime} = 0.42$$

The values of the column voidage calculated for the different flow rates were as follows:

flow rate (cm ³ /h)	column voidage
50	0.48
410	0.42
820	0.51
1230	0.55

The average voidage was $\varepsilon_{av} = 0.49$ which was used to calculate the residence time within the column. For the flow rate of 1BV the residence time would be

$$Rtime = 60.61\text{min} \cdot 0.49 = 29.69\text{min}$$